Construction of In-situ Cast Flat Slabs using Steel Fibre Reinforced Concrete

Robert Jarratt

MSc. Structural Engineering Candidate

Stellenbosch University

Student Number: 16370236

Supervisor: Prof. WP Boshoff

Thesis presented in fulfilment of the requirements for the degree of Master of Science in Engineering at Stellenbosch University

December 2011

Declaration

By submitting this thesis electronically, I declare that the entirety of the work contained therein is my own, original work, that I am the sole author thereof (save to the extent explicitly otherwise stated), that reproduction and publication thereof by Stellenbosch University will not infringe any third party rights and that I have not previously in its entirety or in part submitted it for obtaining any qualification.

Robert Jarratt ……

Date:……..

Abstract

Fibre reinforced concrete (FRC) transforms concrete from a characteristically brittle material to one with a post-crack tensile residual capacity. Its application in industry has varied over the past of which the tensile properties have generally been used in the form of crack mitigation. More recently, the introduction of steel fibres has broadened this scope to structural applications in which the resisting tensile stresses that develop within a steel FRC (SFRC) element can be rather significant. This thesis reviews the existing practices and design models associated with SFRC and the suitability of its implementation as the sole form of reinforcement in in-situ cast flat slab systems.

As a material SFRC is dependent on a number of factors which include the fibre type and volume, fibre distributions, element size, as well as the support and applied load conditions. Thus, its performance can be considered rather variable in comparison to conventional concrete should the incorrect practices be implemented. In order to adequately define the material characteristics, it is necessary to use test procedures that accurately reflect on the intended structural application. As a result a number of test procedures have been developed. In addition to this, the post-crack material performance is associated with a non-linear behaviour. This attribute makes the design of structural SFRC elements rather difficult. In an attempt to simplify this, existing design models define stress-strain or stress-crack width relations in which assumptions are made regarding the cross-sectional stress distribution at specified load states.

This thesis takes on two parts in defining the suitability of SFRC as the sole form of reinforcement in flat slab systems. The first is a theoretical investigation regarding the micro and macro scale material performance of SFRC, the practices that exist in defining the material properties and its application in structural systems (particularly suspended slab systems), and a breakdown of the existing design models applicable to strain softening deflection hardening SFRC materials. The second part is an experimental program in which

the fresh state and hardened state material properties of specified SFRC mix designs defined through flow and beam testing respectively. These properties are then implemented in the design and construction of full scale flexural and punching shear test slabs in an attempt to verify the theory applied.

The investigation reveals that the use of SFRC significantly improves the ductility of concrete systems in the post-crack state through fibre crack bridging. This ductility can result in deflection hardening of flat slab systems in which the redistribution of stresses increases the load carrying capacity once cracking has taken place. However, the performance of large scale test specimens is significantly influenced by the construction practices implemented in which the material variability increases as a result of non-uniform fibre distributions. The results indicate that the load prediction models applied have potential to adequately predict the ultimate failure loads of SFRC flat slab systems but however cannot account for possible non-uniform fibre distributions which could result in premature failure of the system.

Opsomming

Vesel versterkte beton (VVB) verander beton van die kenmerkende uiters bros material na ‘n material met ‘n residuele post-kraak trekkapasiteit. Die toepassing daarvan in die bedryf het in die verlede gewissel en die trek eienskappe is oor die algemeen gebruik vir kraak vermindering. Meer onlangs het die bekenstelling van staal vesel hierdie omvang verbreed na die strukturele toepassings waar trekspannings wat ‘n VVB element kan weerstaan noemenswaardig kan wees. Hierdie tesis ondersoek bestaande praktyke en ontwerpmodelle met die oog op staalvesel versterkte beton (SVVB) en die geskiktheid van die implementering daarvan as die enigste vorm van bekisting in in-situ gegiete plat blad stelsels.

As ‘n materiaal, is SVVB afhanklik van ‘n aantal faktore wat die tipe vesel en volume, vesel verspreiding, element grootte, sowel as die randvoorwaardes tipe aangewende las insluit. As gevolg hiervan, kan die gedrag van SVVB, wat korrek geïmplimenteer word, as redelik varieerbaar beskou word wanneer dit met konvensionele beton vergelyk word. Ten einde die materiaaleienskappe voldoende te definieer, is dit noodsaaklik dat prosedures wat die strukturele toepassing akuraat voorstel, getoets word en daarom is ‘n aantal toets prosedures ontwikkel. Verder het die post-kraak materiaalgedrag ‘n nie-lineêre verband wat struktuurontwerp met SVVB redelik moeilik maak. Om dit te vereenvoudig, definieer bestaande ontwerpmodelle spanning-vervorming of spanning-kraakwydte verhoudings waarin aannames gemaak word ten opsigte van die spanningsverdeling oor ‘n snit, gegewe sekere lastoestande.

Hierdie studie bestaan uit twee dele wat die geskiktheid van SVVB as die enigste vorm van bikisting in plat blad stelsels definieer. Die eerste deel bestaan uit ‘n teoretiese ondersoek wat handel oor die mikro- en makro-skaal materiaalgedrag van SVVB, die praktyke wat bestaan om die materiaaleienskappe en toepassing in strukturele sisteme (spesifiek opgelegde blad stelsels) te definieer, en ‘n uiteensetting van die bestaande ontwerpmodelle wat van

toepassing is vir defleksie as gevolg van vervormingsversagting wat SVVB material verhard. Die tweede deel bestaan uit ‘n eksperimentele program waarin die materiaaleienskappe van gespesifiseerde SVVB meng-ontwerpe in die vars toestand en in die verharde toestand gedefinieer word deur middel van vloei- en balktoetse onderskeidelik. Hierdie eienskappe word dan toegepas vir die ontwerp en konstruksie van volskaalse buig- en ponsskuif toetsblaaie ten einde die modelle en teorie wat toegepas is, te bevestig.

Die ondersoek toon dat die gebruik van SVVB die duktiliteit van beton sisteme noemenswaardig verbeter in die post-kraak toestand deur kraak oorbrugging. Hierdie duktiliteit kan defleksie verharding van plat blad stelsels veroorsaak waarin die herverdeling van spannings, nadat kraking plaasgevind het, die lasdraende kapasiteit verhoog. Die gedrag van die grootskaalse toetsmonsters word egter noemenswaardig beïnvloed deur die konstruksiemetodes wat geïmplementeer word waarin die materialveranderlikheid toeneem as ‘n gevolg van nie-uniforme vesel verdelings. Die resultate dui daarop dat die modelle wat toegepas is om die laste te voorspel, die potensiaal het om die grens falingslas van SVVB plat blad stelsel voldoende te voorspel, maar neem nie moontlike nie-uniforme veselverdelings wat kan lei tot vroeë faling van die stelsel in ag nie.

Acknowledgements

I would like to thank Prof. Billy Boshoff for his assistance and guidance throughout the project research, in which he gave me the freedom to pursue the topic as I felt fit whilst giving valuable input and support when it was needed. I would also like to acknowledge the laboratory staff whom made the practical side of the research project a much easier and enjoyable experience.

I am grateful for the opportunity to have undertaken this research of which would not have been possible without the support from my bursary provider Jeffares and Green. A special thank you must go to Tim Davidson and Gerry Poswell who turned my goals into a reality.

In order for the full potential of this project to be exploited, a number of contributions had to be made from those in the construction sector. I would like to thank Lafarge Ready Mix suppliers for their donations regarding the concrete and materials used, with a special thanks to Rhuyawda Lalla whose patience I often tested. In addition I would like to thank Tim Davidson and Gareth Randel of Jeffares and Green, Chris Steffen of DV Cape and NMC Contractors for their contributions.

I would like to thank my fellow students whom have made my experience at Stellenbosch University a most enjoyable and memorable one. And lastly I would like to thank my family for encouraging me throughout my student career and helping me to believe in myself.

Stellenbosch, 2011

Robert Jarratt

Table of Contents

Symbols and Notations

Symbols:

A_c concrete area

α ratio for average punching strain

b width in mm

β experimentally determined x/h_{sp} ratio

β_a allowable tensile strain

β_{crit} critical tensile strain

c_u depth of compression zone in mm

d effective depth in mm

d_f fibre diameter

δ_{Ri} mid span deflection

ε strain

ε_{fu} allowable tensile strain in outermost face

F applied force

f_{ck} characteristic compressive strength in N/mm^2

f_{ct}' reduced concrete principle tensile strength in N/mm^2

f_{ft} flexural residual stress in N/mm^2

f_{Fts} serviceability residual tensile stress in N/mm^2

f_{Ftu} ultimate residual tensile stress in N/mm^2

f_{pc} axial residual tensile stress in N/mm^2

$\overline{f_{pc}}$ average axial residual stress in N/mm^2

f_{Ri}	residual flexural tensile strength in N/mm^2
f_t	concrete cracking stress in N/mm^2
γ_m	material factor
h	section height in mm
h_{sp}	test specimen height in mm
I	second moment of inertia
k	size factor
k	neutral axis depth ratio
k_∞	neutral axis ratio at theoretical infinite compressive strain
K_{Rd}	redistribution factor
L	span length
l_f	fibre length
l_{cs}	structural characteristic length
λ	normalised compressive strain
λ_s	size factor
m	normalized moment
M_L	applied moment at limit of proportionality
M_i	resistance moment at strength interval
M_∞	moment resistance at theoretical infinite compressive strain
μ	post-peak tensile stress ratio
μ_{crit}	minimum post-crack ratio for deflection hardening materials
P_{cr}	applied cracking load
ρ_1	reinforcement ratio
σ	stress in N/mm^2
σ_a	assumed stress

σ_{cr} flexural cracking stress in N/mm^2

σ_{cy} compressive yield stress in N/mm^2

σ_{fi} flexural residual stress in N/mm^2

σ_{p} flexural residual stress in N/mm^2

σ_{real} real stress in N/mm^2

t element thickness in mm

ϕ normalized curvature

$\overline{\phi}$ average shear cracking angle

ϕ_p post-peak reduction factor

V_c shear resistance of compressive zone

V_d shear resistance through dowel action

V_{fr} shear resistance of fibres in tension zone

V_u ultimate shear resistance

w crack width

W_u maximum allowable crack width

ω compressive yield stress ratio

x neutral axis depth

X_f flexural neutral axis

X_s shear neutral axis

χ curvature angle

Y neutral axis depth

Notations:

AR Aspect Ratio

APC Anti-progressive Collapse

CMOD Crack-mouth Opening Displacement

FRC	Fibre Reinforced Concrete
ITZ	Interfacial Transition Zone
LOP	Limit of Proportionality
LVDT	Linear Voltage Displacement Transducer
NA	Neutral Axis
SCC	Self-compacting Concrete
SCSFRC	Self-compacting Steel Fibre Reinforced Concrete
SFRC	Steel Fibre Reinforced Concrete
SLS	Serviceability Limit State
SP	Superplasticizer
ULS	Ultimate Limit State
UTT	Uni-axial Tensile Test

List of Tables and Figures

Tables

Figures

Chapter 1

Introduction

1.1 Overview of Fibre Reinforced Concrete:

The investigation of the properties of Fibre Reinforced Concrete (FRC) as a structural material has been a widely researched and debated topic over the last 30 years. To date there remain a number of theories as to the behaviour of the material of which all have a similar underlying concept (Soranakom & Mobashir, 2009; Chiaia et al., 2009; Walraven, 2009): the addition of fibres to concrete transforms the material from characteristically having purely compressive properties, in design terms, to that with a tensile capacity. Thus, much interest as to its application in industry has come to light in recent times.

Traditionally FRC application has been relatively limited to the construction of ground slabs that require higher levels of durability and in the prevention of plastic shrinkage of the concrete surface in extreme circumstances as with, for example, marine structures. In recent times the application of this material has become more widespread, especially throughout Europe, and has been used in the construction of tunnel linings (Chiaia et al., 2009), precast bridge deck panels and composite pedestrian bridges (Walraven, 2009), raft foundations and suspended floor slabs in various structures including shopping malls (Oslejs, 2008). These

more recent applications have started implementing the beneficial tensile properties generated through the addition of fibres, in particular steel fibres, to concrete to their full potential. Thus, a number of design methods and applications have been developed and proposed in which the use of conventional reinforcing may be reduced and, in some cases, even eliminated completely (RILEM Technical Committee, 2003; Chiaia et al., 2009; Soranakom & Mobashir, 2009). The use of such a material can thus reduce construction time significantly and produce tough, durable structures with longer life spans.

The tensile capacity of FRC is as a result of fibres bridging cracks that have formed through tensile stresses which may be generated as a result of several load applications (Bentur & Mindess, 2007). Fibres that bridge the cracks transfer the generated tensile stresses within the element to the concrete matrix surrounding the fibre through frictional shear stress, chemical adhesion or mechanical anchorage induced by fibre deformities. The ultimate tensile strength of FRC composites is thus predominantly controlled by the mode of failure of the fibres themselves. As a result, much research has been conducted in order to define methods and standards in which the tensile properties of FRC can be accurately determined. The behaviour of steel FRC (SFRC) as a material is viewed as variable due to its inherent random fibre distribution characteristic (Walraven, 2009) and as a result of this variability a number of differing test procedures have developed for the determination of SFRC material properties. The generally accepted test procedure is the 3-point bending test recommended by the RILEM committee (RILEM Technical Committee, 2003) but it is the opinion of some that this procedure does not adequately illustrate the behaviour of SFRC. It is thus an important task to determine a suitable and accepted test procedure, in combination with a conversion to design rules taking into account the effects of this material variability (Walraven, 2009).

The application of SFRC in structural systems is relatively new, however, a number of structural design methods using the post-crack material properties of SFRC do exist. These models are generally theoretical, such as that proposed by (Soranakom et al., 2008), in which they suggest the defining of the non-linear behaviour of SFRC through parameters which enable the introduction of tensile residual properties into the design methodology. These

suggested methods differ from conventional concrete design where the concrete tensile capacity is ignored and a linear material behaviour is adopted. This deviation from the conventional concrete design approach has led to reluctance in the implementation of SFRC in industry from a design point of view.

Further to this is the practical use of SFRC as a construction material. A defining factor of the materials tensile strength is the volume of steel fibres added to the concrete mix, as an insufficient volume percentage will yield no significant improvements to the concretes tensile capacity. An increased fibre volume percentage, however, results in a decrease of concrete fresh state workability and increases the difficulty in obtaining a uniform distribution of fibres, which is required to achieve the optimum benefits of the material (Grunewald & Walraven, 2001). Thus construction using SFRC has to be performed by specialists of which a specific construction technique is implemented. Should these methods be adequately implemented in which material variability is reduced it may be possible to consider SFRC as an alternative to conventional concrete structures.

This alternative, if proven to be technically viable, will inevitably have economic implications. SFRC can generally be considered an expensive material but when considered in a broader context may prove to be economically beneficial. Under the correct circumstances with adequately determined, reliable material properties it may even be possible to eliminate the requirement of conventional reinforcing when using SFRC, which in turn will reduce labour requirements as fixing of steel is no longer necessary and thus significantly reduce the construction time required. Other influences such as transport and storage of materials to and on site as well as issues regarding on-site quality control may become mitigated through the implementation of this somewhat automated material. Although there is limited literature regarding the economic implications of the use of SFRC the general consensus is that the material, if implemented correctly, can be an economically viable alternative.

1.2 Outline of the Study

Application of SFRC in industry is becoming more widespread throughout Europe (Oslejs, 2008; Destree, 2009). Use of the material has been viewed as an advancement in concrete technology in producing tougher, more economical structures with a longer life span. Although the use of this material is seen as largely beneficial there is still reluctance over its application and use in industry. The aim of this investigation is to determine the feasibility of its use in the design and construction of in-situ cast flat slabs in South Africa. This work is thus targeted at addressing the issues that concern the implementation of SFRC on a structural level which includes both a theoretical and practical understanding of the material behaviour.

In order to sufficiently predict the behaviour of SFRC systems it is necessary to adopt suitable methods in which the material design parameters are determined. A widely accepted procedure in determining SFRC flexural tensile properties is the three-point bending test recommended by RILEM TC 162-TDF (RILEM Technical Committee, 2002). The test method evaluates the tensile properties in terms of areas under the load-deflection curve or by the load bearing capacity at a certain deflection or crack mouth opening displacement (CMOD) obtained by testing a simply supported notched beam under three-point loading. The introduction of a notch in the beam creates a localized crack of which the width can be measured during the test procedure. This methodology allows for measurement of crack propagation but may eliminate the beneficiary property of SFRC that is the distribution of tensile stresses through multiple crack formation. As the crack is locally formed only the properties of the localized area are measured and the effects of fibre orientation and distribution will inevitably lead to variable results. The author thus undertook a theoretical evaluation of the alternative test procedures that may be more suitable in determining SFRC material properties for use in flat slab design. Both the positive and negative aspects of each method are highlighted but unfortunately not experimentally verified due to restraints in resources and time.

In conjunction with adequately determining SFRC material properties the design models implemented need to accurately represent the actual material behaviour and performance under the specified load conditions. A number of design models have been developed for SFRC structures where, in some cases, these models have been used in the design of real structures constructed within Europe (Destree & Mandl, 2008). The author investigates the methods and practices used in the construction of these projects as background to developing a thesis outline targeted at specific aspects of SFRC flat slab construction. It was found that in some of these real cases, where a large dependence has been placed on the applied load and support conditions implemented in order to meet the serviceability requirements, the requirement for conventional reinforcing has been significantly reduced or completely eliminated. This work thus focuses on implementing such systems and discusses the methods implemented in a practical context for both flexural and punching shear analysis in flat slab systems. These design models and their assumptions were then verified through large scale testing.

As limited studies have been conducted to determine if small-scale test specimen behaviour can adequately represent the true response of full scale structural slabs (Roesler et al., 2004) a significant part of this work conducted was targeted at evaluating the transition between the two. Theoretically, in flexural structures a significant redistribution of internal forces is expected in larger test specimens through multiple micro-cracking with an increased moment capacity as a result of deflection hardening. Furthermore, it is expected that a ductile, non-catastrophic mode of failure will occur in the ultimate limit state. It is also believed that steel fibres in combination with conventional reinforcement can contribute to the shear capacity of flat slab systems, thus increasing the viability of the implementation of such systems. A large-scale SFRC flat slab test specimen was constructed based on the evaluated design models upon which loads in the SLS and ULS load states are imposed on the test slab. In conjunction with yield line theory the flexural response was monitored, where crack formations and propagation were of key interest leading up to the ultimate failure mode of the slab. Three identical large scale punching shear specimens were also constructed and tested so as to evaluate prediction models and the failure mode associated with ULS loading. It must

be noted that the practical concerns regarding the use of such materials in industry has been investigated and discussed through the construction of these large scale test specimens. Recommendations regarding the material workability and distribution of fibres is made through adequate mix design and casting techniques.

Chapter 2

Mechanical Behaviour of SFRC:

The mechanical behaviour of SFRC under applied stresses is dependent on complex interactions between the concrete matrix and the embedded fibres. Under tensile loading the material performance is characterised by its residual tensile strength, i.e. the tensile stress resistance provided by the fibres after the concrete has cracked, which is dependent on several factors of which include the fibre material type, length and diameter of the fibre, concrete strength and the matrix density, the fibre volume fraction and their distribution throughout the matrix. As the fibres are considered as a smeared reinforcement, i.e. the residual tensile resistance is isotropic throughout the concrete volume, the design mechanics of the SFRC system differ to that of conventionally reinforced concrete. The full benefits of a SFRC mixture can only be utilized under certain conditions and aspects of which include factors such as the load application type, element size, and the support locations which may have a significant influence on the material performance. It is thus important to have an understanding of both the micro and macro behaviours and interactions of SFRC before one can predict the final composite behaviour.

2.1 Fibre-cement Interactions on a Micro Scale

There are a number of fibre types available which can differ in the material from which they are made to the geometry of the fibres themselves. The different fibre types have suitability for certain applications and it is necessary to use these materials appropriately. The benefits of fibres are generally utilised in the post cracking stage of the concrete, where the fibres are activated through crack bridging. For the composite material to have a sufficiently sustained residual strength it is necessary for the fibres to have a pull-out mode of failure as opposed to rupture of the fibres which will result in a brittle composite failure (Dupont, 2003). Due to the associated tensile stresses steel fibres are generally regarded as the most suitable for structural applications (as explained in Section 6.1). Within this category of fibres there exist a number of varying geometries and a higher aspect ratio, the length of the fibre divided by its diameter, yields a larger surface area in contact with the concrete matrix which provides a greater resistance to the applied stresses (Dupont, 2003).

The behaviour of the fibre during debonding and the following desired pull-out mode is largely dependent on the interfacial transition zone (ITZ) surrounding the fibre (Lofgren, 2005). The ITZ is the region at the interface between the fibre and the surrounding concrete matrix (see Figure 2.1) and its composition differs from that of the rest of the concrete matrix due to the presence of the fibre (Dupont, 2003). Due to wall effects caused by the presence of the fibre the surrounding ITZ is generally made of a cement paste layer of varying thickness, in which there may be a number of voids present due to bleed water becoming trapped in this region during the concrete setting process or inefficient packing of the cement grains surrounding the fibre (Lofgren, 2005; Dupont, 2003; Bentur & Mindess, 2007). An increased concrete strength or matrix packing density, achieved through improved mixing techniques and the use of cement fillers, will improve the strength of this region and thus increase the load required to initiate and maintain fibre pull-out (Lofgren, 2005; Bentur & Mindess, 2007). The size of the ITZ can also be decreased through the use of fibres with a smaller diameter in which the presence of voids is less likely (Bentur & Mindess, 2007).

However, although an increased ITZ strength may improve the composite performance through improved adhesion and friction between the surrounding matrix and the fibre the greatest benefits are achieved through mechanical anchorage of the fibre (Bentur & Mindess, 2007). In steel fibres this can be achieved through the modification of the fibre shape, through the introduction of hooked ends or using crimped wires for example (see Section 6.1), in which the efficiency of the fibre mechanism is improved (Brandt, 2008).

a) 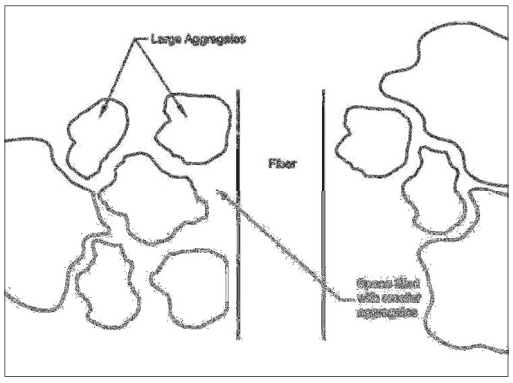

b) 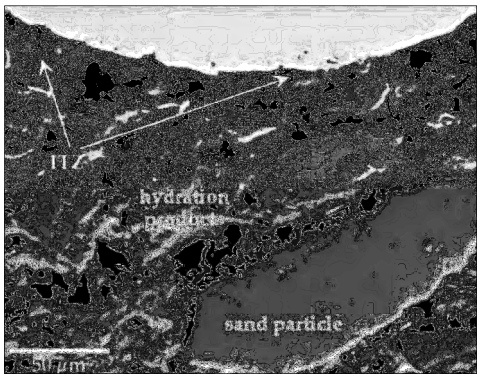

Figure 2.1 a) Schematic of particle packing around fibre (Dupont, 2003)and b) image of ITZ (Lofgren, 2005)

The above mentioned mechanisms refer to the pull-out resistance of the individual fibre itself but the behaviour of the composite is largely governed by the volume of fibres within the matrix and the interaction between the fibres. It is clear that an increase in the volume of fibres will increase the tensile residual strength of the composite, as the potential for a greater number of fibres bridging developed cracks is higher, but complications do arise for fibre volumes above a certain limit. Apart from difficulties encountered due to fibre 'balling' and workability restrictions for increased fibre volumes (see Chapter 6) the increase in residual tensile strength is linear with increasing fibre volumes up to a certain fibre volume range, after which the improvement in strength through the addition of fibres is not as significant (Dupont, 2003; Khaloo & Afshari, 2005). This is caused by an insufficient concrete matrix volume surrounding individual fibres, which results in reduced bond strength, and multiple fibre pull-out occurs as opposed to individual fibres resisting the applied force. However, this

behaviour occurs only at extremely high fibre volume fractions which may be considered impractical due to construction restrictions.

For fibre volumes above a specific minimum volume percentage for that fibre type, known as the critical fibre volume fraction (Fantilli et al., 2009), the cracking regime changes from a single crack formation pattern under tensile loading to that of multiple cracking which results in either strain or deflection hardening (see Section 2.2). This behaviour is desirable in structural applications as multiple cracking results in a larger number of fibres being activated through crack bridging which thus increases the resistance to the applied force and improves ductility.

In addition to the number of fibres bridging the cracks formed in the concrete the fibre orientation can also influence the composite material behaviour (Bentur & Mindess, 2007). As a result of boundary conditions, casting procedures and material fresh state properties (Lofgren, 2005) the orientation of the fibres can range from a generally 2-D orientation to a 3-D orientation (see Figure 2.2). Thus, depending on the orientation of the fibres, the angle at which the fibre bridges cracks formed may vary from 0° to 90°. Generally, a more 2-D fibre alignment is desirable as the potential of fibres to bridge cracks formed is higher when their orientation is 90° to the propagating crack, in which case a larger number of fibres would become activated.

The orientation will also influence the mechanism in which the individual fibre resists the applied pull-out force. For a fibre orientated at 90° to the crack the resistance is provided through mechanical restraint provided, for example, by hooked ends and the frictional resistance caused by shearing between the fibre and surrounding matrix. Should the fibre have a different orientation to this an additional resistance is provided by 'snubbing' effects (Dupont, 2003; Bentur & Mindess, 2007). Instead of a pure pull-out mode the fibre is bent over the crack and the additional resistance is provided through increased friction, much like a rope passing over a pulley. This mechanism may result in a brittle composite failure for weak fibres (as the fibre snaps under increased stress localization) or, in the case of a weak,

porous concrete matrix, the concrete in this zone crushes and spalls under the stress concentration (Bentur & Mindess, 2007). However, for a strong fibre and concrete matrix the stress resistance may be increased from that of standard frictional resistance. The changes in the fibre pull-out mechanism resulting from randomly orientated fibres within the composite matrix is in a large part the reason as to why FRC is characterized by material variability and casting procedures can thus largely have an important role to play in improving the material repeatability (Walraven, 2009).

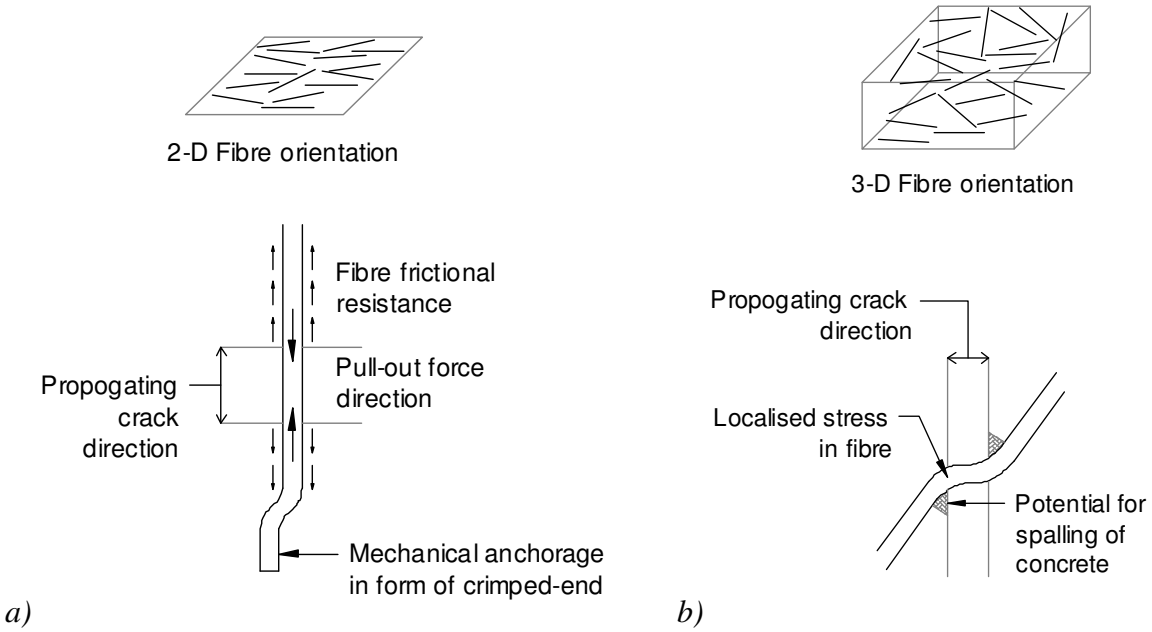

Figure 2.2 a) 2-D and b) 3-D fibre orientation with more likely associated fibre resistance mode

In addition to the fibre orientation it is clear that the fibre distribution throughout the matrix volume will make a significant contribution to the material performance. For regions within the structure volume where there may be a reduced number of fibres the residual stress potential in this region may be reduced or even eliminated, which may result in a brittle failure once the concrete has cracked. It is thus critical to ensure that an even fibre distribution is achieved through adequate mix design (see Chapter 6) and construction

techniques (see Chapter 7) to ensure that the assumptions made during the design process are met.

The contribution of the fibres in structural applications is also largely dependent on the significance of the size effect, which is as a result of the shift in the neutral axis under increased load conditions (see Section 2.2). As fibre lengths are generally 60mm or less in length the residual stress range is geometrically limited (see Figure 2.3). In thin elements imposed to bending forces the associated curvature may result in a stress on the element outer tensile face that is compatible with the residual stress resistance provided through fibre crack bridging in this region. As the crack propagates upwards into the element more fibres are activated whilst the fibres at the outer face still provide a pull-out resisted residual stress, thus the overall resistance of the section is increased. In deeper structural elements the same imposed curvature will result in much higher strain levels on the outer tensile face. Thus, as the crack propagates upwards into the element the activation of fibres near the crack tip is associated with a loss of residual pull-out resistance provided by fibres at the base of the crack near the outer tensile surface. In such a case, the resistance provided by the fibres is limited to a specific regional depth and as this region moves upwards the element sectional stiffness is reduced and the resistance mechanism will most likely be insignificant to the applied load, resulting in failure. Thus, the use of fibres in structural applications has been generally limited to thin structural elements unless used in combination with conventional reinforcing.

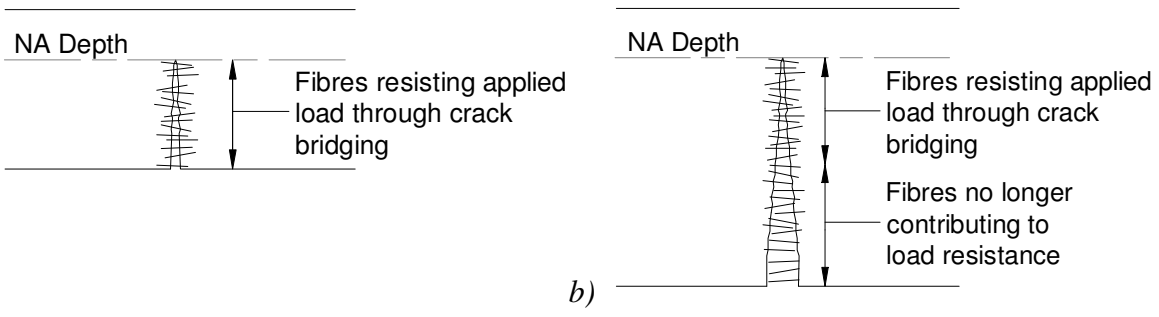

Figure 2.3 Illustration of the influence of size effect in a) thin elements and b) deep elements under imposed bending loads

2.2 Fibre-cement Interaction on a Macro Scale

SFRC is a ductile material when compared to the brittle nature of conventional concrete. The addition of fibres above a certain volume percentage gives the material a post-crack tensile residual strength, which can be attributed to fibres bridging cracks formed on the tensile face. This tensile residual strength is characterised by a non-linear behaviour, where the performance of the material during this stage is dependent on several factors. These factors include the fibre mechanical characteristics as well as the fibre shape and size, the volume of fibres within the matrix and the fibre orientation as well as external conditions such as the concrete curing procedure, load application rates and ambient temperatures to which the material is exposed (Chanvillard et al., 1990).

The behaviour of SFRC under increasing load conditions can be characterised by three distinct phases (see Figure 2.4):

- The linear elastic phase in which the material performance is similar to that of conventional concrete before the formation of cracks on the tensile surface
- A non-linear phase in which cracks form on the tension surface thus activating fibres through crack bridging, providing a resistance to crack propagation
- And finally the phase in which ultimate failure occurs due to rupture of the fibres, associated with a rather brittle failure mode, or more preferably pull-out of the fibres resulting in a ductile failure mode.

In general, for normal fibre volume fractions employed, the addition of fibres does not significantly modify either the initial elastic behaviour of concrete or its modulus of rupture before the initiation of the first crack (Chanvillard et al., 1990; Lofgren, 2005). Some research has indicated that the concrete tensile splitting strength does increase with an increasing fibre volume fraction (Bayramov et al., 2004) but this can be considered negligible

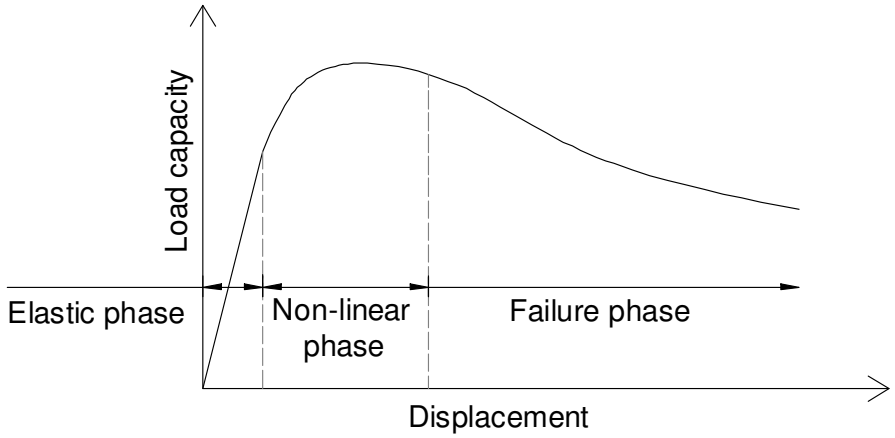

Figure 2.4 Three macro phases of SFRC with a ductile failure mode

as for fibre volume fractions limited to 1% the structural performance of SFRC is generally characterised by it post-cracking behaviour (Dupont, 2003). Thus, the composite behaviour in the initial elastic phase can be considered similar to that of conventional concrete.

Once cracking has occurred at the SFRC surface the fibres in this region become activated through bridging of the cracks. The material behaviour in this stage is dependent on a number of micro-scale factors (as described in Section 2.1) and is characterised by a non-linear response. The material response under pure tensile conditions can be directly recorded through testing such as the uni-axial test (Lofgren, 2005) (see Chapter 3) but it is the behaviour of the composite under flexural bending conditions that leads to complications. At the onset of cracking on the material surface the tensile capacity of the composite changes, to the resistance now provided by the fibres bridging the crack, and the depth of the neutral axis changes accordingly to maintain a balance of the tensile and compressive forces that exist in the flexural element (see Figure2.5). Under increased loading additional cracks may form along the surface and increase in their depth thus activating additional fibres and once again altering the depth of the neutral axis. The prediction of the material behaviour under imposed loading has thus led to a number of models which have been proposed for the design of such elements (see Chapter 5). These models all incorporate a stress-strain relationship which is converted to a stress-crack relation or vice versa (Dupont, 2003) and make a number of

assumptions in an attempt to simplify the complex behaviour of the composite imposed to bending forces.

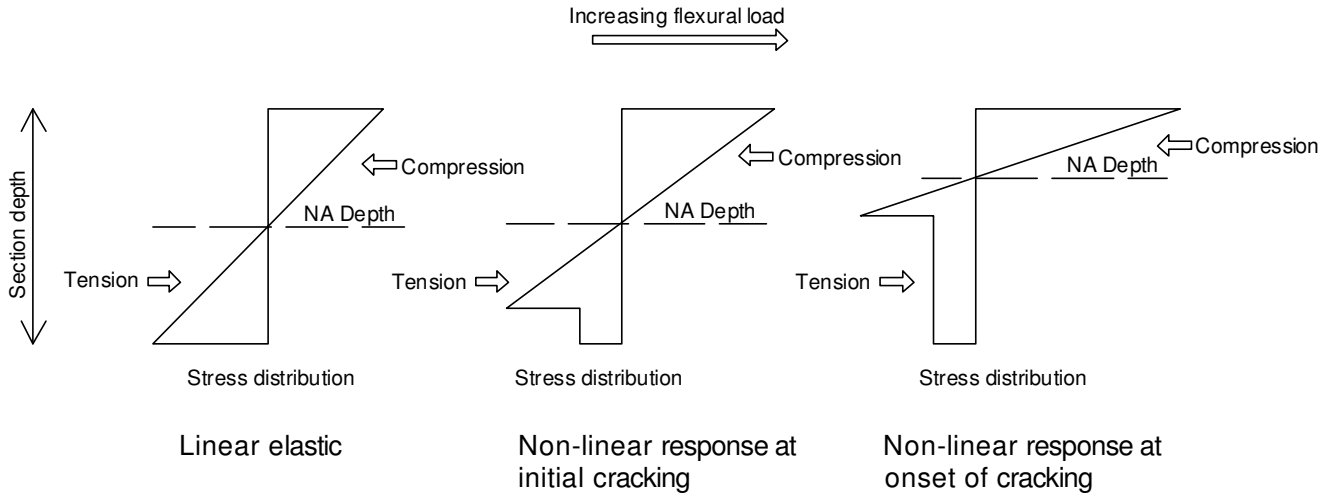

Figure 2.5 Representation of the shift in the neutral axis depth according to simplified residual stress distribution through section height

As the flexural load increases so does the depth and number of the cracks formed which in turn activates more fibres to resist the imposed load. Once the material has reached its maximum load capacity failure of the material begins to take place which can be either of two responses: a brittle failure in which the fibres rupture as a result of stress concentrations, or pull-out of the fibres from the concrete matrix. Rupture of the fibres is generally associated with weaker fibres such as those manufactured from synthetics where the modulus of elasticity can be considered rather low but this mode of failure can also occur in steel fibres used with ultra-high strength concretes. When the matrix-fibre bond strength is greater than the strength of the fibre itself an increasing load results in fibre stresses that cause the fibre to partially elongate and eventually rupture (Bentur & Mindess, 2007), resulting in a rather 'brittle' composite failure. However, generally when using steel fibres failure due to rupture of the fibres is unlikely and one can expect a pull-out mode of failure. Fibre pull-out occurs as the bond strength between the fibres and surrounding concrete matrix is exceeded, thus breaking the bond, and resistance to crack propagation and the imposed loads is provided by

frictional forces between the fibres and surrounding concrete matrix. This behaviour gives the composite a ductile response (Fantilli et al., 2009) as the decrease in resisting stresses from bond strength to frictional resistance in some cases may not be that significant. When using longer fibres there is the possibility to extend the ductility of the composite as the range of the residual tensile strength is extended (Brandt, 2008), giving SFRC a much higher energy absorption capacity than conventionally reinforced concrete.

2.2.1 Non-linear Tensile Strength Composite Behaviour

SFRC composites are characterised by their behaviour in the post-crack non-linear tensile phase. Depending on the fibre characteristics and their volume percentage within the mix, SFRC composites can either undergo strain hardening or strain softening during this post-cracking stage. Strain hardening is a property in which the tensile strength of SFRC increases at the onset of cracking whereas strain softening is when the tensile strength after cracking reduces to a residual tensile strength (see Figure 2.6). Generally, for a certain fibre type there is a volume fraction that exists for a specific mix in which the transition between these two responses is defined known as the critical fibre volume fraction (Fantilli et al., 2009).

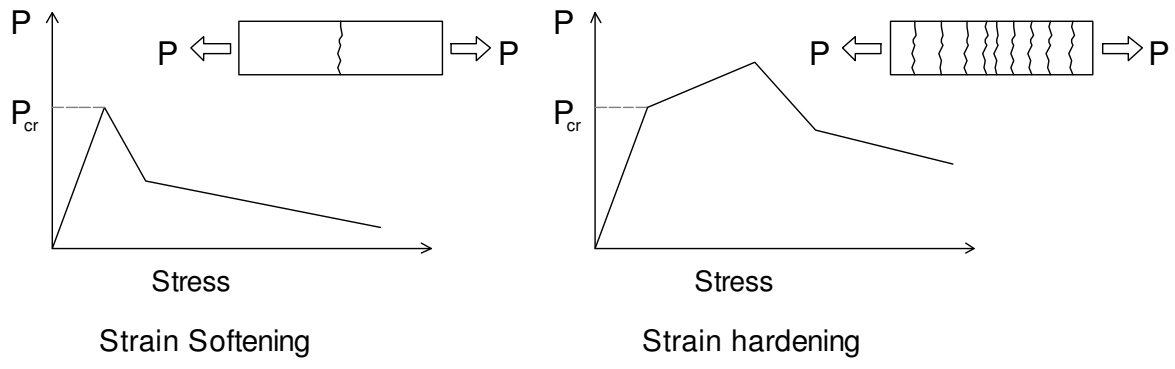

Figure 2.6 Strain hardening vs. strain softening with associated crack pattern under an axially applied load (fib Special Activity Group 5, 2010)

Strain hardening is generally associated with high fibre volume fractions and can be characterised by multiple cracking before reaching the peak value under applied axial loads, whereas strain softening is associated with a decrease in the tensile resistance to an applied axial load once the composite has cracked and is characterised by a single crack formation in a localised area (fib Special Activity Group 5, 2010). When induced to flexural load conditions strain softening materials will undergo either deflection softening or deflection hardening.

Deflection softening is when the material fails with no increase in load capacity once cracking has taken place, whereas deflection hardening occurs when an increased flexural capacity is observed at large deflection levels due to contributions from the stiffness provided by fibres in the cracked zones of the tensile regions (Soranakom & Mobashir, 2007). For deflection hardening to occur it is required that the strain softening material has a sufficiently high residual tensile strength with a relatively large range and for adequate support conditions to exist which will enable the redistribution of tensile stresses during increasing deflection levels. This response occurs when a load applied to a deflection hardening flexural member initiates cracking at the material tension surface in a localised area resulting in a decreased tensile resistance for this cracked region. The fibres bridging the cracks provide a residual tensile strength that gives the material a ductile response, resulting in an increasing deflection of the member under the applied load with a constant residual force resistance provided at the crack locations. As the member deflects, additional cracks form on the tension face and activate fibres at the new crack locations (see Figure 2.7). This multiple cracking regime can be considered as the redistribution of tensile stresses and, should the support conditions be adequate, will lead to an increased load capacity for the flexural member.

For such an element response to occur the residual tensile strength has to be a minimum of 35% of the initial cracking stress (Soranakom, 2009) with an indeterminate support system sufficient enough to enable the onset of two way action and multiple cracking (Destree & Mandl, 2008). The potential for stress redistribution in strain softening materials has been recognised in the *fib* Model Code 2010 (fib Special Activity Group 5, 2010), in which a

factor has been incorporated for experimentally verified redistributive support conditions. It also specifies that for simply supported conditions SFRC with no conventional reinforcement may only be implemented if the material is characterised by a strain hardening behaviour.

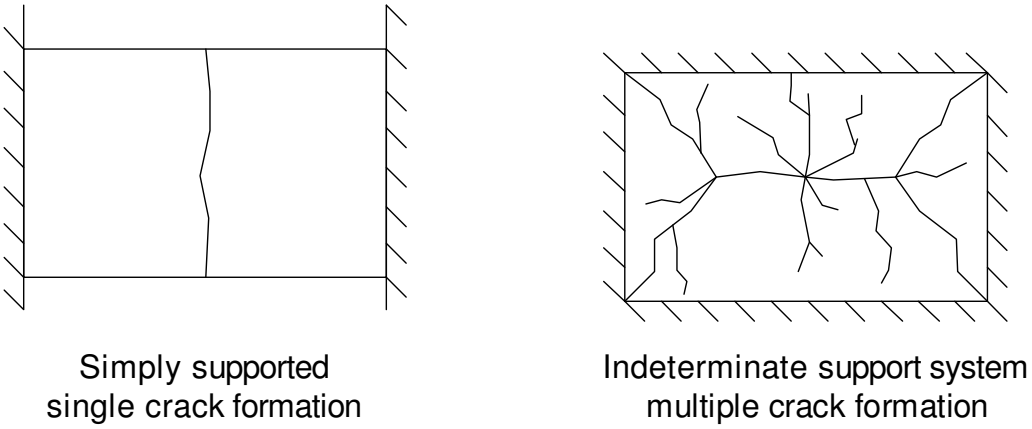

Figure 2.7 Example of the influence of the support system on the SFRC cracking regime and thus the deflection hardening potential

As a result of the many contributing influence parameters associated with both the micro and macro scale properties the design of SFRC structures can be viewed as rather complex. To simplify the structural analysis of such a composite material a number of assumptions have to be made in which the material behaviour as well as the support and load conditions are considered. This approach leads away from the conventional practice in which standard concrete solutions are implemented to systems that are tailor made with regards to the concrete mix constituents and structural layout in meeting the design requirements.

Chapter 3

Determining Material Properties: Evaluation of Test Methods

3.1 Requirements of SFRC Characteristic Testing

The classification of SFRC properties can be done on both a micro and macro scale depending on the purpose of the parameters to be determined. Properties of SFRC on a micro scale refer to the direct interaction of the steel fibre with the surrounding concrete matrix and how its behaviour can influence mechanisms regarding fibre bond strength, stress transfer and eventual fibre rupture or pull-out modes. These parameters can be used in conjunction with coefficients for fibre orientation, snubbing effects, volume of fibres used, expected pull-out length ratio's, etc. to predict the behaviour of a SFRC composite material without performing any further tests. However, the tests involved for this type of analysis can be rather difficult and require specialized equipment in some cases, where the predicted material behaviour is purely theoretical with no validation of the actual final composite behaviour unless macro testing is performed.

Testing on a macro scale refers to the actual SFRC composite behaviour in which testing can relate to the intended use and the material performance can be evaluated under specified

conditions. These tests can be targeted at the influence of the fibres on concrete behaviour such as compressive strengths, stress-strain relations (in the pre-cracking stage) and cracking strengths. However, the influence of steel fibres on these mentioned properties is negligible (di Prisco et al., 2009; Bentur & Mindess, 2007; Rostasy & Hartwich, 1985) and the true benefits are realised in the SFRC post-cracking state. In the post-cracking stage the fibres become activated (see Section 2.2) and their influence under imposed tensile stresses on the composite behaviour is referred to as the residual tensile strength. The two main methods of applying tensile stresses for material characterization are in the form of a pure tension, as with the uni-axial tension test, or through flexural loading such as beam testing.

Due to the complex interaction between fibres and the concrete matrix the determined residual strength material properties can vary according to the test procedure. Results obtained through uni-axial tension testing will differ from those obtained through flexural testing, where in some models factors have been assumed to convert properties between the two based on the test procedure (RILEM Technical Committee, 2003). Even within flexural testing different test procedures will yield different results, such as between beam testing and round panel testing (Destree & Mandl, 2008), as the nature and behaviour of a SFRC material is also dependent on the support conditions. Various authors have also noted that the test specimen size (di Prisco et al., 2009; Giaccio et al., 2008) and the mixing procedure (Walraven & Grunewald, 2001; di Prisco et al., 2009) can influence the material behaviour and thus the properties obtained.

It is clear that the behaviour of SFRC is dependent on complex interactions between a number of variable factors. To develop robust design procedures for particular applications using the mechanical properties of a SFRC mix design it is necessary to evaluate and standardise test procedures upon which these design model parameters can be based. Generally, it has been accepted that fracture mechanics is used when determining these desired properties and Lofgren (2005) has summarised the requirements of test procedures in determining these properties as follows (Lofgren, 2005):

- The test procedure must provide results which readily can be interpreted as constitutive material parameters (the stress-crack width relationship);
- it should, preferably, provide a relationship between load and crack mouth opening displacement (or CMOD) which can be used for inverse analysis;
- the specimen should be designed such that a single, well-defined crack is formed, which generally means that the specimen has to be equipped with a notch of sufficient dimensions;
- it should give representative values;
- it should, if possible, not require too advanced testing equipment or demand a high machine stiffness;
- it should be easy to handle and execute; and
- the specimen size should be as small as possible but still be representative.

Based on the above requirements and recommended test procedures found in various literatures, the author has chosen to evaluate the uni-axial tension test, three and four point beam testing, and the ASTM round panel test in the form of a literature survey. The wedge splitting test was also considered but as it has been described as difficult to determine a constitutive relationship due to the uncertainty regarding stress distributions (Dupont, 2003) the author chose to omit this test procedure from the survey.

3.2 Test Descriptions and Procedures

In determining the properties of a SFRC for structural applications it is important to evaluate how the properties were determined and the limitations associated according to the test procedure used. The test procedure needs to be closely related to the final application so as to give representable and robust material properties upon which design models can be based. As the residual tensile strength is the critical parameter when using SFRC for structural applications test procedures are focused on imposing tensile forces resulting in crack formation on specimens through direct tension, giving an indication of the fibre pull-out

behaviour and resisting forces, or in flexure in which the behaviour and properties of the composite are revealed under a common type of load application.

3.2.1 Uni-Axial Tension Test (UTT)

The uni-axial tension test (UTT) is a material test in which a direct tensile load is imposed on a SFRC specimen in which the stress-crack opening relationship is determined. The test method has been standardised, generally, according to recommendations from RILEM TC 162-TDF Uni-Axial Tensile Test (2003 Part 1) in which an investigation was conducted in determining the robustness of the test method (RILEM Technical Committee, 2003 Part 1). Test specimens are cylindrical in shape with a diameter and height of 150mm which can be made from larger samples cut down so as to eliminate surface imperfections. In order to ensure localised crack formation a 15mm circumferential notch is sawn into the specimen at mid height. At the notch location three linear voltage displacement transducer's (LVDT's) are placed at 120° from each other from which a closed loop system records the average of the three readings as the feedback signal (see Figure 3.1). The stress is then simply calculated by dividing the applied tensile load over the effective area at the notched section and can be compared to the deformation response and crack opening respectively. For further information regarding the test procedure refer to RILEM TC 162-TDF Uni-Axial Tensile Test (2003 Part 1).

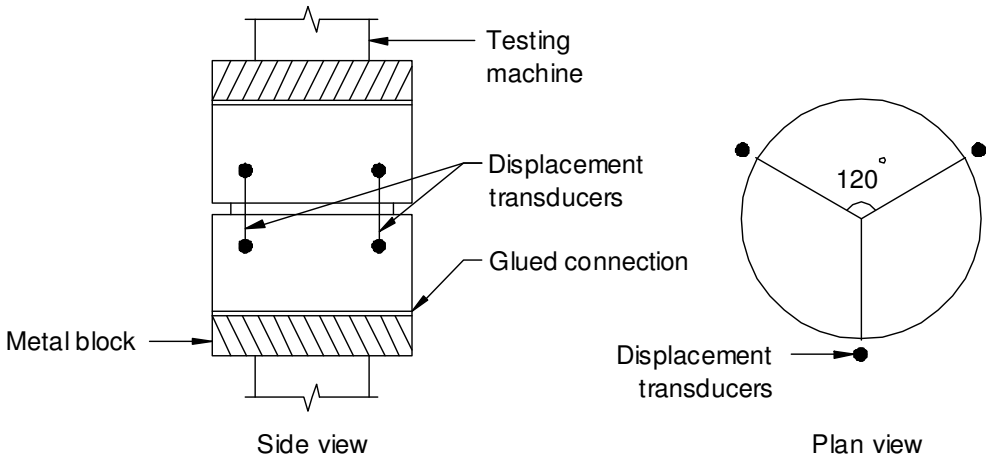

Figure 3.1 Uni-axial tensile test setup (RILEM Technical Committee, 2003 Part 1)

3.2.2 RILEM Three-point Bending Test

The three-point bending test is a standardised beam test proposed in RILEM TC 162-TDF (2002) in which the tensile behaviour of SFRC is obtained by testing a simply supported notched beam under three-point loading (see Figure 3.2). A relationship can be established according to the applied load capacity and displacement or crack mouth opening displacement (CMOD), from which the residual tensile strength is determined at certain crack width intervals.

The standard test specimen is a beam of 150 x 150mm in cross section with a minimum length of 550mm, of which the span length is 450mm in the final test position. A 25mm deep notch is sawn through the width of the beam at mid-section, 90° to the casting surface. LVDT's are placed at the notch location to measure the deflection and the increase of crack width during load application to an accuracy of 0.01mm using an electronic closed looped recording machine. The test procedure is deflection controlled during load application, and material properties are determined according to the relative load capacity at a specified crack width interval. The determination of the residual tensile stresses is based on the theory of an equivalent residual tensile strength from which assumptions are made according to the crack width state (see Section 5.2). For further information regarding the test procedure refer to RILEM TC 162-TDF (2002).

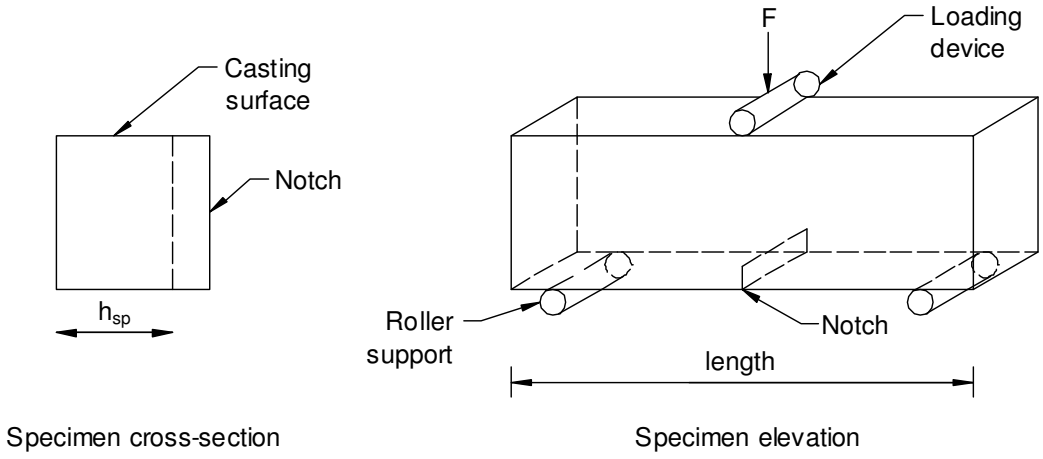

Figure 3.2 Three-point Bending specimen as per RILEM TC 162-TDF (2002)

3.2.3 Four-point Bending Test

The four-point bending test is a method used in several international standards such as the NBN B15-238 1992, JCI-SF4, ASTM C78-94, ASTM 1018-97 and DBV 1992 (Dupont, 2003). The test sample is simply supported and loaded by two point loads at a third span distance from each end (see Figure 3.3). The sample dimensions are similar to that of the RILEM three-point test beam; however, a notch is not located at mid-span. A region of constant moment is applied between the two point loads and the specimen is able to crack at areas of weakness within this zone as there is no induced crack location. Deflections are recorded at mid-span using LVDT's and the loading rate and intervals at which material parameters are determined are dependent on the standard used. Due to the nature of the test setup, when using SFRC only without conventional reinforcing the formation of an unstable crack is common and a number of test specimens have to be discarded (Dupont, 2003). This phenomenon does not exist in the three-point bending test and the four-point bending test can be considered a less economical deterministic procedure. Thus the four point bending test procedure will be discussed no further in this thesis.

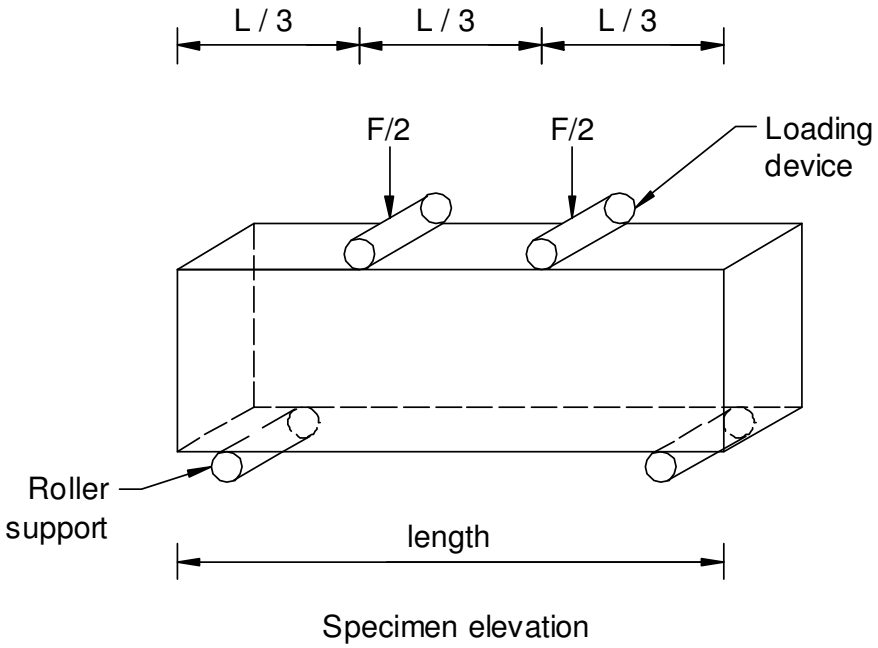

Figure 3.3 Four-point Bending test setup schematic (Dupont, 2003)

3.2.4 Round Panel Test

The round panel test is a flexural test to assess the post crack performance of fibre reinforced concrete that had been standardised by the ASTM Committee as ASTM C 1550-02 (Bernard, 2003). The test involves the application of a point load to the centre of a round panel on a statically indeterminate support system (see Figure 3.4) from which the residual tensile properties are derived using Johanssen's yield line theory (Destree & Mandl, 2008). The test sample is a round panel of 800mm diameter and 75mm thickness (Bernard, 2003) but depending on the application may be adjusted in size to give more comparable results to the actual final application, as is the case with Destree & Mandl (2008) in which circular specimens of 1.5m net span diameter and 150mm in thickness were used to determine material properties for the design of suspended slabs. The support system may be in the form of three symetrically arranged pivots or a continuos simple support along the perimeter. Depending on the method in which the properties are determined the test specimen may be loaded up to failure or a deflection of 40mm. The stress-strain relations are then determined through inverse analysis. For more information regarding the test procedure refer to Bernard (2003), Destree & Mandl (2008) or Walraven (2009).

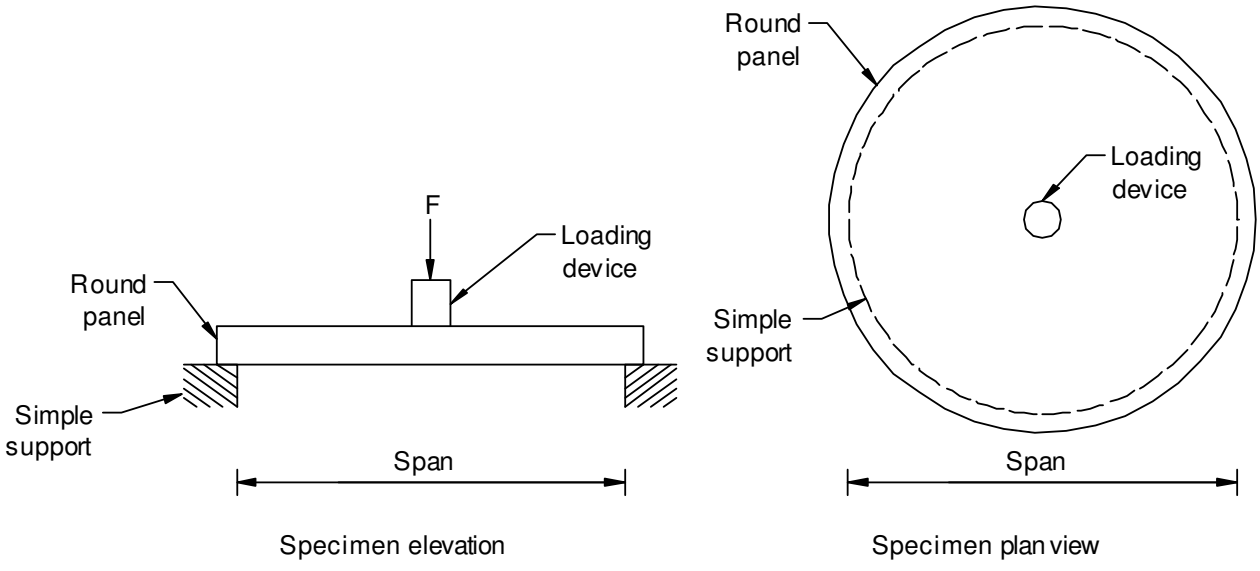

Figure 3.4 Round Panel test setup schematic (Destree & Mandl, 2008)

3.3 Test Procedure Evaluation

Residual tensile material properties used in the design of SFRC structures have to be determined using standardized laboratory procedures as described above. The design values are based on characteristic values determined through statistical analysis and due to the intrinsic nature of SFRC the level of scatter of results can be high, reducing the characteristic value. Thus, a number of applicable test procedures are evaluated according to their repeatability of results regarding a particular SFRC mix design. In addition to this, the test procedure has to represent results that are closely related to the final application and this is influenced by both the form of the load application, i.e. pure tension or flexure, as well as the size of the test specimen as issues regarding size effects (see Section 2.1) and boundary conditions may have an influence. It is also necessary that the test procedure is practical in that the sample size is manageable and testing equipment and procedures are simplistic and economical.

3.3.1 Uni-Axial Tensile Test (UTT)

The UTT is performed by applying a direct tensile force on the test specimen in which an induced crack occurs at the notch location at the mid-height of the sample. Readings are recorded by three LVDT's in which one can compare the average sample deflection or crack width according to the tensile load applied. In principle the procedure sounds simplistic and representative of SFRC tensile behaviour although a number of investigations have revealed that there exists complexities associated with the procedure.

As the test setup and equipment is rather specialised a round robin investigation was conducted to determine the repeatability of the test procedure between different laboratories and the accuracy of results determined (RILEM Technical Committee, 2003 Part 1). It revealed that the repeatability of results was possible, although only when conducted by experienced personnel, but that there were additional concerns with regards to the validity of

the results with respect to the actual behaviour of SFRC under pure tensile load conditions. Due to the intrinsic nature of SFRC a large scatter of results occurred but this is further influenced by the fibre distribution and orientation differences between different samples (Walraven, 2009). It is evident that the effect of casting procedures have a significant influence on the results as fibres in some instances were found to segregate, with a non-representative volume at the notch location where failure occurred, and that through table vibration the orientation of fibres tended to be more horizontal than vertical thus reducing the crack bridging potential of the fibres (RILEM Technical Committee, 2003 Part 1). This was also reported by Lofgren (2005) whom found a number of UTT test samples with half the expected volume of fibres at the fracture surface which had resulted from the sample sensitivity to the casting and compaction procedure (Lofgren, 2005). However, it was found that generally the test results increased in toughness linearly with fibre dosage volumes as expected up to a specific fibre volume in which this relationship would plateau (RILEM Technical Committee, 2003 Part 2) which can be attributed to multiple fibre pull-out (Dupont, 2003).

The rotational stiffness of the experimental setup and accuracy of data loggers also plays a significant role in the sample behaviour and validity of the results acquired under the test procedure (RILEM Technical Committee, 2003 Part 1). Cracking initiates at the notch location as expected but the crack growth is not uniform as would be desired. Due to the setup and load conditions the sample begins to crack on one side, where the majority of the load resistance is then provided by the un-cracked section (Dupont, 2003). This results in an induced moment due to the eccentric tensile load application and a non-uniform tension gradient exists (see Figure 3.5) which complicates the determination of the resisting tensile stresses (Dupont, 2003; RILEM Technical Committee, 2003 Part 2; Walraven, 2009). This again was revealed by sample testing conducted by Lofgren (2005) in which sample deformation remained linear up till 70% of the peak load resistance upon which the sample behaviour began to deviate from this behaviour (Lofgren, 2005) which can be assumed as the on-set of initial cracking and rotation within the sample.

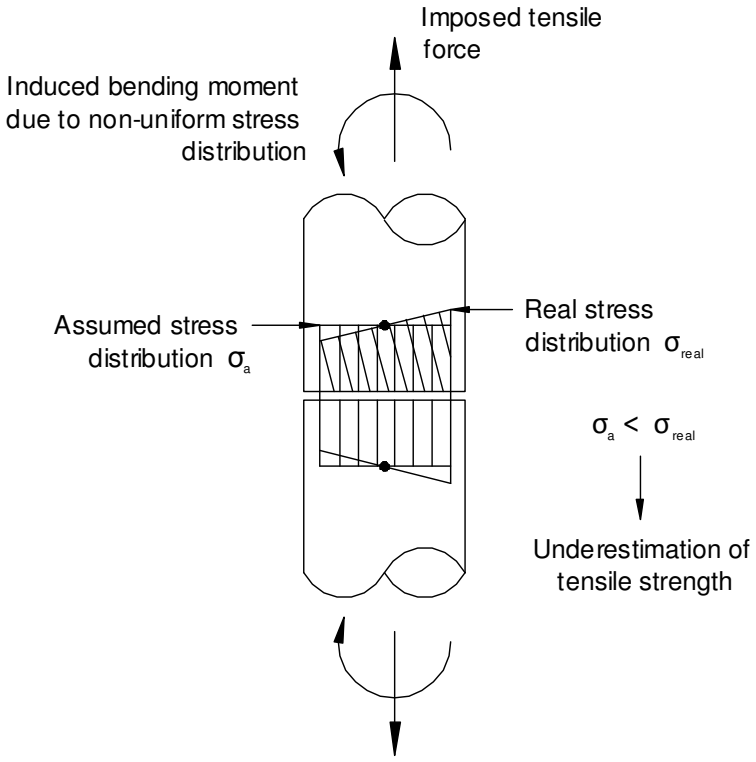

Figure 3.5 UTT non-uniform stress gradient (Dupont, 2003)

The test procedure can be modified to reduce this behaviour but involves fixing the test sample to the test device in which other effects begin to influence the sample behaviour or through using sophisticated recording equipment which compensates for these rotations, both of which complicate the test procedure and make it expensive (Dupont, 2003; Lofgren, 2005). The level of sophistication of the test procedure makes it unsuitable for industrial use (Walraven, 2009). The test procedure is also not entirely suitable for determining the tensile strength of SFRC in the pre-cracked stage or in the region just after cracking, of which results are generally required for serviceability design, but may however be used in determining the fibre resistance to pull-out and stress-crack width relations as the rotational effects decrease after initial cracking and tend to an approximately constant response with increased displacement (RILEM Technical Committee, 2003 Part 2) and can be directly measured as no inverse analysis is required (Lofgren, 2005).

3.3.2 RILEM Three-Point Bending Test

The three-point bending test is a much simpler test procedure than the UTT (Dupont, 2003). When including the initial time in preparing the test setup the test period is half that of the UTT (Dupont, 2003) and the simplistic setup itself makes the test a much easier one to perform (Walraven, 2009) making it more suitable for industrial applications. The procedure involves placing a simply supported beam under flexure and recording the load-deflection and/or load-CMOD relationship under a displacement controlled point load application at mid-span. A notch is located at mid-span to induce cracking at a specific location where an LVDT placed on either side of the specimen (so as to compensate for small rotations of the beam (Dupont, 2003)) can record the crack growth under the applied load. The use of a notch allows one to make this recording, as the crack location is fixed, but its use alters the behaviour of the beam substantially (Walraven, 2009) and thus raises concerns as to the validity of this procedure in determining the material properties of a SFRC mix.

Due to the nature of SFRC the fibre distribution is random and not always isotropic as assumed when using the material for structural design. Therefore, the inclusion of a notch at mid-span may not always correspond with the weakest zone in the beam section and may, in some cases, over-estimate the specimen residual strength (Dupont, 2003; Walraven, 2009). However, due to the large scatter of results within the test batch, which can be greater than 18% (Bernard, 2003), the characteristic value determined for the material property will significantly reduce and eliminate this over-estimation. As a result, the variability has led to over-conservative design (Walraven, 2009) and eroded confidence of using the material in structural applications (Bernard, 2003). The RILEM Committee has tried to reduce this variability by prescribing casting procedures (RILEM Technical Committee, 2002) but this may not be representative of real structures where the casting procedure is not as predefined (Walraven, 2009). Another consideration is the depth of the notch and how it may reduce the positive effects caused by boundary conditions. When casting, the fibres near the boundary will tend to align along a horizontal plane parallel to the casting surface thus increasing the crack bridging potential. This is true in both real structures and in small beam samples, but

the 25mm depth of the notch eliminates the benefits as the fibres towards the centre of the sample tend towards a more 3-D alignment and thus, again, results may not be fully representative (although this may depend on the design application). This is particular in thin structural elements, where the positive effects of boundary conditions may increase the expected moment resistance through a more suitable fibre alignment (Giaccio et al., 2008). This aspect illustrates that the test sample must be representative of the final application and that limitations may be introduced according to the test procedure.

As the test procedure is deflection controlled the crack formation is stable (Dupont, 2003) and thus the procedure is preferred over four-point bending when using SFRC only in determining the material properties. For low volume fibre contents the material properties can be determined through inverse analysis and a good agreement can be found for the stress-crack width relation (Lofgren, 2005). For higher fibre volumes the lowered rate of load application enables test samples to undergo deflection hardening (di Prisco et al., 2009) and may reveal the SFRC potential as a structural material under specific conditions. For a suitable SFRC during three-point bending an initial crack forms at the notch location and under increased deflection the on-set of additional cracking will occur as the stresses are redistributed within this area (see Figure 3.6). Although this material behaviour is a positive sign it distorts the stress crack-width relation. This relationship cannot be directly measured through the test procedure and the material properties have to be determined through inverse analysis, where the results obtained may not always agree with the actual crack width relation (Lofgren, 2005). This effect however may not have a significant influence for structural systems with suitable support conditions, as redistribution of stresses is possible, but it is important to note as the material properties determined may be an over-estimation under certain conditions such as punching shear design (see Section 5.3). It has been suggested, however, that the inclusion of a notch weakens the cross section at this location (Walraven, 2009) and results in stress concentrations. This stimulates localised deformation and the potential for deflection hardening is reduced (Walraven, 2009). This has been acknowledged in the *fib* Model Code (2010) where it has been suggested that one may apply a statistically determined factor to compensate for this reduction during testing when designing structural

applications where the redistribution of stresses, and thus deflection hardening, is possible (fib Special Activity Group 5, 2010).

a)  *b)* 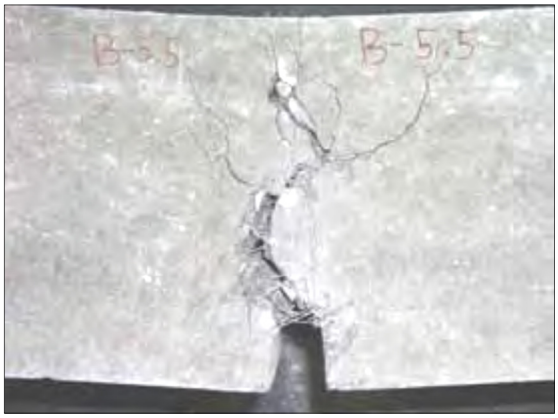

Figure 3.6 a) Single crack formation resulting in deflection softening and b) multiple cracking due to deflection hardening (Lofgren, 2005)

3.3.3 Round Panel Testing

The round panel test is a procedure that produces much lower in batch variability of results than the three-point bending test and has shown superior repeatability in determining test results than regular beam testing (Bernard, 2003). This can be attributed to the larger surface area and the formation of a number of yield lines at failure (Destree & Mandl, 2008; Walraven, 2009). The procedure involves placing a flexural load on a circular slab simply supported either continuously along its perimeter or on three pivots. Under an increased point load application the formation of multiple yield lines (see Figure 3.7a) takes place in the post-elastic phase from which one can determine the moment resistance from Johansson's yield line theory (Destree & Mandl, 2008) or using inverse analysis to determine the stress-strain relation (Walraven, 2009). The support conditions assist in reducing the scatter of results and utilize the full potential of SFRC to redistribute stresses, but as a result may over-estimate the structural properties due to these idealised support conditions.

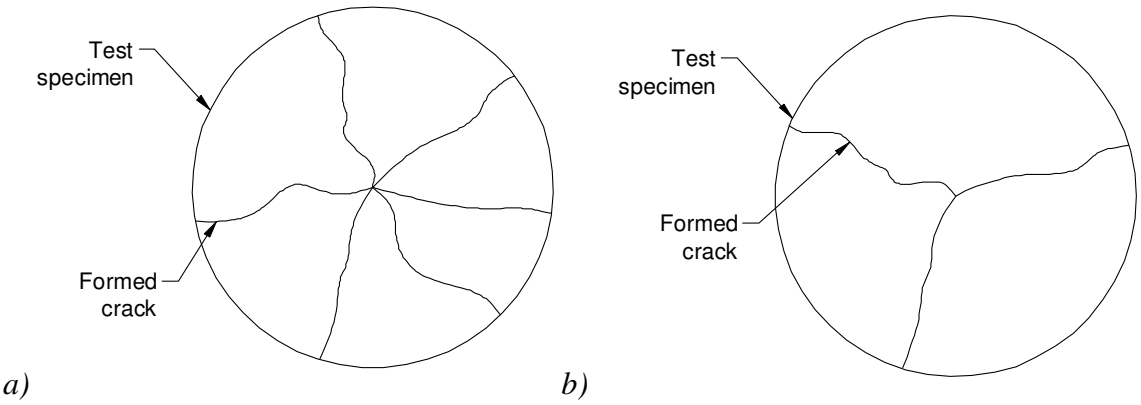

a) *b)*

Figure 3.7 a) Multiple cracking in round panel testing with continuous support and b) Standard cracking with three point pivot supports

An investigation was conducted to determine the degree of variation between beam testing and round panel testing and it was found that a variation of 7% was found in round panel testing as opposed to 18% for beam testing (Bernard, 2003). Although the results are more consistent when using round panel testing one must consider that real structures may not always have such potential for redistribution of stresses and that the intrinsic nature of SFRC is to have degrees of variability throughout the constructed element. It must also be considered that the amount of defects as a result of construction procedures will be much greater in large structures than in small test samples (Soranakom et al., 2009). Thus, depending on the structure, the bearing capacity may be reliant on a small area where it may be possible to have a low volume of fibres with unfavourable orientations in this region. A higher safety coefficient during the design phase will have to account for this lack of redistribution (Walraven, 2009). Although the test procedure may instil a greater confidence in the material properties obtained (Bernard, 2003) the properties will have to be used objectively according to the actual structural application.

However, the test procedure is a convenient method in determining the biaxial flexural behaviour of a SFRC mix (Soranakom et al., 2009). It demonstrates the potential for a SFRC mix to undergo deflection hardening and this is further illustrated by the change in cracking pattern for an increase in fibre volume fraction under continuous support conditions. Under

these support conditions the increase in volume fraction leads to a finer cracking pattern with an increased number of yield lines (Destree & Mandl, 2008). This, however, defeats the purpose of the round panel test as the level of scatter in results is increased due to these unpredictable cracking patterns and the use of a three pivot support system produces three predictable cracks (see Figure 3.7b) and reduces the scatter (Soranakom et al., 2009). The reduced scatter in comparison to results obtained from beams is thus solely as a result of the increased area resisting the load as opposed to the potential for redistribution of stresses (Destree & Mandl, 2008) but this may be suitable in determining material properties as the idealisation of the support conditions is reduced and the larger specimen size in comparison to beams is a better representation of the final structure.

A larger test sample may be more representable of the final structure but one must consider how practical a large sample is to handle and whether it is suitable for industrial applications. In order to determine material properties for full scale slab design Destree et al. (2009) tested circular panels of 1.5m in diameter and 150mm in thickness making these extremely heavy test samples. However, as the process of saw cutting is eliminated the reduction in costs may be as much as 40% when compared to conventional beam testing (Bernard, 2003) and the reduced level of scatter decreases the number of samples to be tested in order to obtain a characteristic material property. Another consideration is the testing equipment required to perform the test and it has been noted that a limited number of institutions have the capabilities to perform such tests, especially for the larger scale samples (Bernard, 2003).

3.4 Selected Test Method to Determine Material Properties

For determining SFRC properties the three-point bending test was selected for this thesis. The procedure was viewed by the author as simplistic and as a well-practiced test procedure both globally and at Stellenbosch University. In addition, it was selected as a suitable procedure as the final results were to be used in the design of a full scale test slab to be tested in flexure. The three-point bending test would give insight to the material performance under flexure where deflection-hardening potential could be interpreted, the neutral axis position could be

visually approximated during loading (thus verifying assumptions made in particular design models), the bending test would show the crack bridging potential of fibres within the concrete matrix, the sample casting procedure allowed one to further evaluate the flow potential of a particular SFRC mix design in the fresh state and the test itself would also show the failure mode behaviour of SFRC under flexure in the hardened state.

The steel fibres most suitable for structural applications are 60mm in length and thus the test sample size has to be compatible, as is the case with a standard RILEM beam test sample (Lofgren, 2005). The use of a 25mm mid-span notch increases the amount of scatter for in batch results which reduces the material tensile residual characteristic strength but this is considered as an intrinsic property of SFRC and thus may be a more suitable test procedure than those with a higher level of repeatability in results. In addition, as properties were to be used in the design of a full scale slab structure any scepticism would be confirmed or denied through the testing of the slab.

Chapter 4

Use of SFRC in Flat Slabs

The use of SFRC to date has been generally in the form of a measure of crack mitigation and as a method to improve the ductility of concrete which is an inherently brittle material. Authors such as Brandt (2008) and Walraven (2009) have noted the use of fibres to improve durability, impact resistance, fatigue and in the reduction of conventional steel in certain structural elements. However, the use of steel fibres as the sole form of reinforcement is still a relatively new concept and there exists much sceptisism as to its implementation in this format. For the potential of SFRC to be fully utilized a number of conditions need to be met of which are possible when designing and constructing flat slabs. This has been achieved in over 40 projects to date (see Figure 4.1 for structure examples) in which the use of SFRC without conventional reinforcing in flat slab construction has been succesful leading to both cost and time effective structures (Destree & Mandl, 2008).

Other than these relatively few projects the use of SFRC only in slab construction is limited and this is mainly due to the lack of design standards and practices. The inherent property of SFRC is its material variability which has impeded the progress of suitable design models. This variability has been further exagerated by the test procedures used to determine these properties which are generally rather small in scale and not representative of the final application, especially that of slabs. In order to fully utilize the potential of steel fibre

Figure 4.1 Structures in which SFRC only slabs have been implemented (Oslejs, 2008; Destree & Mandl, 2008)

reinforcing a large volume of concrete needs to be involved during the failure mechanism so as to activate a greater number of fibres (di Prisco et al., 2009). For such a failure mechanism to occur the support conditions used are to a large degree highly influential, where a greater redundancy results in the formation of a larger number of yield lines. Roesler (1998) found that ground slabs in flexure had a 30% higher strength than that predicted using material properties determined through beam testing (Roesler et al., 2004) which can be attributed to the higher potential for redistribution of stresses. Further testing by Roesler et al. (2004) showed that this increase in flexural strength was as a result of multiple cracking engaging a larger portion of the fibres in the moment resistance (Roesler et al., 2004).

In cases where slab structures have been tested under simply supported conditions (see Figure 4.2) there has been no significant increase in the flexural resistance, although there has been an increase in the energy absorped during the test procedure (Khaloo & Afshari, 2005) which further illustrates the importance of the support system. Under redundant support conditions the formation of multiple yield lines is possible which results in a process known as deflection hardening (see Section 2.2.1), in which the flexural resistance is increased as the deflection increases. The failure mechanism can be described in three phases (Ellouze et al., 2010): under loading in the initial post-crack phase the formation of yield lines can be considered to correlate with yield line theory, increasing the load results in multiple crack formation as the moment resistance in the initial crack does not increase and the resistance is

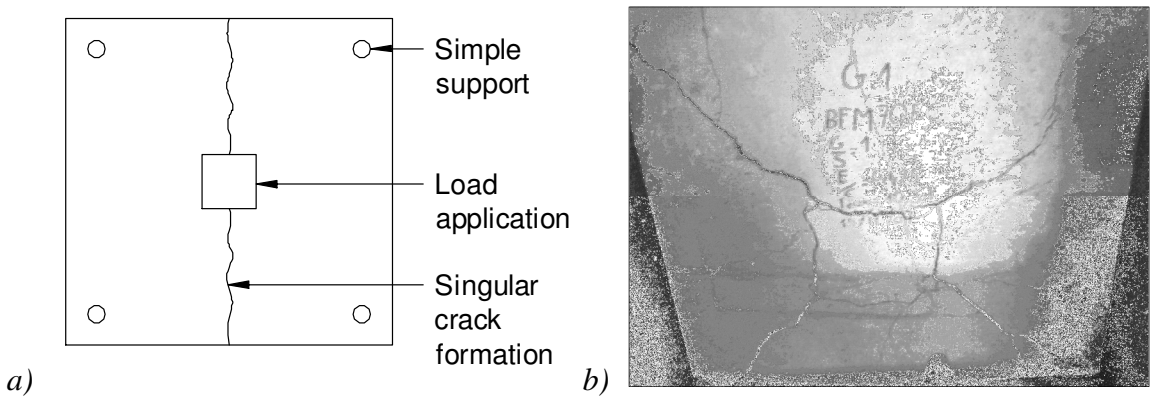

Figure 4.2 a) Simply supported slab yield line formation (Khaloo & Afshari, 2005) and b) continuously supported slab multiple yield line formation (Ellouze et al., 2010)

provided through additional cracking caused by increased deflection, at failure the resistance that was provided by the initial cracks is lost and plastic hinges form at these locations resulting in a ductile mode of failure. This process is possible due to the increased energy absorption capacity of SFRC in comparison to that of conventional concrete. As the fibres pull-out energy is absorbed and this residual strength exists for as long as the fibre pull-out is resisted by shear forces caused by friction between the fibre and surrounding concrete matrix, hence the recommended use of longer steel fibres for structural applications.

The potential for deflection hardening thus creates a possibility to eliminate the use of conventional reinforcing (Soranakom et al., 2009; Oslejs, 2008; di Prisco et al., 2009) which in turn will result in faster construction times and a possible reduction in overall costs. This has been proved through the construction of tunnel linings using only SFRC in parts of Italy (Chiaia et al., 2009) and a number of multi-storey and suspended slab construction projects under taken by ArcelarMittal (Destree & Mandl, 2008). For these systems to become a more common practice it is essential to ensure that the required level of safety is achieved and that local failure in both flexure and shear do not occur. This places a large emphasis on achieving a uniform fibre dispersion which is significantly influenced by the casting process (Ferrara & Meda, 2006).

The use of a self-compacting concrete when using steel fibres is generally preferred as a more even fibre distribution and reduced fibre balling potential is possible to achieve (Grunewald & Walraven, 2001). However, the steel fibres restrict flow characteristics and where used in combination with conventional reinforcing have a tendency to create blockages. These factors become insignificant if the material is used in flat slab construction where the reinforcement has been eliminated and the concrete can be placed by means of a pumping process, which is possible using SFRC. The elimination of the requirement to vibrate the concrete thus reduces the potential for fibre segregation and creates a more suitable 2-D fibre orientation at the tension surface of the element (Ferrara & Meda, 2006).

It is believed that this 2-D fibre orientation at the tension surface has the potential to increase post-crack load carrying capacity (Giaccio et al., 2008), although it is difficult to account for this in the design process, and may reduce the crack widths under SLS load conditions which leads to an improved structural durability. As a measure to ensure the safety of the structural system, it has become standard practice to include anti-progressive collapse (APC) reinforcement within the element (as shown in Figure 4.3) to ensure that a system collapse does not occur in the event of a structural failure (Oslejs, 2008). This is possible in slab systems where the detailed reinforcement can run between support columns to create strong bands in these regions forming a secondary support mechanism.

Figure 4.3 SFRC slab systems where APC reinforcement has been implemented (Oslejs, 2008)

Although the safety of the system is a priority it is also necessary to guarantee that the use of SFRC without conventional reinforcement can meet both the SLS and ULS design requirements. There have been limited studies investigating the performance of SFRC in large structural systems such as flat slabs although the information that is available is positive.

Four full scale tests were conducted on SFRC elevated slabs (see Figure 4.4) so as to investigate the actual structural behaviour in these elements in comparison to the design models based on material properties determined through small scale testing (Destree & Mandl, 2008; Soranakom et al., 2009). The load applications varied according to the loading state and the layout of the test setup, where in some cases SLS load conditions were simulated through the application of distributed pattern loading provided in the form of water barrels and ULS load conditions were applied in the form of a point load at the centre of the slab (Destree & Mandl, 2008). The punching shear resistance was also tested through the application of a point load near a central column support. Under the applied loads the cracking patterns and the crack size were monitored in conjunction with the deflection in the load state. The mode of failure was monitored at ULS load application and the ultimate load resistance was recorded and compared to design predictions.

a)  *b)* 

Figure 4.4 Full scale SFRC slab testing: a) SLS checker board load application and b) point loading at the centre of corner slab (Destree, 2009)

In all cases it was found that under the predicted SLS load conditions no cracking in the slabs occurred due to the application of the external load (Destree, 2009) and the behaviour of the

slab in terms of its deflections can be predicted from the elastic behaviour of round panel testing (see Section 3.2.4) subjected to a central point load (Soranakom et al., 2009). In all cases initial cracking was observed to take place only for load applications greater than that predicted as the SLS load resistance, where the crack width was reported to be no larger than 0.2mm at loads 20-30% higher than the recommended resistance. After the onset of initial cracking significant non-linearity was observed under increasing loads up till the failure load (Soranakom et al., 2009). During the increasing load slabs showed extreme ductility with a large number of micro-cracks forming near supports as the stresses were distributed (Destree, 2009). The results indicate that ultimate failure of the slabs occurred at loads at least double the initial cracking load which gives a positive indication of the reliability of the system.

In addition to this, it was found that at deflections of 30mm the residual resistance provided by the slab was still 40-50% of the ultimate load (Soranakom et al., 2009) giving insight into the ductility of the failure system. The deflections that were reported were in the region of 1/1200 of the span length under SLS test loads (Oslejs, 2008) and that the maximum long-term deflection of the implemented slab systems was no greater than 1/1000 of the span length (Destree, 2009), which is well within the serviceability requirements of 1/500 of the span length as stated in SANS 0100-1 (2000). This reduced level of deflection has also been reported by Ellouze et al. (2010) and is a property that has enabled the implementation of slab systems with a span to depth ratio as high as 30 to be used as a design guidline in which spans of up to 8m in length can be achieved (Soranakom et al., 2009).

Under point loading near the internal column supports it was found that the punching shear resistance of the SFRC system was high and that the performance of the slab structure was flexurally dominated, where a point load of 600 kN was resisted with no sign of failure (Destree, 2009). In other studies where the ultimate punching shear resistance of SFRC in small slabs was tested the ultimate resistance was found to increase linearly with fibre volume percentage and the failure mode was reported as ductile in nature in comparison to conventional concrete systems (Choi et al., 2007; Harajli et al., 1995).

The results discussed above give an indication of the potential of such a system to be further utilized in suitable construction projects. However, there still remains the concern of accurately predicting load resistance. Due to the material variability finite element design models currently tend to over predict the load resistance response based on properties determined through round panel testing (Soranakom et al., 2009), and properties determined through beam testing under predict the response to a large degree (Destree & Mandl, 2008). This reflects back to the test procedures used to determine the material properties, where beam testing is too simplified in its support structure and round panel testing with a continuous support system is an idealized scenario (see Section 3.3). The final slab system can be considered as one in between these two procedures where redistribution of stresses does take place but the paths of least resistance with respect to fibre dispersion are most likely to develop initial cracking under increasing loads. It has been noted that a simplified analytical procedure such as Johansson's Yield Line Theory can more accurately predict the failure loads but this practice requires a certain level of experience and becomes difficult in complex real structures (Soranakom et al., 2009). In conclusion it is clear that much more research is still required in this area before an efficient design approach to sufficiently predict the load carrying capacity of the SFRC flat slab system can be implemented.

Chapter 5

Design of SFRC Flat Slabs

5.1 Design Models for Structural Moment Response

There are a number of design and analysis approaches which are either analytical in nature, primarily developed for performing cross-sectional analysis, or based on the finite element method (Lofgren, 2005). Research has been conducted on generating moment response models based on various material and mechanical properties.

This section is focused on models concerning cross sectional analysis which are applicable on a structural level to Johansen's yield line theory. Yield line theory is a commonly used technique for the analysis of ultimate load carrying capacities of structures and the simplicity of this theory makes it more convenient to estimate the load capacity of the floor slab system (Soranakom et al., 2008). For further information regarding the application of yield line theory refer to Mills (1970) or other relevent literature.

When real structures are to be designed using SFRC it is necessary to have a simplified material law depicting the behaviour of the steel fibres and concrete matrix as a single composite material (Dupont, 2003). The analytical models available are based on assumptions regarding the pre and post-cracked state of SFRC under flexural loading. These

assumptions are primarily focused on the material behaviour of SFRC in the post-cracked state and make reference to either the residual strength or residual stresses within this state. The post-cracking tensile properties are often determined using the three-point bending test (see RILEM Technical Committee, 2002).

The following models have been selected for evaluation by the author in determining the moment response of structural members: the σ-ε-design method as proposed by the RILEM Technical Committee (2003), the linear and rigid plastic models as proposed in the *fib* Model Code 2010 (fib Special Activity Group 5, 2010), and the closed-form solutions for flexural response of fibre reinforced concrete elements proposed by Soranakom & Mobashir (2007).

5.1.1 RILEM σ-ε Design Method

The σ-ε-method is based on the same fundamentals as the design of normally reinforced concrete and is valid for steel fibre-reinforced concretes with compressive strengths of up to C50/60 (RILEM Technical Committee, 2003). The design methodology is intended for cases in which the steel fibres are used for structural purposes and not *e.g.* for slabs on grade. They also do not apply for other applications such as those in which increased resistance to plastic shrinkage, increased resistance to abrasion or impact, etc. are targeted.

The method proposes a representative equivalent flexural tensile strength in describing the post-cracking behaviour of an SFRC material, which is determined through testing of beam samples under the RILEM three-point bending test, as described in Chapter 3. Readings used to determine the equivalent flexural tensile strength are recorded at intervals governed by the CMOD (crack mouth opening displacement) during the deflection controlled bending test.

Residual flexural tensile strengths, $f_{R,1}$ and $f_{R,4}$ respectively, are defined at the crack mouth opening displacement ($CMOD_i$) or mid span deflections ($\delta_{R,i}$) shown in Table 5.1:

Table 5.1 $f_{R,1}$ and $f_{R,4}$ Recording increment

$f_{R,1}$	$CMOD_1$ = 0.5mm	$\delta_{R,1}$ = 0.46 mm
$f_{R,4}$	$CMOD_4$ = 3.5 mm	$\delta_{R,4}$ = 3.00 mm

The residual flexural tensile strength can be determined by means of Equation 5.1:

$$f_{R,i} = \frac{3\,F_{R,i}\,L}{2\,b\,h_{sp}^2} \tag{5.1}$$

where:

$F_{R,i}$ = force applied to specimen at time of measurement (N)

b = width of the specimen (mm)

h_{sp} = distance between tip of the notch and top of cross section (mm)

L = span of the specimen (mm)

The above equation is based on the limit of proportionality (see RILEM Technical Committee, 2002) and is derived from the flexure formula of Bernoulli-Euler beam theory:

$$\sigma = \frac{M_L y}{I} \tag{5.2}$$

where:

σ = flexural tensile strength ($f_{R,i}$)

$$M_L = \frac{F_L}{2} \cdot \frac{L}{2} \tag{5.3}$$

$$y = \frac{h_{sp}}{2} \quad (5.4)$$

$$I = \frac{bh_{sp}^3}{12} \quad (5.5)$$

Equation 5.1 can be used in determining the stresses at the notch tip of the test specimen during the linear elastic phase of deformation (i.e. before the specimen has cracked) with the assumption of the neutral axis being located at $h_{sp}/2$. Note that this assumption assumes an isotropic material i.e. fibres evenly distributed throughout the section. The Rilem model proposes that this linear elastic phase is maintained up till a crack width of 0.05mm and that the cracking force F_L be the highest force within this interval.

In reality after cracking the neutral axis shifts to maintain equilibrium between the compressive and tensile flexural forces. This is as a result of the concrete tensile stress decreasing to a residual stress as described in Chapter 2. Thus, the stress calculation in equation 5.1 is no longer technically valid as the neutral axis can no longer be assumed to be located at the centre of the section.

The σ-ε-method proposes that during this post-cracking stage the behaviour of the SFRC beam can be described by a theoretical *residual tensile strength* such as $f_{R,4}$ (as opposed to a *residual tensile stress* $\sigma_{R,4}$). This theoretical relationship is illustrated in Figure 5.1. Using the theoretical residual tensile strengths' calculation's regarding the moment resistance of a section are based on Equations 5.6 and 5.7 shown below, simplifying the complicated material behaviour to an analogy that is comparable to normally reinforced concrete design.

$$M_1 = \frac{bh_{sp}^2}{6} f_{R1} \quad (5.6)$$

$$M_4 = \frac{bh_{sp}^2}{6} f_{R4} \quad (5.7)$$

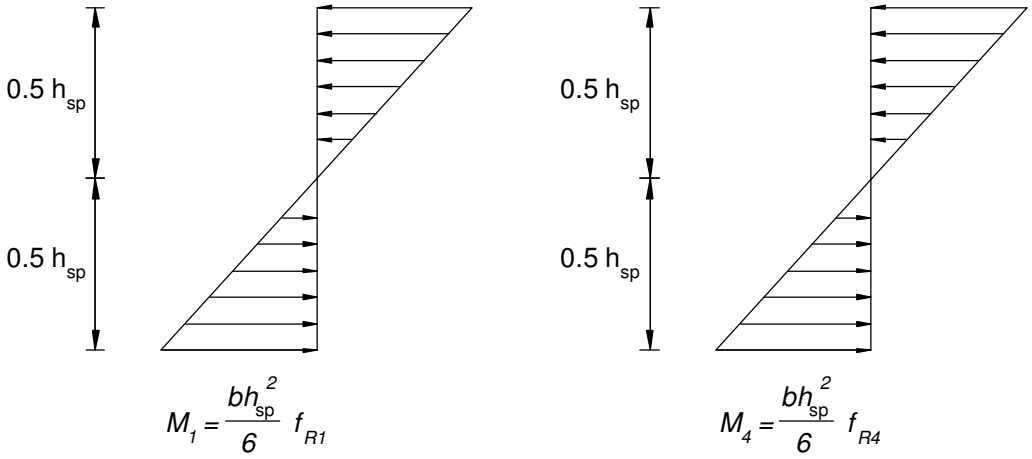

Figure 5.1 Representation of the simplified stress-strain method

The analogy based on residual flexural tensile strength in combination with the assumption of a linear elastic stress distribution provides a simplified model for moment calculations but is unrepresentative of the actual stress distribution through the section. Thus, an alternative representation of the stress distribution has been proposed for the model. The alternative has been proposed as the residual stresses provide more certainty about the material capacity at a certain crack width, whereas the equivalent strengths give a more average value over a certain interval (Dupont, 2003).

Due to the post cracking behaviour of SFRC assumptions have been made regarding the position of the neutral axis and residual stresses at a specific crack width (see Figure 5.2). Equations 5.8 and 5.9 below allow one to determine the moment resistance based on a more realistic stress distribution through the section.

$$M_1 = b\ 0.66h_{sp}\ 0.56h_{sp}\ \sigma_{f1} \tag{5.8}$$

$$M_4 = b\ 0.9h_{sp}\ 0.5h_{sp}\sigma_{f4} \tag{5.9}$$

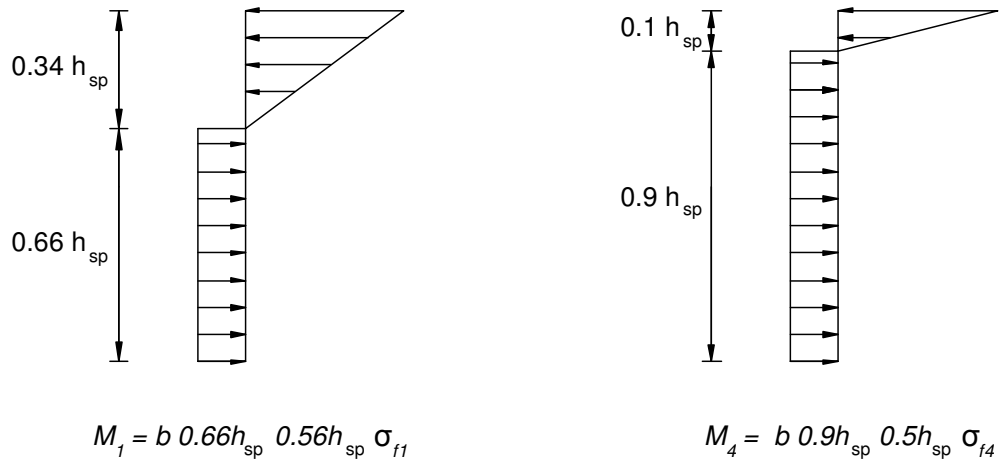

Figure 5.2 Representation of more realistic stress distribution through section

The assumptions are based on the reduction of the section tensile capacity to a residual tensile stress after cracking, resulting in a shift of the neutral axis to maintain equilibrium between the compressive and tensile forces through the section. The position of the neutral axis can be represented by the height of the crack (this represents the rotation axis for rigid body deformation) which reportedly has been experimentally validated to be located at approximately $0.66h_{sp}$ at f_{R1} and $0.9\ h_{sp}$ at f_{R4} respectively (RILEM Technical Committee, 2003).

To maintain continuity between the proposed methods moments determined using the residual stress relationship illustrated above using Equations 5.8 and 5.9 must equal those determined using equivalent flexural strength Equations 5.6 and 5.7 respectively, thus expressing the residual stress $\sigma_{R,i}$ as:

$$\sigma_{R,1} = 0.45\ f_{R1} \tag{5.10}$$

$$\sigma_{R,4} = 0.37\ f_{R4} \tag{5.11}$$

The moment resistance determined for M_1 and M_4 can be considered as the moment resistance at limit state design SLS and ULS respectively.

5.1.2 FIB Linear and Rigid-Plastic Models

The design principles reviewed in this section are those based on the *fib* Model Code 2010-First complete draft Volumes 1 and 2. There are namely two models investigated- the linear and rigid-plastic models. These proposed models are for the design of fibre reinforced concrete (FRC) for structural applications through the use of design constitutive laws considering the post-cracking residual strength provided by the fibre reinforcement. FRC's used in structural applications must provide a guaranteed minimum mechanical performance according to the model code and these limitations shall be described later in this section.

For the determination of material properties the compressive relations valid for plain concrete apply to FRC as well. Tensile properties can be determined using various bending tests aimed at determining the load-deflection relations, with results being used to determine stress-crack width relations through inverse analysis. It is recommended that nominal properties be determined through performing a three-point bending test on a notched beam according to EN 14651 (similar to that of RILEM TC 162-TDF, 2002).

Residual flexural tensile strength parameters, $f_{R,i}$, are determined using the same equation as used for the Limit of Proportionality (LOP) shown in Equation 5.1. These strength parameters differ from that used in the RILEM σ-ε-method as readings are taken at $f_{R,1}$ and $f_{R,3}$ with a CMOD of 0.5mm and 2.5mm respectively. These parameters are then used to develop the constitutive laws that govern the rigid-plastic and linear models.

Rigid-plastic Model:

The rigid-plastic model takes the static equivalence into account under the assumption that the entire compressive force is concentrated within the top fibre of the section. This assumption is based on rotational equilibrium at ultimate behaviour resulting in the residual tensile stress, f_{FTu}, being the unique reference used to form a tension stress block throughout the section (see Figure 5.3):

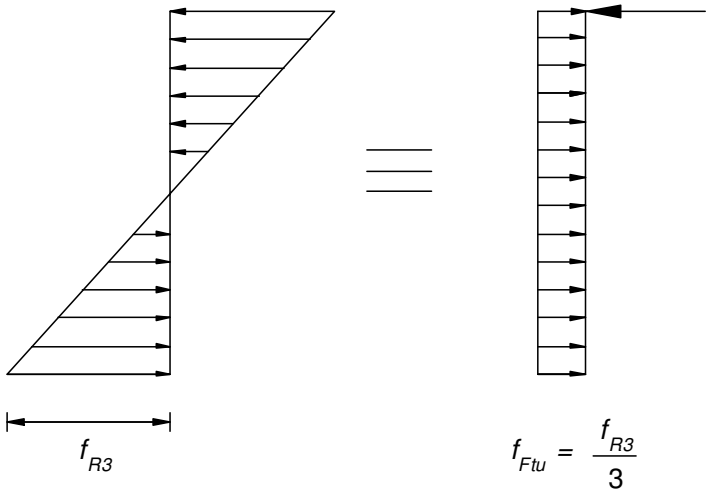

Figure 5.3 Representation of tension stress block used in the Rigid-plastic Model (fib Special Activity Group 5, 2010)

From the assumption of a concentrated compressive force the ultimate moment resistance is determined using equation 5.12 below:

$$M_u = \frac{f_{R3} b h_{sp}^2}{6} = \frac{f_{FTu} b h_{sp}^2}{2} \tag{5.12}$$

For slab elements without conventional reinforcement and prevalent bending actions the resistance moment per unit length, m_{Rd}, can be determined using a rigid plastic relationship.

The equation proposed in the model code is based on the rigid-plastic model shown in Equation 5.12 above:

$$m_{Rd} = \frac{f_{FTu} \cdot t^2}{2} \tag{5.13}$$

Linear Model:

The linear model is derived from an assumed post-cracking behaviour of either a hardening or softening material determined according to serviceability residual strength f_{FTs} and ultimate residual strength f_{FTu}. The constitutive law is determined between points with abscissa crack widths $CMOD_1$ and $CMOD_3$, resulting in the simplified post-crack behaviour as shown in Figure 5.4 below:

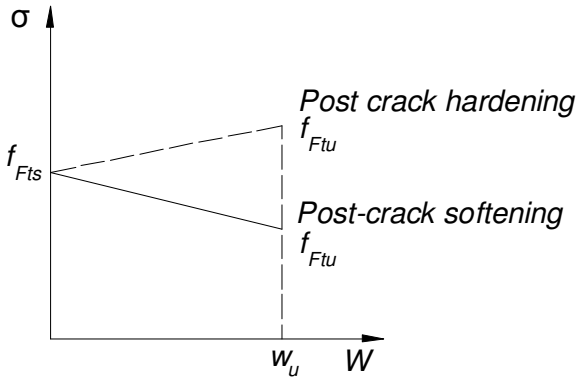

Figure 5.4 Simplified post-crack linear constitutive law (fib Special Activity Group 5, 2010)

The linear model identifies two reference values, f_{FTs} and f_{FTu}, which are defined with reference to residual strength values determined at $CMOD_1$ and $CMOD_3$. These values are then used to determine the limit state stress parameters shown in Equations 5.14 and 5.15 shown below:

$$f_{Fts} = 0.45\, f_{R1} \tag{5.14}$$

$$f_{Ftu} = f_{Fts} - \frac{w_u}{CMOD_3}\left(f_{Fts} - 0.5\, f_{R3} + 0.2\, f_{R1}\right) \geq 0 \qquad (5.15)$$

where:

$f_{R,i} = \frac{3\, F_{R,i}\, L}{2\, b\, h_{sp}^2}$

w_u = maximum allowable crack width

$CMOD_3$ = 2.5mm

From this relationship the moment resistance models are generated according to serviceability and ultimate limit states as shown below in Figure 5.5:

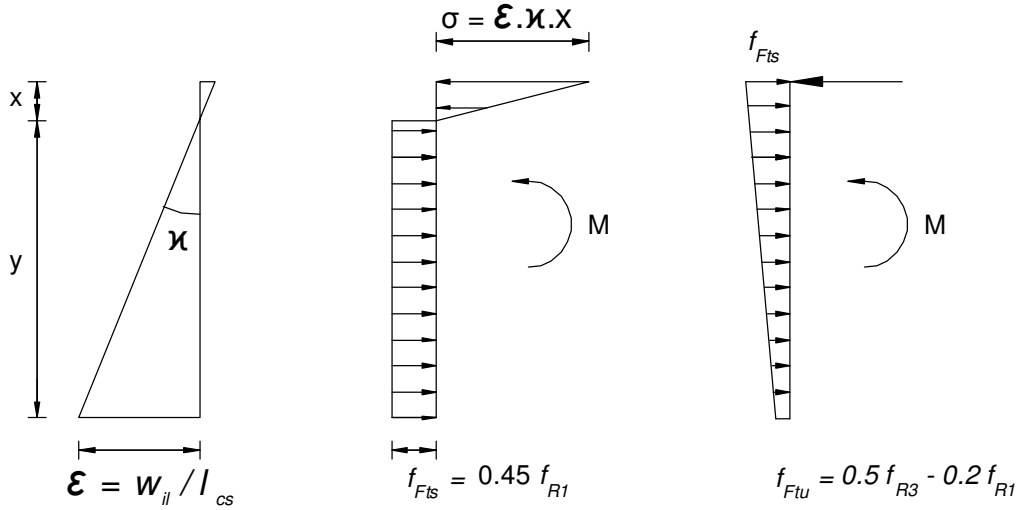

Figure 5.5 Representation of Linear Model limit state stress distributions (fib Special Activity Group 5, 2010)

Under serviceability limit state conditions it is assumed the compressive stress distribution is linear and its force component is equal to the tensile force component as a result of

equilibrium. Under three-point bending test conditions the position of the neutral axis can be determined as the applied moment is known (i.e. M = FL/4).

For ultimate limit state conditions it is assumed that the compressive force is concentrated at the top fibre of the section and that the resultant tensile stress distribution is linear. It must be noted that the above relationship in Figure 5.5 for ultimate limit state is at the absolute maximum allowable crack width of 2.5mm. According to the assumed stress distribution the maximum allowable crack opening can be calculated from Equation 5.16:

$$w_u = l_{cs} \cdot \varepsilon_{Fu} \qquad (5.16)$$

where:

l_{cs} = is the structural characteristic length

ε_{Fu} = is the ultimate allowable tensile strain in the outer most face

Here w_u is the maximum crack width opening accepted in the structural design under ULS conditions and its value depends on the ductility required. The ductility is governed by the ultimate allowable tensile strain ε_{Fu} which is equal to 2% for variable stress distribution through the cross section and 1% for only tensile stress distribution through the cross section. In slabs we assume only tensile stress distribution through the section, as at ULS the compressive force is concentrated in the top fibre, and thus a maximum strain of 1% is permitted. In sections without traditional reinforcement under bending or combined tensile-flexural forces and compressive-flexural forces with resulting force external to the section, the structural characteristic length l_{cs} = h (h=height of section).

With reference to the maximum allowable crack opening the input ultimate residual strength f_{FTu} is determined according to Equation 5.15. This value defines the linear model at ultimate limit state as shown in Figure 5.6 below:

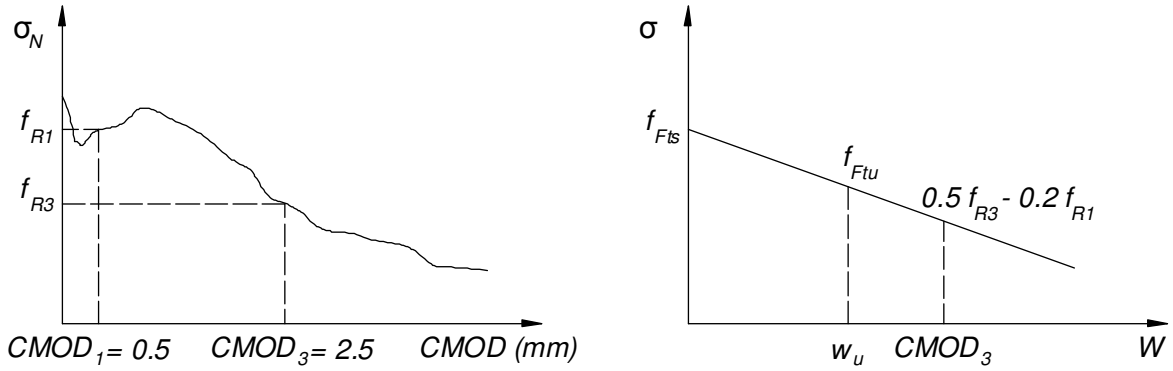

Figure 5.6 Linear model characteristic ultimate tensile stress distribution (fib Special Activity Group 5, 2010)

The model code makes no reference to moment calculations at either SLS or ULS load conditions and it is the decision of the designer as to how these will be calculated. The author suggests that based on the applied test loads and acquired material properties, SLS design loads can be determined in accordance with the limiting crack width and the associated residual flexural tensile stress. The neutral axis position can be determined using expression 5.17 below:

$$m_{applied} = f_{Fts}\left(\frac{3h_{sp}^2 - 2xh_{sp} - x^2}{6}\right)b \qquad (5.17)$$

where:

$m_{applied}$= applied test moment at f_{R1}

x = neutral axis position

h_{sp} = test specimen ligament height (= 125mm)

b = test specimen width

A ratio of the neutral axis position to the specimen ligament height is determined which can be applied to other sections constructed with the associated material. Thus, for a particular SFRC material the sectional SLS moment resistance can be calculated using:

$$M_s = f_{Fts} h^2 b \left(\frac{3-2\beta-\beta^2}{6}\right).\left(\frac{1600-h}{1600-h_{sp}}\right) \qquad (5.18)$$

where:

h = section height

b = section width (= 1000mm for slab design)

β = experimentally determined x/h_{sp} ratio at SLS loading

$\frac{1600-h}{1600-h_{sp}}$ = size factor (Dupont, 2003)

At ULS design loads it is assumed that the compressive force is concentrated at the top fibre of the section and the moment resistance can be determined using the expression:

$$M_u = h^2 \left(\frac{f_{Fts}+2f_{Ftu}}{6}\right) b \left(\frac{1600-h}{1600-h_{sp}}\right) \frac{1}{\gamma_f} \qquad (5.19)$$

where:

h = section height

b = section width (= 1000mm for slab design)

γ_f = 1.5 (*fib* material factor at ULS loading)

$\frac{1600-h}{1600-h_{sp}}$ = size factor (Dupont, 2003)

Design Principles: Required Material Properties

As stated in the model code the structural design must satisfy requirements for resistance and serviceability for the expected life of the FRC element. A distinction has been made between linear elements (e.g. beams), where redistribution is limited and critical zones are identified, and structures with a higher degree of redundancy where stress redistribution concerns the system as a whole (as in slabs).

In all FRC structures without the minimum conventional reinforcement, one of the following conditions has to be satisfied:

$$\delta_u \geq 20\ \delta_{SLS} \tag{5.20}$$

$$\delta_{peak} \geq 5\ \delta_{SLS} \tag{5.21}$$

Where δ_u is the displacement at ultimate crack width, δ_{peak} is the displacement at the ultimate load and δ_{SLS} is the displacement at service load. In addition to these requirements the load applied at the ultimate deflection has to be greater than the initial cracking load:

$$P_{ud} > P_{cr} \tag{5.22}$$

As previously stated the model code makes a distinction between linear elements and structures with a higher degree of redundancy. In the case of linear elements, a strain hardening behaviour in tension is required of the FRC. When the structure is able to

significantly redistribute the applied loads at failure, a factor K_{Rd} takes into account the favourable effects of redistribution:

$$P_{Rd} = K_{Rd}\, P\,(f_{Fd}) \tag{5.23}$$

K_{Rd} is influenced by the structure volume involved during the crack propagation process at failure (V) with respect to that used in the material identification procedure of the post-cracking residual strengths (V_0), and by the ratio between the maximum load reached and the first cracking load P_{cr} that quantifies the redistribution capability:

$$K_{Rd} = K_{Rd}\,(V/V_0\,, P_{max}/P_{cr}) \tag{5.24}$$

Different methods are proposed to evaluate these coefficients in various literatures. Essentially the coefficients consider a mechanical global response when large load redistribution occurs that is experimentally validated. These results are then structured to form coefficients which factor the average post-cracking response attained through three-point bending tests. This is as a result of the reduction of the standard deviation in the structures response in relation to the measurable test specimen, where a limited number of fibres and specific notch location lead to a large scatter in results.

The factor K_{Rd} can be computed (fib Special Activity Group 5, 2010):

$$K_{Rd} = \frac{P_{max,k}}{P_{max,m}} . \frac{f_m}{f_k} \leq 1.4 \tag{5.25}$$

5.1.3 Closed Form Solutions for Flexural Analysis

The model proposed by C. Soranakom and B. Mobasher (Soranakom & Mobashir, 2007; Soranakom *et al*, 2009) defines a closed form solution for moment curvature response based

on the relationships between ultimate tensile strength, residual tensile strength and the top compressive strain. This design method is best suited for thin structural applications such as slabs where size effects are minimal and the applied moments are relatively low when compared to the cracking moment.

The behaviour of a SFRC material is defined as either strain hardening or strain softening in tension and within the latter category; either deflection hardening or deflection softening can occur (Soranakom & Mobashir, 2007). SFRC materials with strain softening properties, and a sufficiently high volume fraction of fibres, may have an effective stiffness of the cracked zone which can resist loads in excess of the initial cracking load and is defined as deflection hardening. The methodology proposed consists of the ultimate and serviceability limit state design of strain softening, deflection hardening FRC materials in flexure.

Strain Softening, Deflection Hardening FRC Model:

The model is based on an idealised material behaviour in which three stages of stress distribution are defined (see Figure 5.7): pre-cracking linear elastic in compression and tension, post-cracking nonlinear tension with elastic compression, and finally a nonlinear tension with plastic compression before ultimate failure is achieved.

a)

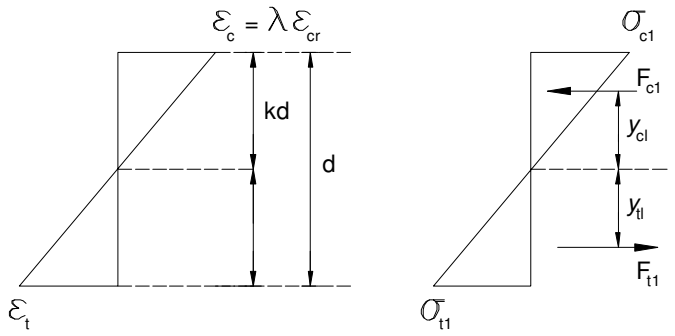

b)

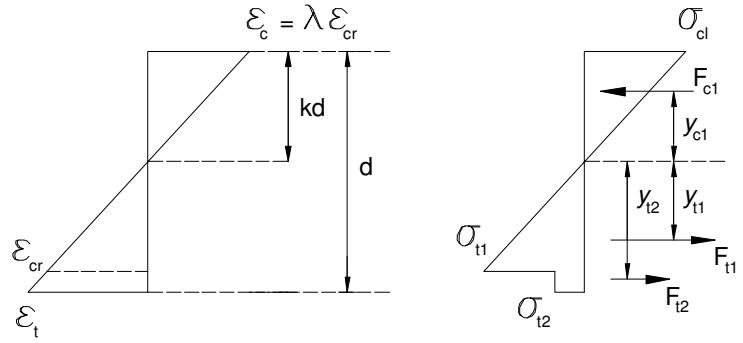

c)

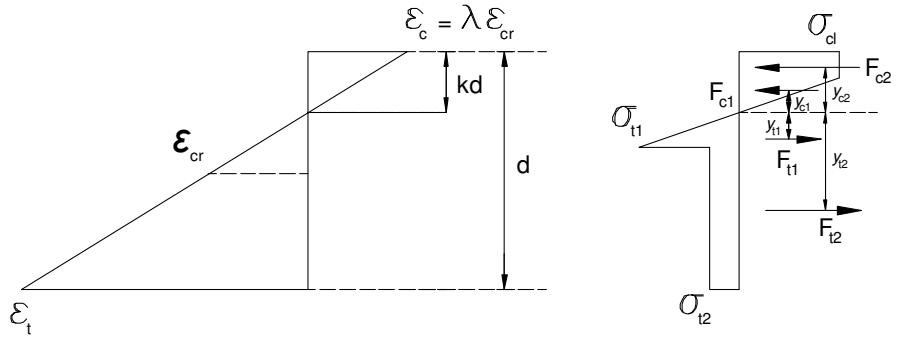

Figure 5.7 Stress and strain distribution for three phases normalized with respect to top compressive strain λ: a) elastic for compression and tension; b) elastic compression non-linear tension; c) plastic compression and non-linear tension (Soranakom & Mobashir, 2007)

The above relationships are derived using conventional beam theory that ignores shear deformation and makes the assumption of a linear distribution of strain across the section

depth. Two parameters are introduced which describe the stress states as a function of the initial cracking tensile stress:

$$\mu = \frac{\sigma_p}{E\ \varepsilon_{cr}} = \frac{\sigma_p}{\sigma_{cr}} \tag{5.26}$$

$$\omega = \frac{\sigma_{cy}}{E\ \varepsilon_{cr}} = \frac{\sigma_{cy}}{\sigma_{cr}} \tag{5.27}$$

The symbol μ refers to the ratio of the post peak tensile stress and ω the ratio of the compressive yield stress in relation to the tensile cracking stress σ_{cr} respectively. Using these parameters both the tension and compression models are expressed as:

$$\sigma_t(\varepsilon_t) = \begin{cases} \varepsilon_t E & for\ 0 \le \varepsilon_t \le \varepsilon_{cr} \\ \mu\varepsilon_{cr} E & for\ \varepsilon_{cr} \le \varepsilon_t \le \varepsilon_{tu} \\ 0 & for \quad \varepsilon_t > \varepsilon_{tu} \end{cases}$$

$$\sigma_c(\varepsilon_c) = \begin{cases} \varepsilon_c E & for\ 0 \le \varepsilon_t \le \varepsilon_{cr} \\ \omega\varepsilon_{cr} E & for\ \varepsilon_{cy} \le \varepsilon_c \le \varepsilon_{cu} \\ 0 & for \quad \varepsilon_c > \varepsilon_{cu} \end{cases}$$

Based on these relationships the internal forces in each sub compression and tension zone are obtained from the area of the stress diagram, in which the neutral axis position is determined through equilibrium of the two resultant forces. The moment response and curvature can then be determined with regards to the neutral axis position. For more information regarding the derivation of relevant closed-form equations refer to Soranakom & Mobashir (2007).

Table 5.2 depicts the neutral axis depth ratio (k) and normalized moment curvature closed-form expressions (m = normalized moment, ϕ = normalized curvature) for the three ranges of an applied normalized top compressive strain λ (where $\lambda = \varepsilon_c / \varepsilon_{cr}$):

Table 5.2 Closed form equations for three phases of applied normalized top compressive strain λ

Range	k	m	φ
$0 \le \lambda \le 1$	$\frac{1}{2}$	$\frac{\lambda}{2k}$	
$0 \le \lambda \le \omega$	$\frac{2\mu\lambda}{\lambda^2 + 2\mu(\lambda + 1) - 1}$	$\frac{(2\lambda^3+3\mu\lambda^2-3\mu+2)k^2}{\lambda^2} - 3\mu(2k-1)$	$\frac{\lambda}{2k}$
$\omega \le \lambda \le \lambda_{cu}$	$\frac{2\mu\lambda}{-\omega^2 + 2\lambda(\omega + \mu) + 2\mu - 1}$	$\frac{(3\omega\lambda^2 - \omega^3 + 3\mu\lambda^2 - 3\mu + 2)k^2}{\lambda^2} - 3\mu(2k-1)$	

As these expressions are normalized with respect to the cracked state they must be multiplied by either the cracking moment or curvature respectively in determining the actual moment response of the section:

$$M = mM_{cr} \tag{5.28}$$

$$K = \phi\, \phi_{cr} \tag{5.29}$$

where:

$$M_{cr} = \frac{1}{6}\, bh^2\sigma_{cr} \tag{5.30}$$

$$\phi_{cr} = \frac{2\varepsilon_{cr}}{h} \tag{5.31}$$

K is the curvature; b and h are the width and height of the beam respectively.

For a SFRC with sufficiently high post-peak tensile strain capacity, the moment response behaves in a ductile manner and approaches a limit value defined as M_∞ at large λ values. The ultimate flexural strength M_u can be reasonably approximated by M_∞ as the moment resistance of the section theoretically converges for large compressive strains λ. Thus,

substituting $\lambda = \infty$ in the expression for k in Table 5.2 to obtain k_∞ and its subsequent substitution into expression for m and ϕ will yield the following expressions:

$$k_\infty = \frac{\mu}{\omega+\mu} \tag{5.32}$$

$$M_\infty = \frac{3\mu\omega}{\omega+\mu} \tag{5.33}$$

$$\phi_\infty = \infty \tag{5.34}$$

It is required that the normalized moment capacity approximated by M_∞ is at least equal to the normalized cracking moment M_{cr} to enable a ductile failure mode. To ensure this mode of failure a critical parameter, μ_{crit}, has been defined and represents the transition from a deflection softening material to a deflection hardening material. For typical ω ranges of between 6-12 for an FRC section the critical normalized tensile strength parameter has been defined as $\mu_{crit} = 0.35$. This indicates that the post-peak tensile stress in a material must be at least 35% of its cracking tensile strength before it can exhibit deflection hardening. For a deflection hardening material, the moment-curvature response can be approximately represented by the bi-linear model as shown dashed lines in Figure 5.8 below. Details of the model can be found in Soranakom & Mobashir (2009).

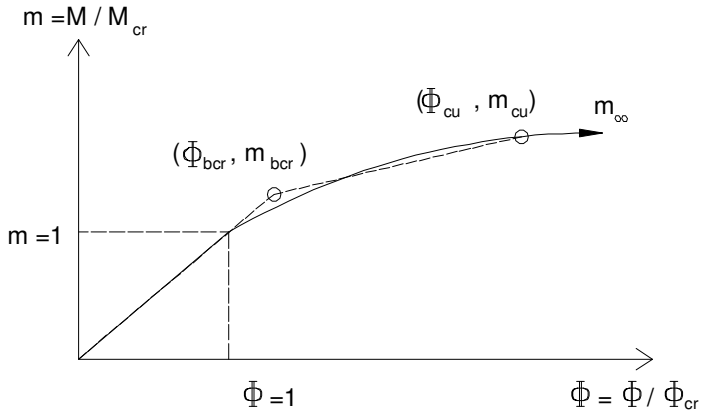

Figure 5.8 Normalized moment curvature diagram and approximate bilinear model for a deflection hardening material (Soranakom & Mobashir, 2009)

Design limits are introduced in the model to limit the allowable tensile strain and crack widths, although ultimate moment capacity can be much greater than the original cracking moment. Depending on support conditions many deflection-hardening SFRC's show multiple cracking, and it is proposed that the nominal tensile strain is averaged from several cracks spaced apart as the serviceability criterion.

A normalised allowable tensile strain, β_a, is introduced to limit crack width and the normalised compressive strain, λ_a, at a balanced condition can be written as

$$\frac{\lambda_a \varepsilon_{cr}}{kh} = \frac{\beta_a \varepsilon_{cr}}{h-kh} \tag{5.35}$$

where

$$\beta_a = \frac{\varepsilon_a}{\varepsilon_{cr}} \tag{5.36}$$

Equation 5.35 is solved in conjunction with the neutral axis parameter *k* in Table 5.2 to solve for the two ranges of either linear elastic compressive strain or plastic compressive strain. This yields two possibilities for λ_a which is dependent on the compressive state:

$$\lambda_a = \begin{cases} \sqrt{2\mu\beta_a - 2\mu + 1} & \beta_a \leq \beta_{crit} \\ \frac{2\mu\beta_a - 2\mu + \omega^2 + 1}{2\omega} & \beta_a > \beta_{crit} \end{cases} \tag{5.37}$$

$$\beta_{crit} = \frac{\omega^2 + 2\mu - 1}{2\mu} \tag{5.38}$$

Where β_{crit} shown in equation 5.38 above is the critical tensile strain and can be regarded as the normalised tensile strain value at which the behaviour of the compressive region changes from linear elastic to a plastic phase.

The normalized allowable tensile strain ratio has been limited to $\beta_a = 20$ with a corresponding normalised compressive strain value $\omega = 6$. An explanation for these limits can be found in Soranakom & Mobashir (2009). The closed-form solutions for the allowable moments corresponding to the limit β_a can be derived by first substituting the values in equation 5.37 above, then substituting the obtained λ_a in the expressions for *k* and *m* in either the compressive linear elastic or plastic phase respectively. With respect to the limiting β_a and ω values stated above, the conservative normalised serviceability moment expression is summarized as:

$$m_a = \begin{cases} \frac{76\mu\sqrt{38\mu+1}+2\sqrt{38\mu+1}+1197\mu+2}{\left(20+\sqrt{38\mu+1}\right)^2} & \beta_a = 20 \leq \frac{35+2\mu}{2\mu} \\ \frac{18\left(1444\mu^2+12.388\mu-343\right)}{(277+38\mu)^2} & \beta_a = 20 > \frac{35+2\mu}{2\mu} \end{cases} \quad (5.39)$$

Thus, based on the sectional dimensions and the cracking moment in conjunction with the above normalised serviceability limit equations, the serviceability moment resistance can be expressed as:

$$M_s = m_a M_{cr} = m_a \frac{\sigma_{cr} b d^2}{6} \quad (5.40)$$

It has been stated that ultimate flexural strength M_u can be reasonably approximated by M_∞. The literature (Soranakom & Mobashir, 2009) recognises that this approximation slightly overestimates the ultimate moment capacity M_u and a reduction factor ϕ_p has been introduced. Based on a statistical analysis of limited data a value $\phi_p = 0.9$ has been proposed. The ultimate moment capacity can thus be obtained using the following expression:

$$M_u = \phi_p m_\infty M_{cr} = \phi_p \frac{3\omega\mu}{\omega+\mu} . \frac{\sigma_{cr} b d^2}{6} \quad (5.41)$$

5.2 Design Model for Punching Shear of SFRC

In flat slab systems the slab is supported directly on columns which result in high stress concentrations at these connection points. The ultimate strength of such slabs is often determined by the punching shear failure load which can be smaller than the determined flexural failure load (Theodorakopoulos & Swamy, 2002). Punching shear failure is generally brittle, occurring without warning as a result of a sudden separation of the slab and column. Literature (Harajli et al., 1995; De Hanai & Holanda, 2008) has shown that the addition of steel fibres significantly increases the punching shear capacity and the ductility of the failure mechanism resulting from an enhanced structural integrity between the slab and the column.

The ability of steel fibres to enhance the punching shear strength of concrete is attributed to the possible transfer of tensile stresses across cracked surfaces (Choi et al., 2007) but the three-dimensional complex behaviour of the slab-column connection makes the enhanced capacity difficult to model and accurately predict. Generally, design codes do not take into account the beneficial effects of steel fibres in determining the punching shear resistance due to inadequate modelling of the failure mechanism and directly linking the failure criterion to the punching shear capacity.

Theodorakopoulos & Swamy (2002) developed a good representation of the physical behaviour of the slab-column connection during load application from which a simple analytical model for the punching shear strength of conventionally reinforced flat slabs was proposed. Using this behavioural concept, Choi *et al* (2007) applied a similar mechanism in determining the punching shear strength of an FRC slab-column connection as a combination of the resistance provided by both the compressive and tensile zones within the section. In addition to the model proposed by Choi et al (2007) the shear resistance determined according to the *fib* Model Code 2010 Volume 2 (fib Special Activity Group 5, 2010) was

also evaluated and served as a benchmark for expected punching shear loads during testing and as a comparison for the above mentioned punching shear model.

5.2.1 Punching Shear Mechanism Design (Choi et al., 2007)

The complexity and uncertainty associated with shear has led to conservative code equations and has become an uneconomical feature of structural design (Gohnert, 2006). In order to predict the punching shear capacity of an FRC slab-column connection the failure mechanism needs to be accurately described and adaptable for use with SFRC. According to Theodorakopoulos and Swamy (2002) the mechanism can be described as a sequence of events such as (1) the formation of a roughly circular crack around the column periphery on the tension surface of the slab and its subsequent propagation into the compression zone of the concrete, (2) formation of new lateral and diagonal flexural cracks on the tension surface, and (3) the initiation of an inclined shear crack near mid-depth of the slab, observed at about 50-70% of the ultimate load. Choi *et al* (2007) have suggested that the average cracking angle, $\bar{\phi}$, for the inclined crack is 30° from the horizontal for an SFRC slab-column connection. With increasing loads the inclined crack extends towards the compression zone and the tension steel, but in the final stages, its propagation is prevented as it reaches the compression zone near the column face and by the dowel action of the tension reinforcement. Finally, punching shear failure occurs in the compression zone resulting in ultimate failure of the slab-column connection (Theodorakopoulos & Swamy, 2002). In an SFRC slab-column connection this final step in the failure mechanism is a combination of the punching shear in the compression zone and fibre pull-out or yielding in the tension zone.

Once the inclined shear crack has developed the applied shear load at the support is resisted by the vertical components of the concrete compression zone and residual tensile strength provided by the fibres (Choi et al., 2007) and the dowel action of the flexural reinforcement over the support should any be detailed (Theodorakopoulos & Swamy, 2002). Thus, the total shear resistance V_u of an SFRC slab-column connection without shear reinforcement is described by:

$$V_u = V_c + V_{fr} + V_d \quad (5.42)$$

where:

V_c = resistance provided by compression zone

V_{fr} = resistance provided by fibres in the tension zone

V_d = resistance provided by longitudinal bars through dowel action

The above model neglects the aggregate interlock force contribution as it is assumed that at failure the inclined crack width is too large for this contribution to be significant at ultimate limit state. The above mentioned components will be discussed in detail in the following sections.

Punching Shear Components:

Resistance of Compression Zone (V_c)

The resistance offered by the concrete compression zone, V_c, is equal to that acting on an inclined, uncracked area of the concrete confined between the plane of the slab-column juncture and the neutral axis (NA) plane (Theodorakopoulos & Swamy, 2002). The slab-column connection is influenced by both flexural and shear forces and these forces influence the NA position (see Figure 5.9) as well as the ultimate failure mechanism.

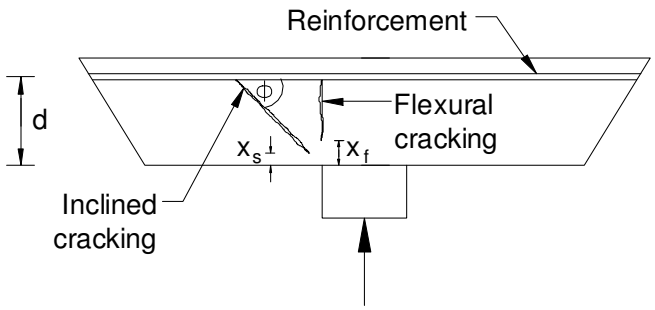

Figure 5.9 Illustration of neutral axis position according to crack mechanism

In flat slabs the behaviour of the slab-column connection is generally dominated by the flexural forces applied at the connection. For an SFRC slab-column connection fibre pull-out and yielding of the tensile reinforcement (should any be detailed) is most likely to occur before punching, as which has been experimentally validated to occur for low tension reinforcement ratios in flat slabs (Theodorakopoulos & Swamy, 2002). Thus, it is assumed that the depth of the NA is equal to the depth of the compression zone at flexure (Theodorakopoulos & Swamy, 2002) where the NA position, X, is represented as:

$$X = X_f \qquad where \quad X_f < X_s \tag{5.43}$$

Where the flexural NA, X_f, can be determined using one of the proposed moment model's for a SFRC material as shown in Section 5.1. As the stresses imposed on the connection are three dimensional, a simplification is made referring to moments in the M_x and M_y span directions. The flexural NA position used for determining the punching shear resistance is thus the smallest compression zone of the two span directions resisting their respective applied moments at the connection. Resulting from the reduced compression zone under an increased applied moment, the shear capacity of the cross-section is reduced with respect to an increased deformation (Choi et al., 2007).

For slabs with relatively low moment forces, high tension reinforcement ratios or drop down panels at the supports the NA may not equal the flexural NA, i.e. $X \neq X_f$, when the slab-

column connection is nearing failure. In this case the NA location may be determined by the shear NA, X_s, which is not varied according to the concrete properties or steel amount and properties (Theodorakopoulos & Swamy, 2002) and can be determined using the equation:

$$X = X_s = 0.25d \qquad where\ X_f > X_s \tag{5.44}$$

Considering the normal and shear stress states at the cross-section, the constitutive material failure mechanism can be defined using Rankine's failure criterion (Choi et al., 2007). Failure of the section thus occurs when the principle stresses reach the material strength. The principle stresses at the section can be compressive, tensile or a combination of the two and it assumed that SFRC behaves in a similar manner to conventional concrete under elastic load conditions. Thus, the shear capacity of the concrete compressive zone is controlled by the cracking tensile strength of the concrete when considering principle stresses. In the *fib* Model Code 2010- Volume 2 in Section 7.7.3.2 it is stated that the principle tensile stress shall not be higher than the design tensile strength (which is in this case the cracking tensile strength):

$$\sigma_1 \leq \frac{f_{Ftuk}}{\gamma_f} \tag{5.45}$$

Thus the failure criterion of the compression zone for an SFRC material controlled by tension can be determined using the concept of a principle tensile stress:

$$\sigma_2 = -\frac{\sigma_c}{2} + \sqrt{\left(\frac{\sigma_c}{2}\right)^2 + v_c^2} = f_t \tag{5.46}$$

where

σ_2 = principle tensile stress

σ_c = compressive normal stress

v_c = shear stress

f_t = concrete tensile strength

With respect to the principle tensile stress the concrete tensile strength can be represented by the concrete splitting strength under axial loading. This can be determined as a function of the concrete characteristic compressive stress should valid experimental data not be available and is defined by RILEM TC-162-TDF (2003) as:

$$f_t = f_{fctm,ax} = 0.3\left(f_{fck}\right)^{\frac{2}{3}} \tag{5.47}$$

Due to the Poisson effect the determined tensile strength of the concrete is reduced by the transverse compressive stress (Choi et al., 2007) to give:

$$f'_{ct} = 0.9 f_t \tag{5.48}$$

The maximum shear stress at each location in the compression zone is defined as a function of the distance from the NA as the compressive stress varies according to the distance from the NA:

$$v_c(z) = \sqrt{f'_{ct}[f'_{ct} + \sigma_c(z)]} \tag{5.49}$$

Where

$$\sigma_c(z) = f'_{cf}\left[2\left(\frac{\alpha z}{c_u}\right) - \left(\frac{\alpha z}{c_u}\right)^2\right], \qquad c_u = \text{depth of the compression zone} \tag{5.50}$$

It is assumed that the compressive strain in the compression zone is linearly distributed and for simplicity in calculation it is considered that the average compressive stress $\bar{\sigma}$ over the

compression zone (Choi et al., 2007). Thus, for the critical compression zone, A_c, the shear capacity of the cross-section controlled by tension is redefined as:

$$v_c \approx \lambda_s \sqrt{f'_{ct}[f'_{ct} + \bar{\sigma}]}\, A_c \tag{5.51}$$

where

$$\bar{\sigma} = \frac{\int_0^{c_u} \sigma_c(z)dz}{c_u} = \left(\alpha - \frac{\alpha^2}{3}\right) f_{cu} \tag{5.52}$$

$$\lambda_s = \sqrt[4]{400/d} \quad (mm) \qquad \text{, size effect factor as per Choi } \textit{et al} \text{ (2007)} \tag{5.53}$$

$$A_c = (2c_1 + 2c_2 + 4\cot\bar{\phi} \cdot c_u)c_u \quad \text{, } c_1 \text{ and } c_2 = \text{column dimensions} \tag{5.54}$$

According to Choi et al. (2007) the experimentally validated average cracking angle, $\bar{\phi}$, can be set at 30° and the maximum compressive strain corresponding to punching shear failure can be described as $\alpha\varepsilon_{cof} = 0.00196$, where ε_{cof} is the compression strain corresponding to the compressive strength of SFRC. Thus α at punching shear failure with respect to the compressive strain of conventional concrete can be defined as:

$$\alpha = \frac{0.00196}{0.0035} = 0.56 \tag{5.55}$$

Resistance of Tensile Zone (V_{fr})

During the punching shear mechanism an inclined shear crack develops near mid-depth of the slab. This crack initiates as a result of the tensile forces developing in the section which can be represented using truss analogy or principal stresses (see Figure 5.10). As the tensile stresses increase the crack propagates towards the compression zone and flexural reinforcement near the top surface (should any be detailed).

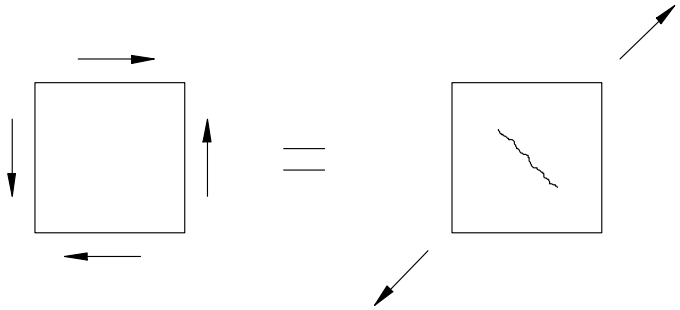

Figure 5.10 Representation of shear and equivalent tensile stress

Once the inclined tension crack has formed in the concrete section the tensile force is resisted by the residual strength of the SFRC material. The tensile force acting on the section can be represented as an axial tension force which is resisted by the post-cracking residual tensile stress which for flexure is defined as:

$$f_{ft} = 0.33 f_{R3} \tag{5.56}$$

However, as the tension failure mechanism is similar to that of a uni-axial load application the flexural residual stress given in Equation 5.56 is no longer applicable. According to the RILEM Technical Committee (2003) the relationship between the tensile flexural strength and the tensile axial strength for a given composite can be approximated by a factor of 0.6 (RILEM Technical Committee, 2003). This factor is applicable to the tensile cracking stress and is thus only relevent in the linear elastic phase. In the plastic tensile phase of a SFRC composite a new factor needs to be determined and the author proposes a factor of 0.4. The factor has been approximated according to punching shear results determined by Choi et al. (2007) and can be justified by the fibre pull-out behaviour where the effects of snubbing and fibre-matrix friction are reduced in uni-axial tension, the properties determined through flexure may also include influences caused by deflection hardening which is non-existent in direct tension testing, and when compared to flexure an approximate 2-D fibre orientation as a result of the casting processes may over estimate the capabilities a SFRC with randomly

orientated fibres when pure tension forces are imposed. The uni-axial tensile residual stress can thus be approximated by:

$$f_{pc} = 0.4 f_{ft} \tag{5.57}$$

The tensile resistance provided by the residual tensile strength of SFRC can thus increase the punching shear strength through the bridging of steel fibres across cracks, and this improvement in strength has been shown to have a linear relationship according to the fibre volume fraction (De Hanai & Holanda, 2008). As proposed by Choi et al. *(*2007), the contribution of the SFRC residual tensile strength over the critical tension zone, A_T, to the vertical resistance of the slab-column separation during punching shear can be represented by:

$$V_{fr} = \overline{f_{pc}} A_t \cos\bar{\phi} \tag{5.58}$$

where:

$$\overline{f_{pc}} = 0.6 f_{pc} \tag{5.59}$$

$$A_T = (2c_1 + 2c_2 + 4\cot\bar{\phi} \cdot d)(d - c_u)/\sin\bar{\phi} \tag{5.60}$$

$\bar{\phi}$ = average angle of the inclined shear crack

d = depth from slab underside to level of reinforcement

As the shear capacity in the tension zone is resisted by only the residual tensile strength an average value $\overline{f_{pc}}$ is used in accordance with the recommendations of Choi *et al* (2007). This value is determined with respect to the axial post-cracking residual strength which can be determined from the flexural residual tensile strength as per Equation 5.57. Based on the

experimental observations of Choi *et al* (2007) the average cracking angle of a SFRC material is lower than that of a conventionally reinforced concrete slab-column connection with a $\bar{\phi}$ value set at 30°.

Where longitudinal reinforcement has been utilised the region resisting the tensile component of the punching shear mechanism shall lie between the reinforcement and compression zone in accordance with recommendations made by Choi et al. (2007). This is a simplification as an assumption is made that the fibres in this region make no contribution to the flexural resistance and that the fibre capacity is thus available to resist punching shear forces. Should more information regarding this composite behaviour and the NA location become available adjustments could be made to this model but the further development of this model is outside the scope of this project.

Contribution of Dowel Action from Longitudinal Reinforcing Bars

The dowel effect is a shear mechanism transferred by longitudinal flexural reinforcement crossing the punching crack (Kinnunen, 2001). The ultimate punching shear resistance offered by dowel action in two-way spanning slabs can be as much as 25-35% based primarily on experimental observations as a theoretical evaluation of its contribution is difficult to determine (Theodorakopoulos & Swamy, 2002). In SFRC slab-column connections the failure mode is generally dominated by flexure. Should any longitudinal flexural reinforcement be required for moment resistance over the support it is expected to yield before punching shear failure occurs, thus considerably reducing the dowel resistance offered. Due to this failure mechanism and the unpredictability of the dowel resistance contribution it is recommended by the author to ignore this component in determining the punching shear resistance of a SFRC slab-column connection.

However, should the concrete section be over reinforced or additional reinforcing be required to resist punching shear, the contribution from the longitudinal reinforcing bars to the

punching shear resistance can be determined in accordance with the *fib* Bulletin 12 (Kinnunen, 2001).

Outline of Analysis Procedure:

1. Determine the NA depth of the flexural section, X_f, in accordance with Section 5.1. If the section contains longitudinal reinforcement we assume the neutral axis depth is fixed in accordance with conventional concrete design.

2. Determine the depth of the NA for the shear section, X_s, using Equation 5.44:
   $X_s = 0.25\,d$
3. Determine the punching shear resistance from the compressive zone with Equation 5.51:

   $$v_c \approx \lambda_s \sqrt{0.9 f_t \left[0.9 f_t + (\alpha - \alpha^2/3) \cdot f'_{cf}\right]}\, A_c$$

4. Determine the vertical contribution to punching shear resistance from the tension zone with respect to the axial residual stress using Equation 5.58:

   $$V_{fr} = \overline{f_{pc}} A_t \cos\bar{\phi}$$

5. Consider the influence of longitudinal reinforcement (should any be detailed) in the punching shear resistance through dowel action, V_d. Should this force be applicable determine the contribution in accordance with *fib* bulletin 12 (Kinnunen, 2001).

6. Calculate the overall punching shear resistance, V_u, as per Equation 5.42:

   $$V_u = V_c + V_{fr} + V_d$$

7. Should the punching shear resistance V_u be insufficient increase the amount of longitudinal reinforcement (should any be detailed) to increase the depth of the

compressive zone and increase the influence of the dowel effect. Alternatively, increase the depth of the section using a drop down panel. Determine the new punching shear resistance according to the above procedure.

5.2.2 FIB Shear in Beams (fib Special Activity Group 5, 2010)

As little is known about the punching shear resistance of SFRC systems the determination of shear resistance in beams without shear reinforcement according to the *fib* Model Code 2010 served as a reference to the punching shear resistance of test samples. The assumption of an inclined crack at 30° to the horizontal was used with reference to the experimental observations made by Choi et al (2007). This value was used to determine the perimeter size upon which calculations were based.

In terms of the determination of the shear capacity in itself little is explained as to the origin or assumptions made for the model where a simplified formula is provided. The origin of the introduced size factor could not be found in the literature. The values for the characteristic concrete tensile strength and the residual tensile strength is determined through direct tensile tests. The shear resistance of beams provided without shear reinforcement can thus be determined in Equation 5.61 below (fib Special Activity Group 5, 2010):

$$V_{Rd,F} = \left\{ \frac{0.18}{\gamma_c} \, k \left[100 \, \rho_1 \left(1 + 7.5 \, \frac{f_{Ftuk}}{f_{ctk}} \right) f_{ck} \right]^{1/3} + 0.15 \, \sigma_{cp} \right\} b_w \, d \qquad (5.61)$$

where:

γ_c is the partial safety factor for the concrete without fibres

k is a factor that takes into account the size effect and is equal to:

$$1 + \sqrt{\frac{200}{d}} \leq 2.0$$

d is the effective depth of the cross section in mm

ρ_l is the reinforcement ratio for longitudinal reinforcement

f_{Ftuk} is the characteristic value of the residual tensile strength at w_u = 1.5mm, in MPa

f_{ctk} characteristic value of the tensile strength for the concrete matrix

f_{ck} is the characteristic value of the cylindrical compressive strength, in MPa

σ_{cp} is the average stress acting on the concrete resulting from an axial force, in MPa

b_w is the smallest width of the cross-section in the tensile area, in mm

5.3 Crack Pattern and Deflection in SFRC Flat Slab Systems

In flat slab systems the support conditions are generally indeterminate making this type of structural application potentially suitable for SFRC. The suitability is attributed to a possibility of a considerable amount of stress, and thus moment redistribution throughout the structure when using SFRC due to its ductile behaviour. However, as a result of this stress redistribution characteristic the prediction of the SFRC cracking patterns and resultant deflections becomes difficult.

5.3.1 Multiple Cracking Pattern

According to Oslejs J (2008) SFRC relies on the development of multiple new yield lines at the ultimate limit state, where existing yield lines act as hinges and newly developed yield lines resist the moments and absorb energy (Oslejs, 2008). This has been experimentally shown by Ellouze et al. (2010) in which 1100x1100x60mm thick slabs with continuous simple supports along the perimeter where tested for flexural behaviour under uniformly distributed loading. It was observed that yield lines form through cracking of the concrete, in which phase the fibre resistance is activated, and additional cracking occurs through the redistribution of stresses before plastic hinges developed at the initial main cracks resulting in an ultimate failure of the system (Ellouze et al., 2010).

This multiple cracking pattern has been described by Soranakom et al. (2008) as smeared cracking in which one can assume an average tensile strain measured over several crack spacing's (Soranakom et al., 2008). As the fibres are randomly orientated and distributed throughout the concrete matrix it is not possible to determine crack spacing and location as with conventionally reinforced concrete, increasing the difficulty in predicting crack widths. However, various models have been developed in an attempt to predict average crack spacing's and width using fracture mechanics with the non-linear material behaviour of SFRC (e.g. Chiaia et al., 2009; Olesen J.F, 2001). An underlying concept within these models is the assumption of a structural characteristic length in defining the region over which the strain is distributed and defining the spacing of cracks within the affected area. This length has been defined by Olesen (2001) as half the sectional depth of the resisting element whereas the *fib* Model Code (2010) refers to this length being equal to the depth of the resisting section for elements reinforced with steel fibres only. These assumptions have been made with regards to three- and four-point bending tests and their application to structural systems such as flat slabs is uncertain. Thus, further investigation with regards to the theoretical prediction of crack widths and spacing will not be covered in this document.

5.3.2 Deflection Prediction

Due to the redistributive cracking nature of SFRC flat slabs the prediction of deflection becomes difficult as it is not possible to directly determine the rotation angle at supports from crack widths and their locations. Soranakom et al. (2007) described a moment area method in which the mid-span deflection of three- and four-point bending tests could be derived with reference to a bilinear moment-curvature diagram. The model was based on an assumption that after cracking of the concrete the moment resistance generated through crack bridging of the fibres had a ceiling for that specific crack, which remains constant over a period as a result of the fibre pull-out resistance during widening of the crack. The curvature distribution would thus depend on the post-crack tensile strength (Soranakom & Mobasher, 2007), as an increase in the applied moment could potentially be resisted through the formation of additional cracks within this localized area before ultimate failure of the initial main crack.

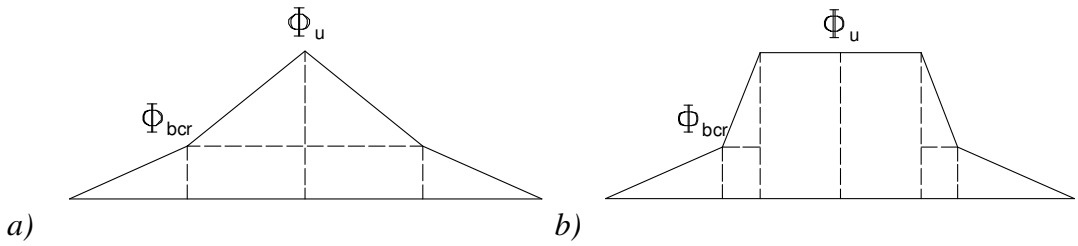

Figure 5.11 Schematic showing the proposed post-crack curvature distribution for a) three- and b) four-point bending for sufficient post-crack tensile strength (Soranakom & Mobashir, 2007)

Using the concept of curvature distribution as illustrated in Figure 5.11 above a prediction to a load-deflection response can be made through a number of load steps along a moment-curvature diagram. This concept is similar to the plastic-hinge theory as proposed by Olesen et al. (2001) in which the mean value of curvature through a section is used to develop a fictitious crack model with a bilinear stress-crack opening relationship (Olesen, 2001). The hinge model assumes a width of the hinge that can be used to determine the theoretical crack width according to the resistance provided by the residual stress of SFRC through the

modelling of spring elements. Using this fictitious crack width the rotation at the supports can be determined and used to predict the overall deflection at mid-span.

The models discussed above have been used to generate closed form solutions suitable for predicting a deflection response under specific loading conditions but are generally applicable to statically determinate situations, e.g. three- and four-point bending tests only. However, the failure mechanism concept described in conjunction with a distributed curvature response may be applicable for use in flat slabs. Ellouze et al. (2010) noted that during an increasing, uniformly distributed load a crack pattern similar to that predicted through yield line theory initially developed. Under increasing load the bending moment resistance of the initial crack no longer increases and the moment is redistributed resulting in additional crack formation. This stress redistribution was maintained until plastic hinges finally developed at the initial main cracks at failure (Ellouze et al., 2010). Thus, the deflection of SFRC flat slabs may be predicted through the use of such models should the curvature distribution be correctly simulated in accordance with the system support mechanism. The modelling of this behaviour, however, is beyond the scope of this research.

5.3.3 Practical Guidelines for SFRC Flat Slabs

The load resistance mechanism and deflections of SFRC flat slabs is difficult to predict as a result of the random distribution and orientation of fibres throughout the concrete matrix and the indeterminate nature of the support system. Although the support system contributes to the difficulty in determining crack widths, spacing and deflections it is recommended to have as much of a continuous support along all edges as possible. This will enable new yield lines to develop over a larger area and thus allow a greater number of fibres to counteract the applied moment (Oslejs, 2008).

Due to the type of support conditions required to make the use of SFRC in flat slabs suitable, the deflections are negligible in most cases as the span to depth ratio is always smaller than

30 and the maximum service bending stress is limited to 5MPa (Destree, 2009). It must be noted that the recommended span to depth ratio for a beam of conventionally reinforced concrete with continuous ends is 28 as per the South African Concrete Design Code (SANS 0100-2, 1992), indicating that expected deflections in SFRC slabs is less than that expected in conventionally reinforced concrete. This is further illustrated through elevated slabs constructed using SFRC as the principal reinforcement by ArcelarMittal in Europe where they have stated that span to depth ratios can be as much as 33. This has been experimentally validated by Ellouze *et al* (2010) and Destree *et al* (2009) in which test slabs, both small and full scale, were reported to show lower deflections than those expected for conventionally reinforced concrete. According to Destree (2009) the maximum long-term deflection of TAB-slab, the patented SFRC slab design incorporated by ArcelarMittal, is in most cases less than span/1000, which is well within the limitations as stated in the South African Concrete Design Code (SANS 0100-2, 1992).

5.4 Other Design Considerations for SFRC

5.4.1 Durability

Durability of concrete is one of the most significant problems within the civil engineering community (Li & Lepech, 2006) which can be attributed to concretes inherent brittle nature as a material. Formation of cracks on concrete surfaces as a result of loading or exposure conditions allows the ingress of corrosives that accelerate the degradation process and thus possibly reduce a structure's life span. The addition of fibres to concrete reduces the size of crack widths through the bridging process but when the fibres are used for structural applications, and not solely to reduce crack widths, it is required to ensure that fibres do not corrode to such an extent that results in failure (whether structural or other).

SFRC fibres are distributed randomly throughout the concrete matrix and surface fibres may lack protection from the alkalinity of the concrete resulting from near zero concrete cover

(Graeff et al., 2009). There is limited information regarding the long-term performance of SFRC structures but there is satisfactory evidence indicating good performance of SFRC in the short and medium terms through laboratory testing. Through the use of applicable laboratory test procedures it is possible to accelerate the corrosion process of a SFRC test specimen which can be used to monitor the external appearance of SFRC during this process and the effect of corrosion on the structural performance through additional testing such as flexure.

Limitation of Crack Widths:

The performance of a concrete structure in terms of its durability is generally influenced by the degree of cracking at its surface. For SFRC's the material can be engineered to limit crack widths at increased strain levels through redistribution of stresses until the material is saturated with cracks (Li & Lepech, 2006). However, this places great dependence on the integrity of fibres especially when used for structural applications. It is thus recommended to limit crack widths as much as possible to minimise the effects of corrosion, these limitations are shown below in Table 5.2:

Table 5.3 Crack width limitations

Regular exposure	0.5mm
Harsh exposure	0.2mm
Severe exposure	0.1mm

The above values are from the *fib* Model Code 2010 (fib Special Activity Group 5, 2010) serviceability limit state design based on crack width limitations (see Section 5.1) and design limits used for precast elements in the construction of the Gold Coast desalination tunnels (Angerer & Chappel, 2008). Generally, it is impossible to estimate crack widths of SFRC without conventional reinforcing as softening occurs at high stresses due to a deviation from a linear behaviour (Angerer & Chappel, 2008). In spite of this, crack widths can be estimated using the RILEM stress-strain design guideline or other applicable models.

Structural Integrity of SFRC Structures:

Fibres bridge cracks formed in the concrete surface and this can be expected to lead to corrosion of the fibres depending on the exposure conditions. According to Graeff et al (2009) three theories exist regarding the corrosion of fibres and the outcomes on the structural performance of the material: a decrease in peak load, a uniform gain in strength resulting from increased fibre friction due to rust formation, or auto-healing of cracks resulting in restoration and an increase in the peak load. The rate of corrosive degradation of SFRC may not be uniform (Graeff et al., 2009) and it is thus necessary to evaluate a structures performance over a long period of time or to perform accelerated material tests.

Graeff et al (2009) performed wet-dry cycle tests to a SFRC material to accelerate and monitor this corrosive process and found that changes in concrete colour resulted from the corrosion of external fibres. The level of corrosion however was reportedly superficial and there were no changes in flexural test results between corroded and non-corroded specimens (Graeff et al., 2009). Li V and Lepech M (2006) performed hot water immersion tests (to simulate humid conditions) on concrete beams with PVA fibres and found that as a result of multiple cracks with small widths, as opposed to large singular cracks, self-healing is possible from 70% in residual stiffness after loading to a recovery of 90% in stiffness. This resulted in an improved bond between the fibre and concrete matrix but the apparent fibre strength decreased, resulting in breaking of the fibres as opposed to pull-out (Li & Lepech, 2006). Although the fibre type differs to steel fibres the results give an indication of the self-healing potential of such systems. These results were shown to represent corrosion at approximately 70 years exposure to hot, humid conditions and can be considered acceptable for most applications.

The author thus recommends that for normal exposure conditions the structural concerns regarding durability can be ignored (provided the 0.5mm crack width serviceability limit is adhered to). However, for more severe exposure conditions consideration must be made for a possible loss in sectional depth due to corrosion of fibres. Based on durability modelling used

for precast elements in the construction of the Gold Coast desalination tunnel, a loss of 25mm at extreme exposures (e.g. sea water) and 15mm for harsh exposure (ground conditions) should be considered as a possible sectional loss of fibres at the exposed face in the design process (Angerer & Chappel, 2008).

Aesthetic Concerns:

As a result of corrosion to external fibres the concrete surface may change in colour with the level of external, superficial damage increasing with exposure time (Graeff et al., 2009). The degree of this superficial damage, however, can be reduced through the use of an adequate concrete mix design. The most important durability design logic is the achievement of "least voids" through the utilization of fly ash and cement paste. The use of Fly Ash to fill the voids between blended aggregates will increase the density of the material and hence reduce the steel fibre reinforcement corrosion (Tsai et al., 2009). It is also necessary to reduce the amount of cracks and their size and a concrete mixture with low water and cement amounts is recommended to achieve this (Tsai et al., 2009). The cement type can also influence the degree of protection and a Cement Type II- limestone can be recommended as the corrosion protection is expected to be slightly higher than CEM Type I materials through a pH being around 13 (Graeff et al., 2009). A uniform fibre distribution reduces the field variability of mechanical properties and hence the degree of cracking, this can best be achieved through the use of a self-compacting SFRC mix (Ferrara & Meda, 2006). The uniform distribution of fibres will also provide a greater resistance against spalling of the concrete and the material can be considered more durable than conventional concrete (Angerer & Chappel, 2008).

5.4.2 Fire Resistance

For the use of steel fibres as a replacement to conventional reinforcing in flat slabs the effects of fire becomes an important design parameter. In terms of safety it is important for the tensile properties of SFRC to remain intact within specific ranges of temperature increase and

to have indicators that allow one to fully assess any possible defects after the incident by means of inspection. Research regarding the mechanical properties of SFRC after exposure to high temperatures has been conducted (Lau & Anson, 2006; Colombo et al., 2010; Sukontasukkul et al., 2010) which reveals that the influence is negligible up to a certain range in temperature.

During the initial phases of temperature increase the behaviour of SFRC remains generally unaffected at relatively low temperatures up till 300-400 °C (Sukontasukkul et al., 2010). At this range the properties of conventional concrete remain unchanged and the behaviour of SFRC is thus not influenced as the steel fibres are unaffected by this increase in temperature. For temperature ranges between 400-600 °C the compressive strength of concrete starts to deteriorate linearly (Colombo et al., 2010) in combination with the concrete un-cracked tensile capacity. However, steel fibres remain intact within this range and the tensile capacity tends towards the steel fibre pull-out residual strength (Sukontasukkul et al., 2010). In some cases the residual tensile capacity has been found to increase slightly (Colombo et al., 2009; Sukontasukkul et al., 2010) and this may possibly be attributed to a hydration process between unhydrated cement particles and left over water in the fibre/matrix interfacial zone (Sukontasukkul et al., 2010). For temperatures above 600 °C the load resistance begins to decrease, although not drastically, and tends towards a fraction of the initial SFRC residual tensile strength. Thus, the failure mechanism at high temperatures in excess of 600 °C can be assumed to be rather ductile and not catastrophic, allowing secondary support mechanisms to become effective. This failure mechanism can be considered similar to conventionally reinforced concrete systems both in temperature range and behaviour.

During the initial phase of heating the concrete strength is unaffected but there is a marked reduction in stiffness (Sukontasukkul et al., 2010). This will lead to an increased deflection and excessive cracking, activating unused fibres which serve as a safety mechanism against a collapsible failure mode. The degree of cracking and deflection may serve as a tool to analyse the level of any potential structural defects during a forensic investigation. An additional tool may be the colour of the concrete which changes when heated up to temperatures around

400°C (Lau & Anson, 2006). The change in colour will vary according to the concrete composition but will generally be slightly yellow for temperatures between 400-600 °C and more reddish in colour for temperatures in excesses of 600 °C (Lau & Anson, 2006). Thus, it may be possible to inspect and estimate the degree of damage to an SFRC structure and determine whether the structural capacity has been influenced.

5.5 Concluding Summary

In summary a number of design models exist in which the beneficial effects of the residual tensile strength properties of SFRC can be utilized, giving insight as to the potential of such systems on a structural level. However, the models make assumptions regarding the relevant mechanisms in an attempt to simplify the complex post-crack behaviour of these composites, and it is necessary to fully understand these assumptions in order to adequately predict the load resistance of the particular SFRC structural system. In addition, the tensile residual properties need to be determined through test procedures representative of the final application and must also satisfy certain minimum requirements for the application of such models to be valid. It must also be noted that the behaviour of SFRC systems can be somewhat unpredictable due to random fibre distributions and the variability must be considered in structural systems where stress concentrations are expected. This places a large emphasis on construction practices implemented in obtaining an even fibre distribution as the design models all assume an isotropic material behaviour. Should these conditions be met the evidence suggests that such systems will satisfy the safety and serviceability requirements necessary for SFRC to be implemented as a viable alternative to conventional concrete systems.

Chapter 6

Mix Design for SFRC

For the construction of flat slabs with steel fibres as the sole form of reinforcement to be possible, it is essential to achieve the required concrete tensile characteristics whilst maintaining an even distribution of fibres throughout the constructed element. In doing so, the potential to fully utilize the fibre fraction is increased and reduces the risk of the formation of weak areas within the SFRC element. In structural applications specific fibre types and volume fractions are necessary according to the function, where these two parameters can have a significant influence on the SFRC fresh and post-crack hardened state performance.

When using SFRC the difficulty in the fresh state is maintaining workability whilst ensuring that the fibres do not segregate from the mixture. Another aspect is the formation of fibre 'balling' during the mixing process which can result in uneven fibre dispersions and thus a non-isotropic material behaviour in the hardened state. Thus, the addition of steel fibres to concrete is known to enhance the post-cracking tensile residual strength properties (di Prisco et al., 2009) but can be associated with a reduction in the workability and the flow characteristics of plain concrete essentially (Walraven & Grunewald, 2001). As a result alternative mix designs are required depending on the application. The use of higher strength concretes with self-compacting properties is thus more practical, in which a high fluidity and

moderate viscosity can be achieved with reliable and sufficient post-crack material tensile strengths.

6.1 Influence of Fibre Volume, Type and Concrete Properties on SFRC

The addition of fibres to concrete alters the post-cracking behaviour in the hardened state (Bentur, 2007). The changes in behaviour can be attributed to a number of factors which include the number of fibres per unit volume, mechanical characteristics of the fibres as well as their size and shape, concrete strength, matrix characteristics and the curing conditions (Chanvillard et al., 1990). It is clear that specific fibre types and the amount added to a concrete mix need to be selected according to the function for which they are intended. Together with this, the concrete strength and its composition can influence the behaviour of the particular fibre type, the material failure mode and the ultimate residual tensile strengths that can be achieved.

6.1.1 Fibre Volume and Type

There are basic groups of fibres applied for structural concretes and are classified according to their material type (Brandt, 2008):

- Steel fibres of different shapes and dimensions
- Alkali-resistant glass fibres
- Synthetic fibres made with different materials: polypropylene, polyethylene, and polyolefin, polyvinyl alcohol (PVA), etc.
- Carbon, pitch and polyacrylonitrile (PAN) fibres

Fibres improve the tensile performance of concrete through crack bridging (see Section 2.1) and the applications of the different fibre types are generally determined by the fibre strength and its elastic modulus. For flexible fibres with a low elastic modulus, such as synthetic fibres, applications are restricted to that of reducing crack widths caused by non-restrained shrinkage of the concrete. The stress in the fibres resulting from shrinkage cracking at the concrete surface is relatively low and the resistance provided by these fibres is sufficient to assist in crack reduction. For cracks created as a result of more significant tensile stresses these fibres tend to yield and fail as the fibre-matrix bond strength may be too high, or in some cases too low resulting in premature pull-out, or the shear stresses generated in the fibre due to frictional slip are too high for the individual fibres to maintain integrity. Thus, steel fibres are generally regarded as the most suitable for structural applications (Brandt, 2008) due to a higher elastic modulus and, generally, a fibre pull-out mode of failure as opposed to fibre fracture.

Within the steel fibre group variances can be in the form of the material strength, the length and diameter of the fibre (which is considered in fibre classification as the aspect ratio, l_f/d_f), and the geometry of the fibre. When using fibre reinforced concrete the post-cracking behaviour of the composite is the critical characteristic, as the activation of the fibres only takes place in the post-elastic phase of the concrete (see Section 2.2). Changes in any of the above mentioned fibre properties can alter the failure mode and hence its suitability for the particular function.

For the addition of steel fibres to be effective a fibre pull-out mode of failure (see Section 2.1) is necessary as this ensures that some form of residual resistance can be achieved in the post-cracking stage. The required strength of the fibre itself is thus dependent on the tensile strength of the concrete and a mechanical mismatch should be avoided. For weaker concretes where cracking occurs at low stresses the required fibre strength is not as high (although dependent on whether a strain hardening or softening material is required), whereas for high strength concretes a high strength fibre is required. It has been suggested that for high

strength concretes a steel fibre of tensile strength as much as 2000MPa may be required (Bayramov et al., 2004).

In addition to the fibre tensile strength the size and shape of the fibre can have a significant influence on the composite behaviour. Fibre length determines the amount of tensile strain that the composite can undergo before ultimate failure occurs due to a loss in residual resistance (resisting frictional force) of the fibre. The diameter of the fibre influences the size of the interfacial transition zone (see Section 2.1). The smaller the diameter of the fibre the smaller the transition zone surrounding it which leads to a higher performance from the fibre (Bentur, 2007). Thus, when classifying steel fibres, these two parameters have been combined and are referred to as the aspect ratio l_f/d_f. The higher the aspect ratio the better the expected composite performance will be in tension for that concrete mix (bearing in mind that factors such as the fibre compatibility with the specific mix design as described in Sections 6.2 and 6.3 are adhered to) in the hardened state (Walraven & Grunewald, 2001). The shape of the fibre (see Figure 6.1) can also influence its resistance and a number of deformed steel fibres are available.

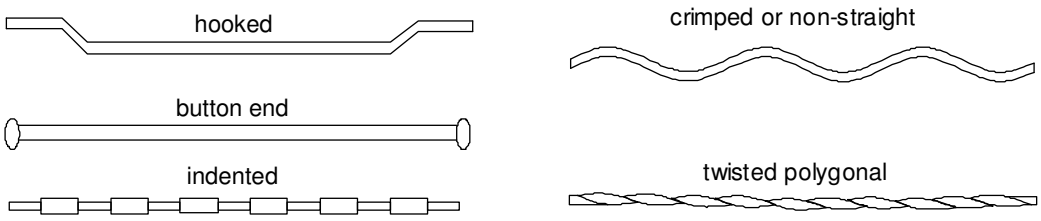

Figure 6.1 Examples of deformed steel fibres (Brandt, 2008)

A deformed fibre has an increased mechanical anchorage as opposed to a straight fibre and this may be considered as the most effective form of resistance provided by the fibre against pull-out (Bentur, 2007). For structural applications, deformed fibres are generally specified due to this higher level of performance.

The fibre strength and shape will influence the behaviour of the composite but a critical aspect determining whether strain hardening or softening (see Section 2.2.1) will occur is the volume of fibres added. For a particular fibre type a critical volume fraction for a specific concrete mix may be determined (Fantilli et al., 2009). According to Fantilli et al. (2009) this behaviour is related to the fibre geometry, concrete tensile strength, bond strength (dependent on both fibre and concrete properties), and the fibre volume fraction. Depending on the concrete mix design and fibre type, fibre volumes below the critical volume fraction will experience a strain softening behaviour in uni-axial tension in which a single crack will form in the test specimen. For fibre volumes above the critical volume a strain hardening behaviour will occur in which multiple cracking patterns form under the same test conditions (Fantilli et al., 2009). This concept can be applied to members in flexure; however, support conditions can alter this behaviour in which deflection hardening occurs (see Section 4). Thus, when considering a SFRC mix design it is necessary to evaluate the element type to be constructed and the support conditions under which it will be imposed. The *fib* Model Code 2010 states that for a material to experience a strain hardening or softening behaviour the primary factor is the volume of fibres within the mix and that for non-conventionally reinforced linear elements (where there is limited stress redistribution for that particular section) the FRC should have a hardening behaviour in tension (fib Special Activity Group 5, 2010).

Due to the potential indeterminate support systems used in flat slabs the use of a strain softening material is possible. However, the material is required to undergo deflection hardening in the post-crack state which is dependent on the composites residual strength value and range, which is in turn dependent on the volume and type of fibres where the length of the fibre type generally determines the range. Thus, for a strain softening material to be structurally viable a longer length fibre is required in which an extended residual strength range is achieved allowing for deflection hardening to occur through the redistribution of stresses over the concrete volume.

6.1.2 Concrete Properties

In addition to fibre type and volume added another aspect to consider is the concrete properties, in particular the concrete strength. For a higher compressive strength there is a higher concrete tensile strength, which will influence the fibre behaviour. As described in Section 6.1.1 above an increased cracking stress may cause the fibres to fracture at activation, eliminating the benefits gained from fibre addition. An increase in bond strength between the fibre and the surrounding concrete matrix will occur with an increasing concrete compressive strength (Xu & Shi, 2009) and this bond strength can alter the failure mode of the particular fibre type from pull-out to fracture or vica versa. The increased bond strength can be beneficial for a sufficiently strong fibre as an increase in the composite tensile strength after initial cracking can be achieved. However, once the fibre-matrix bond has been broken through opening of the crack mouth the residual strength is determined by the density of the surrounding concrete matrix and the fibre mechanical properties, such as anchorage and roughness of the fibre surface (Bentur, 2007). An increase in density of the concrete matrix results in an increase of the frictional force which will improve the strength of the residual stress. In some cases the modification of the concrete matrix with additives such as fly ash, silica fume, polymers, etc. has been practiced to increase the composite residual stress (Bentur, 2007). For an increase in the matrix density benefits in the hardened state such as composite durability (see Section 5.4) and in the fresh state (see Section 6.3) can also be achieved.

6.2 Self-compacting Concrete and its use with Steel Fibres

Self-compacting concrete (SCC) is an innovative concrete in which no vibration is required during placement or to achieve compaction. The fluidity and segregation resistance of SCC ensures a high level of homogeneity, minimal concrete voids and uniform concrete strength, providing the potential for a superior level of finish and durability to the structure (Self Compacting European Project Group, 2005). An important characteristic of SCC is that it can

be designed with materials that are used for conventional concrete mix design in which the high level of fluidity is achieved through the addition of admixtures such as super plasticizers. However, as a result of achieving this high level of fluidity SCC mix designs are generally sensitive to fluctuations in total moisture content and changes to raw material gradations and moisture content can have a dramatic influence on the stability of the mix (RILEM Technical Committee 188-CSC, 2006).The addition of steel fibres to the mix further complicates the design as an increase in fibre volume percentage is associated with a reduced flow and deformability of the self-compacting steel fibre reinforced concrete (SCSFRC) mix (Walraven & Grunewald, 2001). A SCC with a dense matrix and high viscosity is also required of the mix design when using steel fibres. A fluid mixture with a high viscosity will fully suspend the fibres and an increased aggregate packing density will minimize the possibility of fibre 'balling' during the mixing and casting process.

The concrete materials selected and the final hardened concrete product of the SCSFRC need to meet the requirements as per conventional concrete and those set by the SFRC design. With respect to the raw materials used changes in the water (i.e. fresh, recycled, etc.), cement and aggregate type can have a significant influence on the behaviour of the SCSFRC mix and the principles regarding SCC need to be applied. Fibres used with a high aspect ratio, as is needed for structural applications, reduce the workability and flow of the SCSFRC mix, as does an increase in the fibre volume, and a change in either of these criteria may thus require a redesign of the mix in order to achieve the desired performance level (Walraven & Grunewald, 2001).

It has been found that a SCSFRC mix design with a considerable amount of fibres of a high aspect ratio can still achieve self-compacting properties (Walraven & Grunewald, 2001) and the fibre distribution through the element can be influenced according to the casting technique implemented (Mueller & Holschemacher, 2009). In industry, where slabs have been constructed using only SFRC without conventional reinforcing, the use of SCSFRC is dominant due to its practicality and ease of construction (Destree, 2009).

6.3 SCSFRC Design Principles

SCC has an extremely large range of particle sizes from micrometre size fines to centimetres for course aggregates (RILEM Technical Committee 188-CSC, 2006). The fundamental concept is particle suspension, in which course aggregates are suspended throughout the concrete matrix by the finer mortar or paste. This concept is also applied to SCSFRC, in which the fibres are suspended throughout the matrix together with the aggregates.

For a fixed paste density, the fluidity of the concrete mixture is mainly dependent on the thickness of the paste layer coating the aggregate and fibres, where the paste in the interspace among aggregates has little contribution to the fluidity (Zhu et al., 2009). For a SCSFRC mix, sufficient paste is required to enable a self-compacting flow but excessive paste may result in fibre 'balling' due to an insufficient packing density of the matrix. It is thus necessary to have a sufficient particle size distribution to attain the required packing density for the fibre type and volume. In addition, although a sufficient particle size distribution is required, when fibres are used a shift from course to a finer aggregate mix design is required to ensure adequate filling capabilities in reducing fibre 'balling' potential (RILEM Technical Committee 188-CSC, 2006). It has been noted (Construction Competenece and Consulting, 2011) that the larger the maximum size aggregate and aspect ratio, the less volume fraction of fibres can be added. In addition to preventing fibre 'balling' it is necessary to ensure that fibres are suspended throughout the mixture and the introduction of a pozzolanic material such as fly ash will create a more viscous concrete mix. Pozzolanic materials are generally introduced to improve and maintain cohesion and segregation resistance and the addition of fly ash has been shown to be effective, although high levels may produce a paste fraction that is so cohesive that the flow properties are restricted (Self Compacting European Project Group, 2005).

Generally, there are limited theoretical design procedures for SCC and those available can prove to be rather laborious. This is mainly due to the sensitivity of a SCC mix design with regards to the raw materials used. The design concept of SCC is based on the following

principles: limited aggregate content, low water-powder ratio and the use of super plasticizer (Tang & Schouenborg, 2009). Thus, in this investigation the design of a SCSFRC mix is based on proportioning techniques in conjunction with the fibre volume dosage required to achieve the necessary mechanical properties. The higher the aspect ratio and volume of fibres added the higher the level of viscosity, whilst maintaining fluidity, which is required of the concrete in the fresh state. The level of performance is dependent on the grading of the aggregates used and the amount of fines present in the mixture, where the addition of fillers such as fly ash with increased quantities of super plasticizer may allow one to achieve the desired properties should there be a lack of fines within the aggregates. It is not possible to prescribe desired aggregate grading curves for a SCC as this can be misleading (Koehler & Fowler, 2007).

The fresh state material performance is dependent on, among many factors, the shape of the overall grading curve of the mix as well as the actual shape of the aggregates used. The differing aggregate particle shapes relate to the total aggregate surface area for a particular concrete mix, which in turn is highly influential on the paste content required. However, Bhattacharya et al. (2008) found that for a SCC with a more evenly distributed course aggregate grading the better the flow characteristics that were obtained, and that for a higher fraction in large stone aggregate used the potential for static segregation was more likely (Bhattacharya et al., 2008). Generally, the different aggregate partical size ranges can be split into three different chategories (Bhattacharya et al., 2008): particles greater than 9.5mm in size contribute to the strength of the concrete in the hardened state, particle ranges between 9.5mm and 2.36mm are related to the mobility in the fresh state, and particles smaller than 2.36mm influence the workability of the mixture.

The fresh state flow properties will have to be verified through trial mixing and adequate test procedures in the laboratory conducted by experienced personnel. Table 6.1 below is based on the recommendations made by the Self Compacting European Project Group (2005) and is an approximation for material proportion ranges for a SCC mix where aggregate gradations and shape have not been taken into account (note that powder refers to cementitious

materials). Mix designs are not restricted by these values and for SCSFRC the proportions regarding course aggregates will have to generally have a smaller particle size than that used in conventional SCC.

Table 6.1 Material proportion ranges for an SCC mix design (Self Compacting European Project Group, 2005)

Constituent	**Typical range by mass (kg/m^3)**	**Typical range by volume (litres/m^3)**
Powder	380 - 600	
Paste		300 - 380
Water	150 - 210	150 - 210
Coarse aggregate	750 - 1000	270 - 360
Fine aggregate (sand)	Content balances the volume of the other constituents, typically 48 - 55% of total aggregate weight.	
Water/powder ratio by Vol		0.85 - 1.10

6.4 Requirements of SCSFRC and Test Procedures

As discussed previously it is necessary to achieve homogeneous fibre distribution throughout the SCSFRC mix to ensure that the design material properties are consistent throughout the element. When considering SCSFRC the passing ability, viscosity and segregation resistance will influence the homogeneity of the mix, and thus the hardened state properties of the concrete. These factors need to be monitored during the mix design and trial mixing process. For flat slabs constructed without conventional reinforcing the passing ability of the mix is not as critical and thus the number of applicable test procedures can be reduced.

The most suitable test procedure, and most common for SCC, is the slump flow test. The test, using a slump cone, gives an indication of the flow capabilities of the fresh mix in unconfined conditions. Additional information regarding the viscosity and segregation resistance can also visually be interpreted. Should further information regarding the viscosity and flow rate be

required, the V-funnel test can be used so as to give an indication (Walraven & Grunewald, 2001).

Figure 6.2 Approximate circular slump flow shape and close up of even fibre distribution

According to Walraven & Grunewald (2001) a minimum slump flow of 600mm is required to ensure self-compaction in a SCSFRC, but this can be reduced to 500mm depending on the construction specifications and conditions. In addition to this the shape of the test specimen needs to be approximately circular, as fibres tend to bundle in the centre and restrict flow direction which can result in segregation for poorly graded mixes. An adequate mix will thus have a sufficiently high viscosity to evenly distribute and suspend the fibres throughout the mix to the edges of the test sample during slump flow testing. During the test procedure it is essential to monitor that fibres and course aggregate do not segregate from the mix and that surface paste is minimal. The amount of surface paste will give an indication of the design mixtures robustness against fibre and particle segregation as a result of possible variations in raw aggregate moisture levels for the particular mix design, although this evaluation can be subjective.

Chapter 7

Construction using SFRC and Economic Implications

7.1 Considerations when using Steel Fibres

The use of SFRC in structural applications without conventional reinforcing requires that fibres are homogeneously distributed throughout the constructed element. This is particular in flat slab construction where the redistribution of stresses in resisting the applied forces is necessary. To obtain an even distribution of fibres can lead to a number of practical difficulties and calls for greater attention to detail than normal concrete construction (Oslejs, 2008). To reduce the risk associated with SFRC construction it is necessary to use SFRC mixtures of adequate fresh state performance in combination with the correct placement techniques in order to obtain an isotropic material behaviour.

An intrinsic problem associated with SFRC is the reduced workability for an increase in fibre aspect ratio (length/diameter) and volume content within the mix. For a SFRC mix to be structurally suitable a relatively large volume of fibres is required, with a sufficiently high fibre aspect ratio, whilst maintaining adequate workability to allow placement, consolidation, and finishing with a minimum of effort. Thus, to make the use of SFRC more practical the

mix design should be self-compacting (Walraven, 2009). A suitably designed mix will flow during the casting procedure, suspending and distributing the fibres evenly throughout the casting area. It has been noted that when using SFRC it is essential that the mix be self-compacting as this reduces the field variability of mechanical properties (Ferrara & Meda, 2006). It is essential to ensure that the correct concrete mix design is used according to the structural application (see Section 5). In addition, the use of a SCSFRC mix eliminates the requirement for poker vibration which can lead to fibre segregation.

As discussed in Chapter 6, another associated problem with the use of SFRC is 'balling' of the steel fibres. This is also dependent on the volume fraction and aspect ratio of the fibres and can be reduced through adequate mix design. In addition to this precautions may be made during the addition of fibres to the mixture in order to reduce the risk of fibre 'balling'. According to steel fibre manufacturers Bekaert and ArcelarMittal, the fibres must always be the last component added to the concrete mix and can be done so at the batching plant or on site. The rate of steel fibre addition shall generally be in the region of 30-40kg/min (dependent on fibre type) whilst the mixer is rotating at full speed, after which the mixer is reduced to the recommended mixing speed for 40 to 50 revolutions (Construction Competence and Consulting, 2011). The fibre addition can be done by loading the fibres directly into the mixing truck manually or via a conveyor in an evenly distributed manner to prevent dry 'balling'. Alternatively, blast machines may be used to ensure a constant dosage and even distribution of fibres. Steel fibres are generally supplied in fibre bundles (see Figure 7.1) where the individual fibres have been glued to one another, as with the Bekaert Dramix RC-80/60-BN steel fibres, which reduces the chance of fibre dry 'balling' during the addition process and distributes the fibres throughout the concrete mix as the binding glue joining fibres dissolves when added to the concrete.

a)  *b)* 

Figure 7.1 RC-80/60-BN steel fibre bundle appearance as per Bekaert Catalogue and actual fibre apprearance

7.2 SFRC Construction Techniques:

Once a SCSFRC mixture has been designed and selected, it is highly advisable that a full field batch be processed prior to actual start of construction with the mixing equipment that will be used for the project (Construction Competence and Consulting, 2011). The behaviour of SCSFRC is dependable on the mixing procedure. A pan mixer, as used during small scale trial mixing, will mix the different mix constituents more efficiently than a front loaded or truck mixer. This can become an issue when using steel fibres due to the tendency of fibres to form balls and segregate from the concrete mix. Thus, the fibre dosage rate and methodology needs to be strictly monitored and in accordance with guidelines recommended in Section 7.1 above.

The use of a SCSFRC mix will require skilled labour with strict quality control as correct placement techniques will need to be implemented. SCSFRC can be directly discharged from the mixer truck or pumped using a minimum hose size of no less than 125mm in diameter, or a fibre length of no greater than 70% of the hose internal diameter, with no reducers along the hose length (ArcelarMittal, 2010). To ensure fibre dispersion through critical areas the SCSFRC material is placed at either end of the slab and 'flows' towards the centre, distributing fibres throughout. Consideration may also need to be taken with regards to the cross-section shape as this may also influence fibre field homogeneity (Ferrara & Meda, 2006). It is essential that tightly bound fibre clumps be broken up or prevented from entering

the mix (Construction Competence and Consulting, 2011). All conventional concrete finishing techniques may be implemented excluding vibration as this will lead to segregation of the fibres from the concrete matrix. For a quality finish fibres protruding from the surface will need to be levelled off.

During the casting procedure it is essential to check the dosage rate is adequate, this can be done through taking 10 litre samples at the first ¼, middle and the last ¼ of the concrete discharge load. Wash away the cement paste and aggregate and weigh the remaining fibres. The remaining steel fibre mass needs to be 80% or greater of the target mass for the sample and the average value taken from the three samples is at least 90% of the target value. During this step it is also possible to check that all fibre bundles have opened. Whilst casting sample specimens will need to be taken for testing as is with normal concrete practice. Test samples will need to be taken for both compressive and tensile testing. Generally, fibres used for structural applications are around 60mm in length and 150mm cube moulds will be the most suitable for compression testing.

For tensile testing it is important that the test specimen for structural characterization reproduces as closely as possible the stress field that will occur in the structure as well as attaining the fibre distribution properties which are likely to be featured in structural elements (Ferrara & Meda, 2006). Test samples may be similar to that of the initial material characterization test samples such as 700x150x150mm beams or round panels in accordance with the relevant standards. As there are no standards regarding test sample frequency it is recommended that a minimum of three test samples be taken for each day's placing and from at least every $30m^3$ of concrete cast. Samples shall be taken from a batch of concrete chosen on a random basis. When SFRC is used without conventional reinforcement it is imperative to ensure the structural integrity of the material is maintained and an increased sample frequency may be required depending on the importance and circumstances of the work.

Based on a concrete delivery rate of four trucks per hour using one skilled person to load the steel fibres into the trucks, approximately 6000 kg of fibres can be added in an eight hour day

(ArcelarMittal, 2010). This dosage rate can enable a relatively quick construction period as fibre volumes range around 80kg/m^3 in SFRC for structural applications. The increased construction productivity is evident in projects such as the Ditton supermarket in Latvia in which a 1042m^2, 250mm thick suspended floor slab with a fibre dosage of 100kg/m^3 was constructed in one day (Oslejs, 2008) and the sixteen storey Rocca Tower in Estonia in which a construction rate of one floor slab a week was achieved for most of the project (Destree, 2009).

7.3 State of Construction in South Africa

Globally, poor quality construction has resulted in major durability concerns of concrete structures (Rwelamila & Wiseman, 1995; Lofgren, 2005) and failures resulting from durability issues have become a problem. The cost of repairs due to these failures can be as much as 34% of initial costs, as reported for the average 15 year old building in Sydney, Australia (Rwelamila & Wiseman, 1995), and can amount to 3.5% of GNP for some industrialized countries (Mackechnie & Alexander, 2001). These costs can be reduced by simply constructing better quality structures. In South Africa, the majority of construction firms are characterized by poor capacity, poor quality, low productivity and low profit margins (Sidumedi, 2010). This has led to an increasing amount of remedial work in South Africa at great expense to the client (Rwelamila & Wiseman, 1995). As a result consumer organizations, clients and users have become more conscious of the influence of concrete construction quality. It is evident that an indication of concrete quality is the durability of the structure and the owner will have to pay for durability at some stage of the life of the structure (Mackechnie & Alexander, 2001), where the investment in the form of design and construction will bring better rewards than allowing for maintenance.

According to Sidumedi (2009) the economic growth rate in South Africa has increased since 1994 from 0.8% to 3.6% in 2004 yet the construction industries contribution to the GDP has shrunk from 7% in the 70's to 3% in 2002 (Sidumedi, 2010). In order to produce reliable and durable structures on time with little rework and maintenance a quality assurance program is

essential in detecting and eliminating errors. In South Africa it has been reported that as many as 70% of contractors do not have quality assurance programs in place for most concrete construction practices, where concrete quality is regarded as the suppliers concern and reinforcement positioning is only checked through a final inspection by the engineer (Rwelamila & Wiseman, 1995). To produce quality structures it is necessary to have the correct cement ratios, cover to reinforcement, compaction and curing. Adequate compaction and cover to reinforcement will largely influence the onset of corrosion but these two components have the greatest risk of error during the construction process due to inadequate quality control. According to the Hot Dip Galvanizers Association of Southern Africa under normal exposure conditions reinforcement with 24mm nominal concrete cover will give an estimated 100 years until the onset of corrosion, whereas a nominal cover of 12mm reduces this to 15 years for the corrosion initiation. Thus, in order to reduce unnecessary expenditure on repair maintenance and save time during the construction process in reducing the amount of rework the construction industry needs to prioritise service life design and the implementation of the correct construction techniques and technologies.

In order to improve the state of the South African construction industry organised quality management needs to be implemented. With regards to durability this concerns the assurance of correct concrete batching, placement of reinforcing, compaction and curing. Apart from improvements in management control it is possible to have reliability engineered into a product, where the use of cutting edge technology enables organizations to produce products of the highest quality more cost effectively. This is evident in Japan, where the construction industry invests heavily in research and development and has resulted in Japanese contractors being renowned to be the best in the world with high production rates and fewer defects (Sidumedi, 2010). In South Africa the construction industry is epitomized by a lack of research and innovation, reducing the potential of new systems that could be recommended to prospective clients. This lack of innovation has resulted in the construction industry falling behind other manufacturing industries in terms of quality, productivity and value for money (Sidumedi, 2010). In order to improve the performance of South African construction firm's

research development, innovation, benchmarking, and customer orientation need to be prioritized (Sidumedi, 2010).

The introduction of SFRC systems is a step towards improved durability of future structures through technological innovation. The material is characterised by smaller crack widths and a greater resistance against spalling of the concrete (see Section 5.4.1) and, if constructed correctly, is homogenous in nature reducing the risk of weak zones in which corrosion can take place. As the construction sequence is automated the errors introduced through on-site supervision and labour issues can be mitigated. Savings in both the short and long term may be possible through accelerated construction programs and reduced maintenance in the years following the project completion.

7.4 Economic Evaluation of using SFRC

In evaluating SFRC in financial terms it is necessary to look at both the short and long term associated costs. For concrete construction in general there are several considerations for short term costs of which will include that of material choices, labour and associated working hours, including that of the machinery required for the different processes. The long term costs will consider the integrity and life span of the structure along with the relevant maintenance plans, of which the majority of costs will impact the owner. It is thus important for potential construction clients to be well informed of the costs and implications regarding the various forms of construction and for representatives such as engineers to explore and understand these possible alternatives.

As a material, SFRC is considered expensive in comparison to conventional concrete. The use of steel fibres requires special production techniques and, when used in South Africa, fibres will need to be imported as they are not currently manufactured locally. The specific concrete mix design will need to be engineered to suite the fibre type and dosage volume and, in the case of a SCSFRC mix, when compared to conventional concrete will require a smaller

course aggregate particle size, an increased paste volume and the use of admixtures such as a superplastisizer is necessary (see Chapter 6).

However, short term savings are possible. In flat slabs there is potential to eliminate the use of conventional reinforcing when using SFRC. Thus, savings can be made on the reinforcement itself as well as the labour and time required to fix reinforcing in position, which has been noted to take up the second largest portion of man-hours behind formwork (Lofgren, 2005). Lead times associated with reinforcing are also eliminated, which includes design, detailing and the generation of bending schedules as the material is considered isotropic which simplifies the design process. Transportation costs will be reduced as concrete and reinforcing are now combined and the storage of reinforcing on, or off, site will not be necessary, which also reduces the chance of theft which is considered a major problem in South Africa. With the elimination of conventional reinforcing and the automation and mechanisation of using a SCSFRC the potential for a reduced completed construction period is great and savings on potential project "preliminary and general" (P&G's) can be made. This saving may have more than a monetary value for projects with tight and strict time limitations.

Long term savings when using SFRC are also possible. As described previously, construction in South Africa is associated with poor quality and low productivity. Poor productivity can be associated with the intensive labour techniques used in South Africa and the amount of rework that is required. Poor quality is as a result of a lack of supervision and mismanagement of these intensive labour operations. For a correctly designed SCSFRC the increased mechanisation and automation of the construction process has a built in quality assurance. Cover to reinforcing and the concrete compaction are no longer variables and concerns in the construction process and costs associated with rework and repair are reduced or even eliminated for these structures. Maintenance of structures is less regular and intensive as SFRC is, in general, considered far more durable material than conventionally reinforced concrete (see Section 5.4). The savings associated with a more durable structure will

ultimately benefit the owner and the construction of more durable structures will increase the economic productivity of the South African construction industry as a whole.

The use of SFRC is influenced by the market situation regarding the cost of material and labour. Currently, high material production costs in combination with relatively low labour costs may indicate that use of SFRC in structural applications may not yet be feasible in South Africa. However, further research is required regarding the costs and savings associated with using SFRC only for structural applications. Its use will require the integration of the differing disciplines with regards to design and construction due to the high level of skill required in its production. Implementation of SCSFRC may increase the efficiency of the construction process through possible savings in time and improved quality. Thus, applicability of SFRC will be project specific and may only be feasible in large scale structures where fast-track production is necessary whilst maintaining quality. A shift in mind set is required of the industry for SFRC construction in South Africa to become a reality. The focus needs to be taken away from short term savings with extensive maintenance plans to a process of construction focused on life cycle serviceability and investing in quality that ensures long lasting, durable structures.

7.5 Concluding Summary

For SFRC systems to become a viable alternative to conventional concrete systems a number of criteria need to be met. With regards to the mix design the correct fibre type with a sufficient volume fraction is required to obtain the necessary post-crack tensile capacities whilst workability of the material is maintained in the fresh state. In addition to this, the distribution of fibres needs to be even throughout the mixture where adequate construction practices with strict quality control will need to be implemented to ensure this. However, should these criteria be met a more durable structure with an increased service life will result. As the current state of construction in South Africa is plagued by structures with poor service life and durability issues the introduction of SFRC systems can be beneficial. The increased automation with regards to construction practice reduces the need for extensive on-site

supervision and can increase productivity through accelerated programming. This can lead to short term savings as well as long term as the need for extended maintenance programs is reduced through an improved quality in structures.

Chapter 8

Test Setup and Procedures

The objective of this thesis is to investigate, evaluate and possibly reveal issues concerning both the theoretical and practical methods and standards implemented in the construction of SFRC flat slabs in a South African context. Thus, an experimental study regarding the influence of fibres and the different types on concrete material properties in both the fresh and hardened state was required. In addition, as the use of SFRC only (i.e without conventional reinforcing) in the construction of flat slabs in Europe is relatively limited, and non-existent in South Africa, it was also required to investigate the behaviour and performance of full scale structural elements designed according to material properties determined from smaller test specimens.

The test program was constructed accordingly so as to reveal issues that may concern both the theoretical and practical use of a SFRC only system in all phases. Thus, the program was targeted at:

- Defining the influence of aggregate and fibre type on SFRC fresh state performance
- Determining the effects of fibre type and concrete strength on the tensile performance of SFRC through three-point beam testing.

- Evaluating the flexural performance of a full scale flat slab under SLS and ULS load conditions; monitoring crack patterns and size, deflections and load capacities.
- Evaluating the punching shear resistance of SFRC slab panels and to determine the contribution of steel fibres to the resisting mechanism.

The fresh state properties were evaluated for self compacting SFRC with regards to variations in fibre type and raw aggregate materials through a series of flow testing experiments. The hardened state material properties were evaluated with reference to the selected mix designs and certain properties were used for the design of full scale slab test specimens. Full scale slab testing was conducted so as to investigate the applicability of various design models, and their assumptions, based on material properties determined from beam testing, were the focus of the investigation was targeted at revealing slab moment and punching shear resistance together with crack patterns and deflections under applied load conditions.

8.1 Aggregate and Fresh State Properties

8.1.1 Experimental Method

Four self-compacting SFRC (SCSFRC) reference mixtures were developed with different mixture compositions. Initially, it was intended to use the same mix design with different fibre types but after initial testing it was decided to alter the mix design according to fibre type and due to changes in raw aggregate suppliers. Table 8.1 shows the mixture compositions. The mixtures differed in either or both fibre type and/or aggregate type and thus the mix proportions with reference to these changes had to be adjusted. Changes in aggregate type were due to different suppliers used by Stellenbosch University (SU) and those used by the local Ready Mix supplier Lafarge, whom donated the concrete for the construction of the full scale slab test specimen. The steel fibre percentage remained unchanged between the mixes at 1% by volume as this was deemed the most suitable quantity

for structural applications whilst remaining workable enough for standard construction practices.

Table 8.1 Mixture composition for experimental mixes

Materials	**Mix 1** kg/m^3	**Mix 2** kg/m^3	**Mix 3** kg/m^3	**Mix 4** kg/m^3
CEM II 32.5R Cement	350	370	-	-
CEM I 42.5N Cement	-	-	370	370
Dura Pozz Fly Ash	210	235	250	250
Greywacke Stone 13 mm	254	-	-	-
Greywacke Stone 6 mm	382	635	-	-
Hornfels Stone 6 mm	-	-	760	635
Sand (Malmesbury/Klipheuwel)	936	934	835	917
Water	210	195	180	195
Chryso Fluid Premia 310 SP	4.025	3.98	5.6	5.79
30mm Dramix ZP 305 fibres	78.5	-	-	-
60mm Dramix RC 80/60 fibres	-	78.5	78.5	78.5
TOTAL:	2425	2451	2479	2451

All mixes were designed to be self compacting based on investigations by Walraven and Grunewald (2001) and the recommendations by various authors such as Walraven (2009), Destree (2009) and Oslejs (2008) that SFRC should be self-compacting or at least as workable as possible. Thus, characteristics in fresh state flow properties were considered in which an even distribution of fibres without segregation was required whilst maintaining self-compacting properties. Changes in mix design were made when it was evident that for a change in fibre or aggregate type the specific mix design was no longer valid and did not meet requirements. The changes to the design were made using proportioning techniques and the fresh state performance was validated through trial mixing.

8.1.2 Materials

A CEM II 32.5R, supplied by PPC and marketed as Surebuild, was used in Mixes 1 and 2 so as to achieve a concrete compressive strength in the range of 35-50 MPa, ensuring fibre pull-out as opposed to fibre rupture during flexural testing at ultimate loading. For Mixes 3 and 4 a CEM I 42.5N, supplied by PPC and marketed as OPC, was used as this was the cement type used by concrete suppliers at the time within the local area. Cement was used in combination with Dura Pozz fly ash to make up the powder materials and paste, of which the volume ratio was adjusted between the different mixes according to performance during flow testing.

Malmesbury and Klipheuwel sand (which are similar but for the purposes of this work there will be a differentiation between the two) was used for the fine aggregate content in the differing mix designs. Originally, trial mixing was also conducted using a Cape Phillipi sand in the laboratory, as this was viewed to have a lower organic material content, but it was realised that the lack of an even particle grading distribution made the material unsuitable in combination with steel fibres to create a self compacting mix. The course aggregates used were Greywacke stone of sizes 6mm and 13mm and a Hornfels stone aggregate of 6mm in size (see Figure 8.1). It was evident through trial mixing that for an increased fibre length and aspect ratio a finer course aggregate content was required which was in agreement with recommendations made in the RILEM Technical Committee 188-CSC (2006) and findings by Bhattacharya et al. (2008). The stone particles varied in shape and grading between the Greywacke and Hornfels stones as described in Section 9.3. The super plasticizer (SP) Chryso Fluid Premia 310 was used in all mixes of which the volume amount was adjusted between the mix designs to achieve the required flow properties without fibre or aggregate segregation.

a)  b) 

Figure 8.1 a) 6mm Greywacke stone and b) 6mm Hornfels stone

Two fibre types were used which differed in length and aspect ratio. Fibres used in Mix 1 were Dramix ZP 305 with an aspect ratio of 55 (length = 30mm, diameter = 0.55mm) whilst fibres used in Mixes 2, 3 and 4 were Dramix RC-80/60 with an aspect ratio of 80 (length = 60mm, diameter = 0.75mm). Manufacturers Bekaert recommend that 60mm steel fibres are more suitable for structural applications but due to the availability of materials at the time initial testing was conducted using the 30mm long steel fibres to demonstrate the change in fresh state properties and residual tensile properties of the hardened concrete with respect to the fibre type. Both fibre types had hooked ends and were made of galvanised steel. The fibres supplied where in two formats: 30mm fibres were provided (initially) as individual fibres whilst 60mm fibres were supplied in bundles (see Figure 8.2).

a)  b) 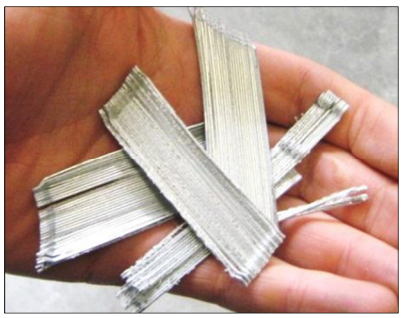

Figure 8.2 Fibre types used in trial mixing a) Dramix ZP 305 fibres (shown here in bundled format) and b) Dramix RC 80/60 fibres

8.1.3 Sieve Analysis

Due to variations in the materials supplied and the sensitivity of a SCSFRC mix design to changes in aggregate properties a sieve analysis was conducted on all aggregates used. The sieve sizes were in accordance with the SANS Method 829, the different sieve sizes being 4.75mm, 2.36mm, 1.18mm, 0.6mm, 0.3mm, 0.15mm and 0.075mm. A pan collected particles less than 0.075mm in size making up the portion of material classified as dust. Preparation of materials for sieving was different to that given in the SANS standard as materials were not washed before drying in the oven. All materials that underwent a grading analysis were dried beforehand in the oven at 150°C overnight to eliminate any moisture within the aggregate. Aggregates were then placed in the top sieve and agitated using mechanical apparatus for 10min, of which the weight retained in each sieve was weighed.

8.1.4 Mixing Procedure

A pan mixer was used during trial mixing and flow testing for all mix types. The mixer was initially cleaned and dried after which the procedure was as follows: powders, sand and aggregate were added to the mixer and mixed for approximatley 10s, after which water was added. Once the water had mixed through SP was added and left to mix further for approximately 2-3 minutes to achieve desired flow properties. Fibres were then added over a period of approximately 90s and the mixture was mixed for an additional 4-5 minutes. The additional mixing time was to ensure that fibre bundles had opened and to achieve a more likely even fibre distribution within the mix.

8.1.5 Test Method

Evaluation of the mix design flow properties was done using the slump flow test in combination with observations made during trial mixing and testing as to the fibre distribution and segregation potential. The slump flow test is performed by filling a slump

cone with fresh SFRC and lifting the cone, allowing concrete to flow outwards. The 'slump flow' is a measurement of the average diameter of the horizontal flow (the largest diameter and the one orthogonal to this) once the flow outwards is completed. Based on observations made referring to flow diameter, final shape and the approximate flow time it was possible to evaluate the design mix stability, segregation resistance and mixture deformability. As the research was focused on the structural use of SFRC without conventional reinforcing no further tests were conducted. For additional test methods refer to Section 6.4 or Walraven & Grunewald (2001).

8.2 Three-point Beam Testing

8.2.1 Experimental Method

Three point beam testing was conducted as a measure for SFRC material characterisation for specific mix types, where the results were used in design models for flexural and punching shear test specimen design. The results also served as a comparative analysis of the influence of fibre aspect ratio and concrete strength with regards to the SFRC material residual tensile strength properties. Through testing the behaviour of SFRC in the hardened state and redistributive potential under flexural loading was revealed. The test procedure was selected for material characterisation as it is a recognised method for use with SFRC and has standardised guidelines as defined by RILEM TC 162-TDF (2002). In addition, the test procedure is relatively easy to perform with test specimens not too large for handling. The test procedure was conducted according to the specifications defined in RILEM TC 162-TDF (2002) (see Section 3.2.2).

8.2.2 Sample Preparation

Beam test samples were constructed for Mixes 1, 2 and 5. Materials used for Mixes 1 and 2 were mixed in the pan mixer (see Figure 8.3) whereas beams cast using Mix 5 (see Section

8.3.2) were constructed from the same material used to cast the flexural test slab and were thus mixed in the Ready Mix truck. In all cases a self-compacting mix design was used and thus no vibration took place. Beams were stripped and placed in curing baths (at 25°C) after 2 days ensuring that the concrete was firm enough for handling. All test beams had a 25mm notch cut into its side a minimum of three days prior to testing after which samples were placed back in the curing baths until the test date. As a measure to determine the concrete compressive strength 100mm and 150mm cubes were cast from the same batch material used to cast the beams and were also stripped and placed in the 25°C curing baths 2 days after casting.

Figure 8.3 Pan mixer and casting of test beams from one side

8.2.3 Test Method

The test procedure was conducted in accordance with RILEM TC 162-TDF (2002), where the test beam was loaded under three-point conditions and the load capacity was measured against the crack mouth opening displacement (CMOD). Test specimens cast using Mixes 1 and 2 were tested at 28day strength whereas specimens cast using Mix 5 were tested on 63day strength so as to coincide with the flexural slab test date.

Specimens were placed on roller pin supports giving a clear span of 450mm (see Figure 8.4). The test load was applied in the form of a point load at mid span above the notch using the

Zwick machine. The load application was deflection controlled at a rate of 2mm/min with termination of the test at a minimum notch crack width of 5mm. Load recordings were made using a 20t load cell. The notch crack width was measured using two LVDT (linear variable differential transformer) deflection sensors placed either side of the specimen of which the average of the two output readings was used to determine the crack width recording. Beam deflection was also recorded using two LVDT deflection sensors placed on the underside of the test specimen. All readings were recorded using an electronic recording system. After testing, beam samples were cut in half so as to give an indication of the fibre distribution and suspension within the sample as a form of evaluation for the mix design resistance to fibre segregation (see Figure 8.5). Cube testing was conducted using the Contest Electronic Load Application machine.

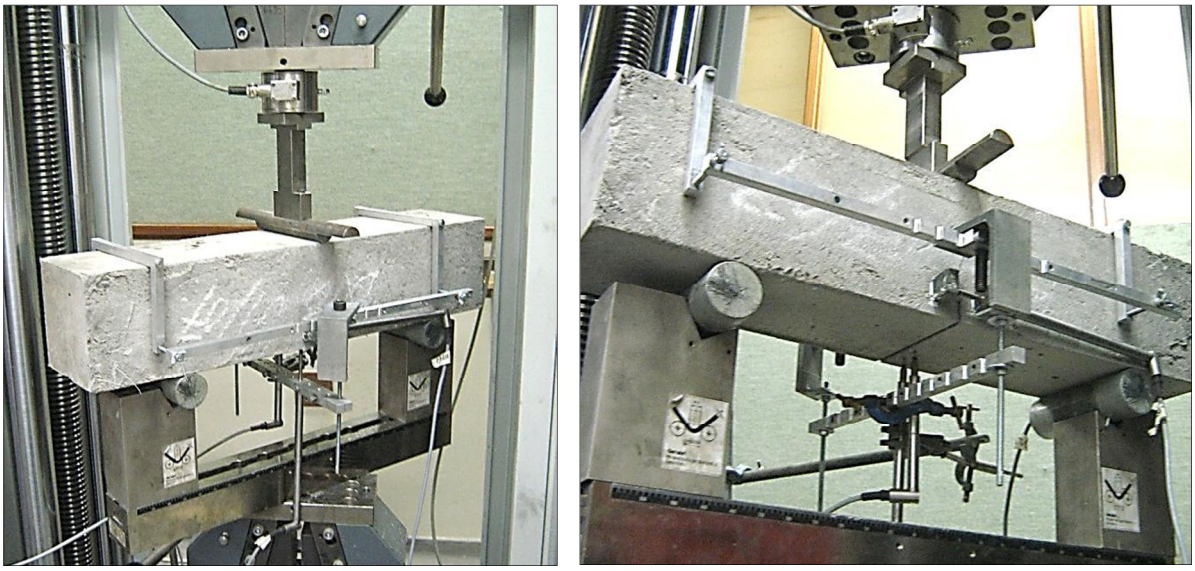

Figure 8.4 Three point bending test setup

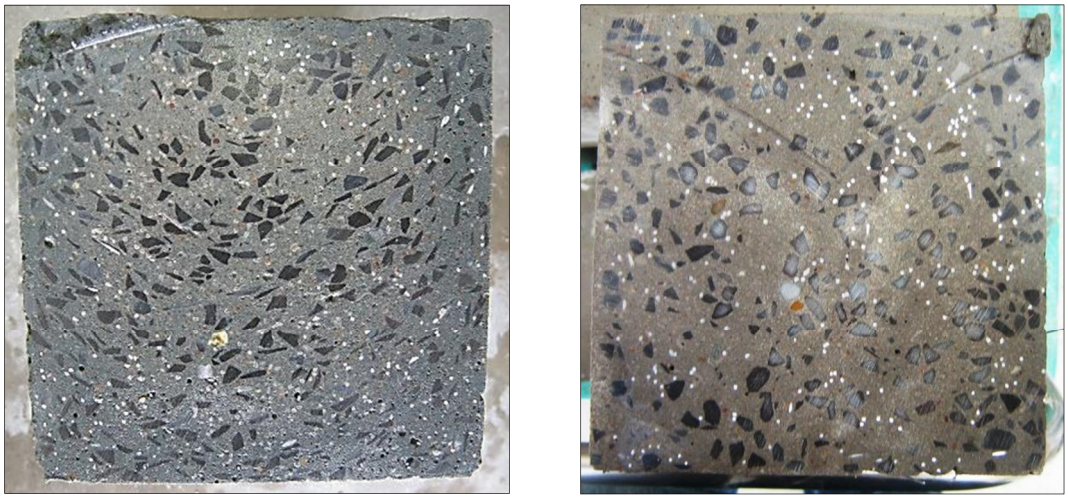

Figure 8.5 Fibre distribution example in test beams for Mix 2 (left) and Mix 5 (right)

8.3 Slab Testing: Flexural Analysis

8.3.1 Experimental Method

A full scale flat slab was constructed to evaluate the structural behaviour of a SFRC only slab under increasing flexural load. The test was aimed at verifying the validity of a number of design models and assumptions made from small scale SFRC test specimens (see Chapter 5). It was also intended to reveal issues regarding the construction process using SFRC and the capacity of the slab to redistribute stresses under increased loading (see Chapter 4).

Initially, a continuous slab system on column supports was considered but as little is known about the moment redistribution properties of SFRC it was decided to construct a 5.7x3.8x0.15m slab with a continuous simple support system along the perimeter so as to create an indeterminate support structure (see Figure 8.6). A slab thickness of 150mm was chosen so as to reduce the influence of the size effect when comparing the slab behaviour to the properties obtained from smaller test specimens. Plan dimensions were chosen so as to

restrict the total slab weight to that of the 10t crane lifting capacity and to suite the support layout to be used.

As the redistribution of stresses under increased loading was considered an important aspect of the structural behaviour it was decided to apply the test load to the underside of the slab allowing one to safely monitor and evaluate the crack development and associate patterns on the top surface. The test load was applied simultaneously in the form of two point loads located at positions deemed suitable to facilitate load distribution within the slab. The structural behaviour of the test slab was then recorded at various loading stages up to and past the ultimate failure load so as to give insight into the ductility of the slab at ULS loading and to verify the various assumptions made in the slab design according to yield line theory.

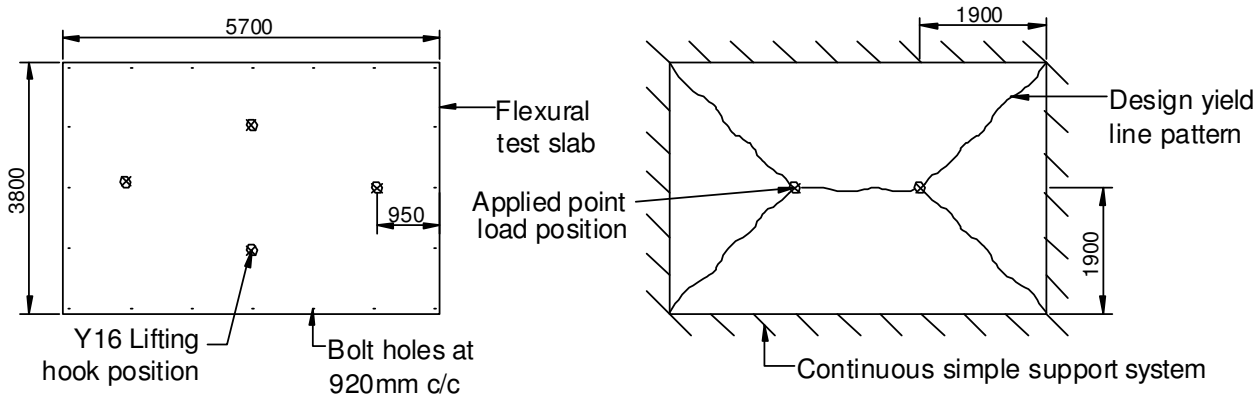

Figure 8.6 Schematic of flexural test slab layout and design yield line pattern

8.3.2 Materials and Mix Design

Originally, it was intended to use SFRC Mix 2 (see Table 8.1) to construct the flexural test slab as both the material fresh state and hardened state performance had been predetermined through initial beam testing. However, as the materials used by the ready-mix supplier differed from those used at Stellenbosch University the mix had to be adjusted accordingly to still meet the construction requirements. Material samples were collected from the Ready

Mix suppliers and trial mixing was conducted to give insight into the material fresh state performance (see Section 8.1), although this was provisional as the mixing procedure used in the laboratory differed from that used in industrial practice.

The aggregate material used in the final test slab mix was a 6mm Greywacke stone (course aggregate) and Klipheuwel sand (fine aggregate) (see Section 8.1.2) in combination with Dura Pozz Fly Ash, CEM I 42.5N cement, water, Chryso Fluid Premia 310 superplasticizer (SP) and 60mm Baekert Dramix RC-80/60 fibres. The water and SP volumes were adjusted during the final mixing process both at the concrete plant and on-site as there was uncertainty regarding the influence of the Ready Mix truck mixing process and the travel time to site (approximately 1 hour) on the fresh state properties. The final mix design labelled as Mix 5 was used to construct the flexural test slab and its constituents can be viewed below in Table 8.2.

Table 8.2 SFRC Mix design 5

Flexural Slab Materials	**Mix 5** kg/m^3
CEM I 42.5N Cement	363
Dura Pozz Fly Ash	242
Greywacke Stone 6 mm	635.7
Sand (Klipheuwel)	923.1
Water	188.3
Chryso Fluid Premia 310 SP	4.2
60mm Dramix RC-80/60 fibres	75
TOTAL:	2435

8.3.3 Mixing and Casting Procedures

The materials used in Mix 5 were mixed in the Ready Mix truck at the concrete plant to a batch volume of approximately 4m^3 of SFRC. The superplasticizer (under batched initially by 1kg) and water (under batched initially by 80 litres) were added to the Ready Mix truck first,

of which were then followed by the powder and aggregate constituents. After approximately 5 minutes mixing time, once all the above mentioned constituents had been added, the fluidity of the mixture was reviewed at the first check point where it was decided to add 20 litres of water to the mix to increase the flow properties. The steel fibres were then added over a 10 minute period to make up a total dosage weight of 300kg (i.e. 30kg/minute). Fibres were added to the truck by hand, done so in an evenly distributed manner so as to decrease fibre 'balling' potential, and were left to mix through the SFRC mixture during the travel to site at Stellenbosch University.

Once on site (approximately 1 hour later) the mixture flow properties were evaluated through two separate slump flow tests (see Figure 8.7). After the first slump flow test it was decided to add 1kg of additional superplasticizer with 60 litres of water in total to achieve the desired flow properties. A slump flow of 400mm, which was less than the targeted 500mm, was obtained in the second slump flow test but was deemed suitable for construction purposes as further addition of water may have risked segregation of the suspended fibres and coarse aggregate. The SFRC material was then transported from the truck to the slab mould via a concrete 'banana' bucket which discharged the material directly into the slab mould at $0.5m^3$ per lift. The concrete was discharged initially at the centre of the slab mould and then at each end alternatively between lifts so as to achieve an even distribution of fibres throughout the slab (see Figure 8.8). Once in the mould, the fresh SFRC was manoeuvred manually using shovels so as to obtain the desired thickness of 150mm throughout the slab (see Figure 8.9).

The casting period lasted for approximately 2.5 hours, after which the surface was floated to obtain a relatively smooth surface with a minimum amount of fibres protruding. The fibres and aggregate were deemed to have remained suspended and evenly distributed throughout the mix during the casting process. To determine material characteristics through small scale testing, twelve beam samples and six 150mm cube samples were cast from the mixture to determine the compressive and tensile strength properties at a later stage (see Section 8.2).

a)  b) 

Figure 8.7 Slump flow specimen appearance a) test 1 and b) test 2

 

Figure 8.8 SCSFRC direct discharge from concrete bucket to flexural test slab mould

 

Figure 8.9 SCSFRC manually distributed to obtain desired levels

8.3.4 Curing, Test Positioning and Test Setup

After casting of the flexural test slab the concrete was left to harden for approximately 24 hours and then cured using wet blankets and water for 14 days. The formation of shrinkage cracking on the concrete surface was considered unlikely due to the presence of steel fibres but curing was conducted so as to reduce the potential of additional tensile stresses being imposed on the fibres. The mould side shutters were removed after one week and no spalling of the concrete was observed. The slab surface was then painted using a white water/chalk mixture which made it easier to spot crack development during the applied test loading.

After 60 days the flexural test slab was lifted into the test position via lifting hooks and placed on four steel struts with bearing pads that offer no rotational resistance (i.e. pinned supports) to the underside (see Figure 8.12). As the test load would be applied to the underside of the slab the implemented test support system was provided by 16mm threaded steel bars passing through sleeves cast in the slab at 920mm c/c, restraining the slab to the laboratory floor system (see Figure 8.11).

The test was performed 63 days after casting. Load application was imposed via two 60t Enerpac loading jacks driven by hydraulic hand pumps, from which load recordings were made using 50t load cells attached to each load jack respectively. Deflections in the slab during load application were recorded on the top surface using eight LVDT deflection sensors (see Figure 8.10). Sensors were positioned so as to give insight into the behaviour of the slab and expected rigid panels that would form within the slab under increasing loads during the test procedure. All readings were recorded using an electronic recording system.

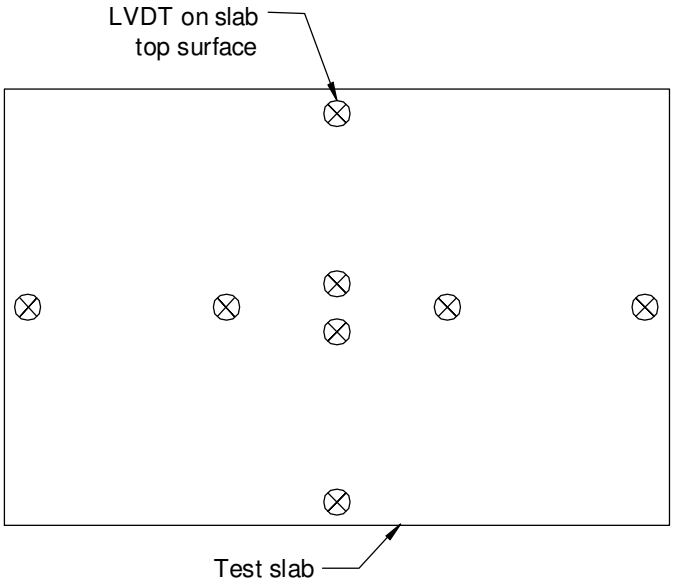

Figure 8.10 Placement of LVDT's on flexural slab tension surface

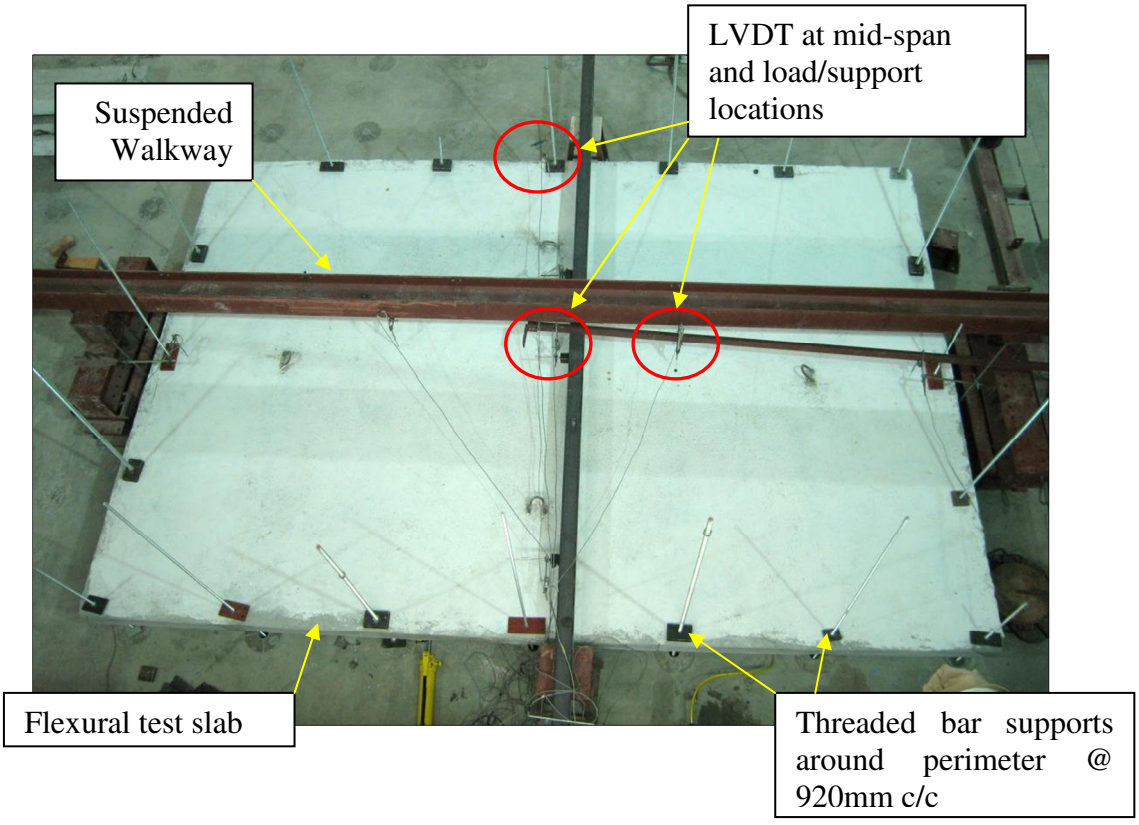

Figure 8.11 Flexural test slab in final test position

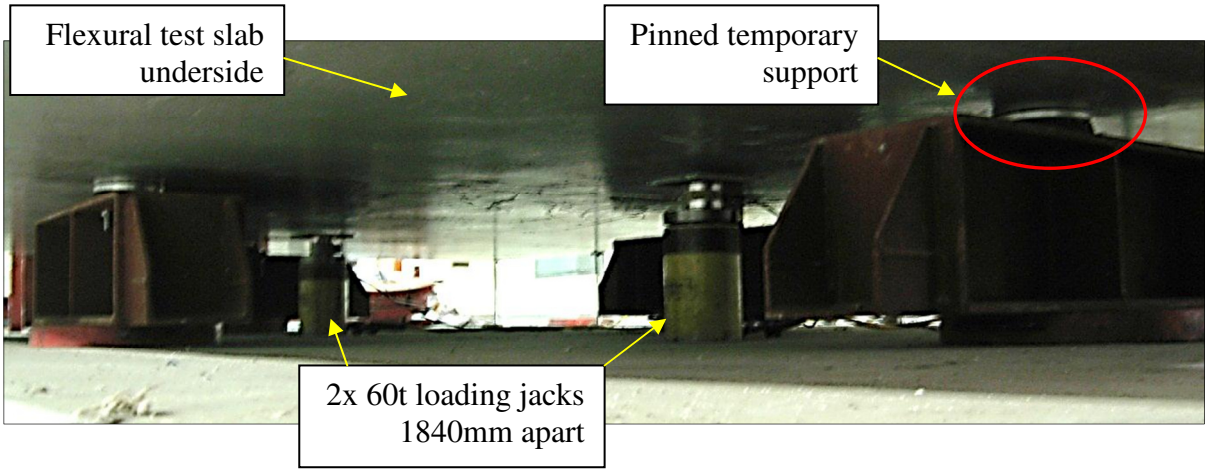

Figure 8.12 Underside of flexural test slab showing load jacks and pinned supports

8.4 Slab Testing: Punching Shear Analysis

8.4.1 Experimental Method

To evaluate the contribution of steel fibres to the punching shear resistance of a flat slab system three identical large scale test specimens were constructed for punching shear testing. As with the flexural test slab the tests were aimed to verify the validity of design models and material properties determined from small scale testing, whilst revealing the structural and failure mode behaviours of a SFRC slab under punching shear conditions. The thickness of each slab was 150mm in depth, so as to be comparable with results obtained from the flexural test slab; with planar dimensions 2m x 2m to eliminate the influence of boundary conditions during the test procedure (see Figure 8.13). An indeterminate support system was applied to all three test specimens to simulate conditions under which punching shear occurs. The test load was applied to the underside of the test specimens via a 150x150x150mm stub column, allowing one to safely monitor and evaluate the crack formation and failure characteristics during the test procedure. Records were made at various load steps to give insight into the specimen behaviours until eventual failure.

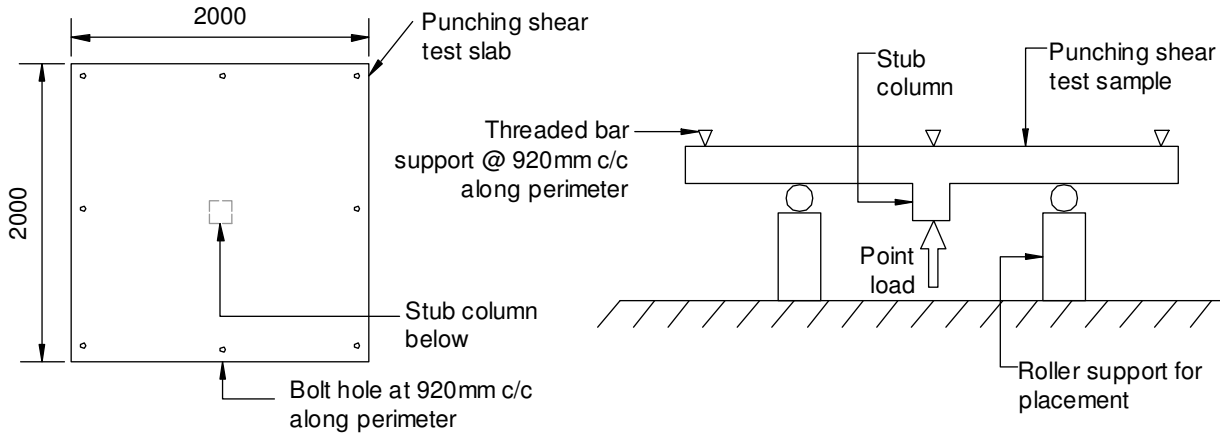

Figure 8.13 Punching shear sample plan layout and sectional support schematic

8.4.2 Sample Preparation

All three punching shear samples were constructed as per Mix 2 in composition (see Section 8.1.1). Materials were mixed using the 0.12m^3 pan mixer making 6 batches (approximately 0.105m^3 per batch) per specimen, adding up to approximately 0.6m^3 of concrete in volume. The fresh material was transported manually using a wheel barrow and placed into the wooden mould directly from one side throughout the casting procedure (see Figure 8.14). The concrete in its fresh state was then evenly distributed in the mould and constantly disturbed so as to reduce the potential for lamination within the cast specimen due to early setting of the lower layers. Towards the end of the casting procedure a 10mm steel mesh with bar centres at 200mm was placed on the to be tensile surface of the sample and covered with an approximate 15mm layer of fresh SFRC. The entire casting process ran over a 4 hour period. The following day after casting of the sample concrete curing was performed using wet blankets and plastic sheeting for a period of no less than 14 days. Test samples could be lifted and moved using the 10t crane and 20mm dowel bars cast into the sample once the test sample had reached a minimum 7 day concrete strength. The slab surface was then painted using a white water/chalk mixture which made it easier to spot crack development during the applied test loading.

a)  *b)* 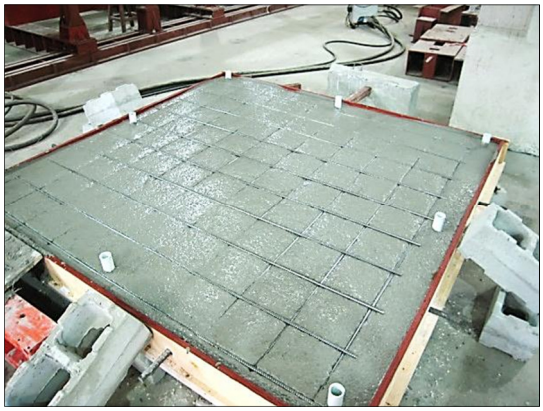

Figure 8.14 a) Punching shear sample casting from one side and b) mesh reinforcing in place before placement of final SFRC topping layer

8.4.3 Test Method

Slabs were lifted and placed on temporary pinned supports and bolted to the laboratory floor slab using threaded steel bars at 920mm c/c along the test sample perimeter, forming the indeterminate support system during the test procedure. As the behaviour of a SFRC only slab panel under applied loading was expected to be dominated by a flexural behaviour a 10mm steel mesh was placed near the tension surface of the test specimen to ensure a punching shear mode of failure. Once the test sample had been lifted into place three LVDT's were positioned in a straight line, one on each edge near the relevant support and one in the centre of the specimen (see Figure 8.15), along the tension surface to record deflections and give a representation of the deformed shape of the test sample during load application.

Due to delays regarding the setup test Specimens 1 and 2 were tested at 30day and 31day age strength respectively, whereas Specimen 3 was tested at the originally intended 28day strength. The load was applied to the stub column using a 60t Enerpac load jack with an electronic hydraulic pump (see Figure 8.16). The applied load was recorded via a 50t load cell connected to an electronic recording system, as were the deflections that were recorded using the LVDT's. The load was applied in 50kN increments until visible cracking had

occurred after which load application was in approximate 20kN increments. At each load step the crack pattern was monitored and marked to allow a progressive analysis of the slab behaviour under increasing load. The slabs were tested until ultimate failure had occurred where the ductility of the failure mechanism was evaluated.

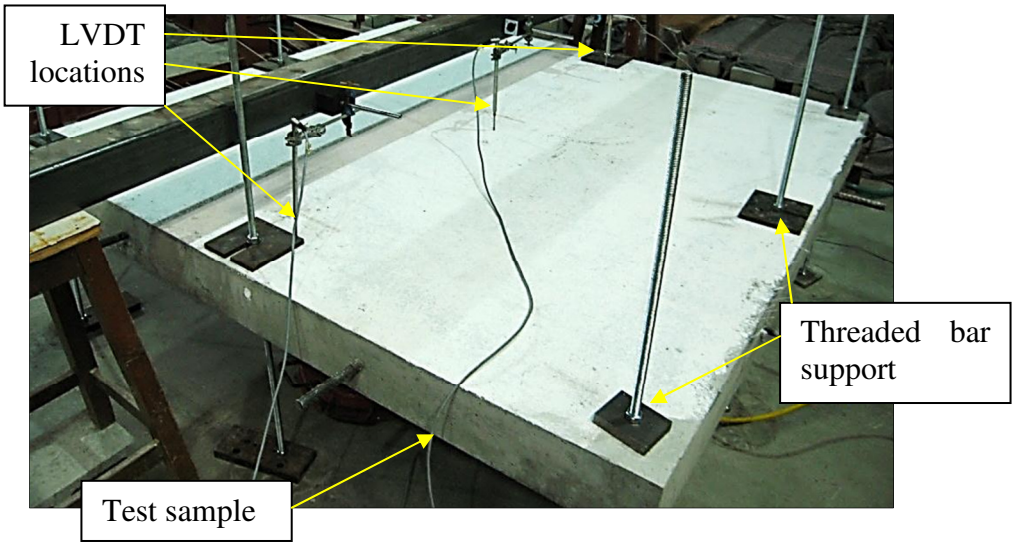

Figure 8.15 Punching shear test setup (top surface)

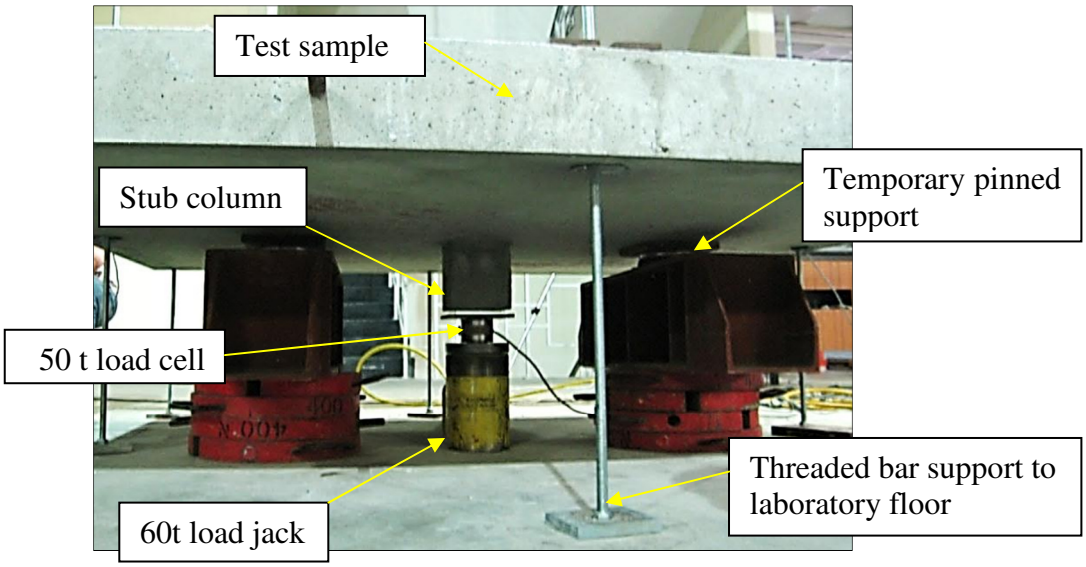

Figure 8.16 Punching shear test setup (underside)

Chapter 9

Test Results and Discussion

The test program conducted revealed the challenges, practical issues and potential of the use of SFRC only systems in flat slab construction. The effects of fibres on the behaviour of concrete can be seen in both the fresh and hardened state behaviour, where adjustments need to be made regarding the conventional concrete methods usually implemented. The results indicate that fibres can significantly improve the post-crack behaviour of concrete through a ductile response but the material performance is highly dependent on the distribution of fibres obtained. It is thus clear that the quality control of SFRC practice needs to be maintained throughout the construction process, from mix design to slab construction and eventual service of the member constructed.

9.1 Aggregate and Fresh State Properties

In order to fully evaluate the influences regarding SFRC fresh state performance the effects of both aggregate and fibre type variance were tested. Fine and course aggregate materials underwent a grading analysis in which the changes of particle distributions could be seen. Through flow testing the effects of the different aggregate types on fresh state performance could be identified with regards to the particular fibre type used, and it was revealed that changes to the mix design need to be made for the different fibre types used. As the aim of

the fresh state tests were to develop a self-compacting mix for full-scale construction slump flow testing was conducted. The results indicate that it is possible to develop a self-compacting SFRC mix although the flow properties are heavily influenced by the presence of fibres within the mix, and adjustments need to be made accordingly.

9.1.1 Aggregate Material Analysis

The stone particle shape of the Greywacke 6mm stone was more angular than that of the 6mm Hornfels stone. The grading of the Hornfels stone aggregate was slightly finer as approximately 25% of particles by mass passed the 4.75mm sieve, as opposed to 5% of aggregate by mass in the Greywacke stone (see Table 9.1). The predominant 6mm stone aggregate used by the concrete supplier is Hornfels, however, initially a 6mm processed Greywacke stone, named as 'concrete' stone, was supplied and initial trial mixing was conducted using this material. The processed Greywacke stone aggregate had a courser particle grading with only 0.65% by mass passing through the 4.75mm sieve, and the aggregate shape was generally more rounded.

Table 9.1 Hornfels, Greywacke and 'concrete' stone aggregate grading's

Sieve Size mm	6mm Hornfels stone Percentage Passing (%)	6mm Greywacke stone Percentage Passing (%)	6mm concrete stone Percentage Passing (%)
12.5	100	100	100
4.75	25.44	5.19	0.65
2.36	6.41	1.37	0.3
1.18	1.69	1.18	0.27
0.6	1.2	0.97	0.27
0.3	1.41	1.2	0.27
0.15	0.85	0.46	0.26
0.075	0.56	0.22	0.1

Three types of fine aggregate were analysed through sieve analysis to identify the characteristics that may influence the behaviour of a SCSFRC (see Table 9.2). The

Klipheuwel sand samples provided by the concrete supplier were collected in separate batches and it was found that slight variances between batches occurred as a result of storage conditions at the plant.

Table 9.2 Cape Phillipi, Malmesbury and Klipheuwel sand aggregate grading's

Sieve Size mm	Cape Phillipi % Passing	Malmesbury % Passing	Klipheuwel Batch 1 % Passing	Klipheuwel Batch 2 % Passing
12.5	100	100	100	100
4.75	100	99.6	99.9	95.74
2.36	100	98.08	99.17	93.26
1.18	100	86.37	85.74	71.55
0.6	96.78	54.65	64.8	37.09
0.3	58.04	31.78	45.93	16.82
0.15	4.48	11.51	16.04	3.82
0.075	0.42	2.04	4.79	0.7

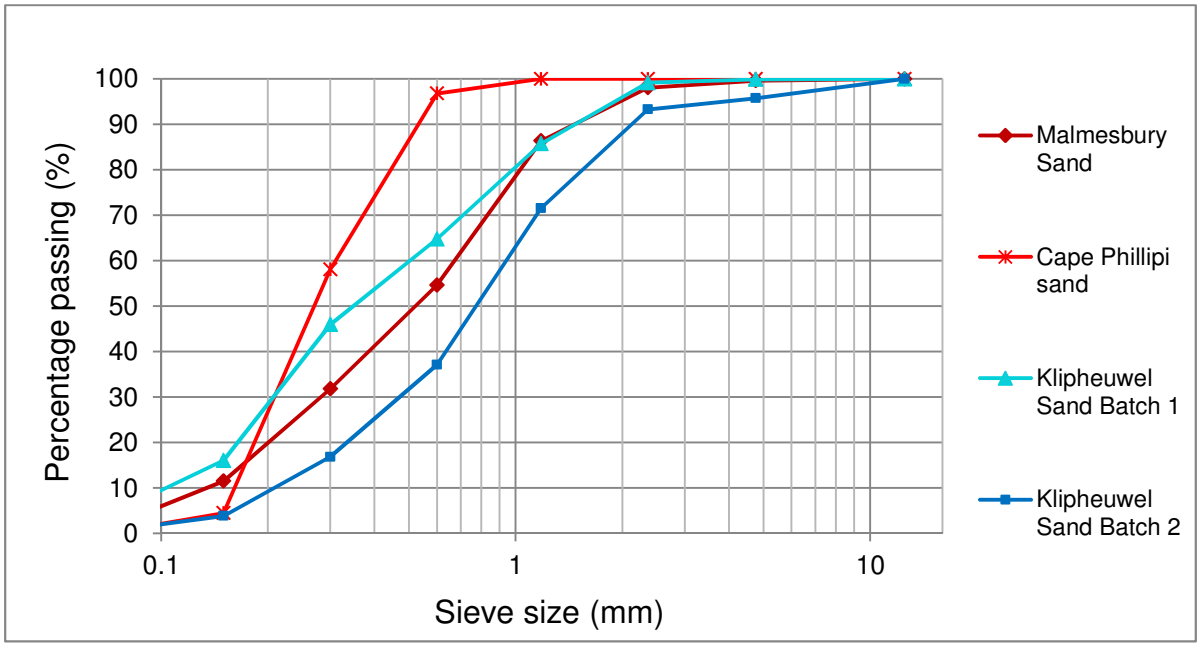

Figure 9.1 *Fine aggregate sieve analysis summary*

As can be seen in Figure 9.1, Cape Phillipi sand is a relatively poorly graded fine aggregate material and not suitable for use in a self-compacting mix. There is a distinct lack in larger particles, which are required to obtain adequate flow properties, as well as in the finer particles which assist in fibre and course aggregate suspension as they increase the mixture viscosity. Malmesbury and Klipheuwel (Batch 1) sand aggregates have a well distributed grading, and trial mixes made with these materials during flow testing produced the most successful and stable test specimens. Klipheuwel Batch 2 sand aggregate, however, had a reduced percentage in finer aggregate particles and it is believed that this was due to storage conditions at the plant. Materials were stored outside in the mixing yard and exposed to varying weather conditions where recent rains may have washed away a percentage of the fines. As a result, the existing SCSFRC mix design was no longer valid and a new mix design was incorporated to compensate for these changes.

9.1.2 SCSFRC Flow Testing

During the mixing procedure it was observed that the addition of steel fibres influences the fresh state properties. The mixture deformability was reduced and, depending on the mixture composition, may have resulted in failure of the mixture through segregation or fibre bundling. Mixtures were tested using the slump flow test.

Table 9.3 Slump flow results for Mixes 1-4

Mix Design	Slump Flow (mm)
Mix 1	525
Mix 2	560
Mix 3	565
Mix 4	500

As can be seen in Table 9.3 above none of the mix designs tested achieved the targeted 600mm slump flow, although results correspond to that recorded by Grunewald & Walraven

(2001) whome achieved a slump flow of 570mm using a 60mm Dramix 80/60 steel fibre (Grunewald & Walraven, 2001). Due to time constraints it was decided that the stability of the mix against segregation was a higher priority than achieving the slump flow recommended by various authors for an idealised self-compacting SFRC mix. The designed mix was intended to be used for the construction of the test slab without reinforcing, thus due to the simplicity of the test slab setup a slightly reduced flow would not significantly impact the construction process.

Results and Discussion

During slump flow testing it became evident that the same mix design could not be used for variations in fibre or aggregate type. SCSFRC Mix 1, which consisted of 30mm steel fibres, could not be used with the 60mm steel fibres as fibre bundling would result. In an attempt to improve the flow of this test mixture when using 60mm fibres the SP volume was increased but resulted in segregation. It is thus clear that when using a longer steel fibre type a finer course aggregate is necessary in order to obtain a sufficient packing density that physically separates the fibres and reduces the fibre 'balling' potential.

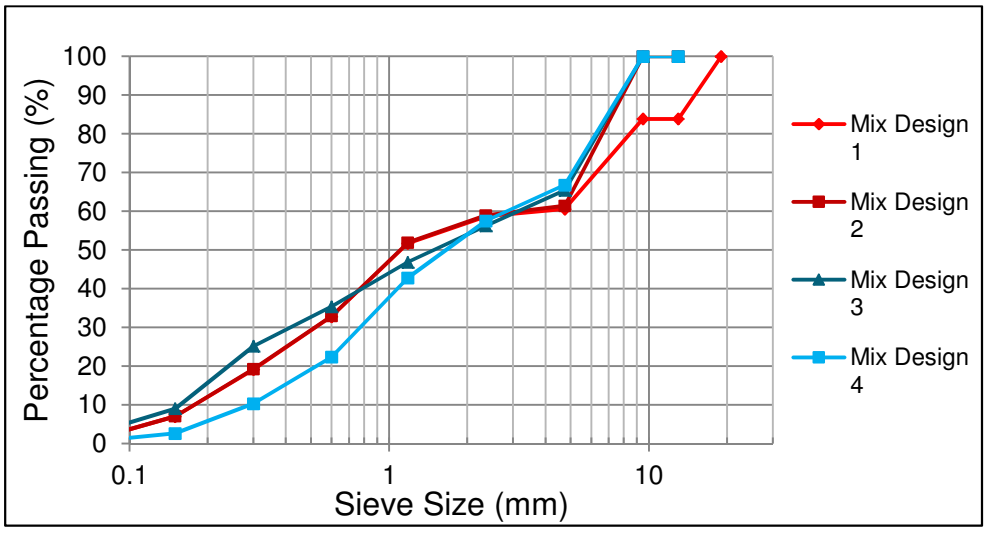

Figure 9.2 *Material grading comparison between various mix designs*

As can be seen in Figure 9.2 the aggregate grading curves of Mixes 1 and 2 were very similar apart from the course aggregate distribution. The mix design was then revised to accommodate the 60mm fibres to create Mix 2, where the 13mm stone aggregate was replaced by the smaller 6mm Greywacke course aggregate by mass, with increased paste content and a reduced water volume. The mix was deemed self-compacting as a slump flow of 560mm was attained whilst maintaining an even fibre distribution (see Figure 9.3).

Figure 9.3 *Even fibre distribution and suspension in fresh state; SCSFRC flow during casting*

Mix 2 was then used with materials supplied by the concrete supplier to check flow properties of the mix with the slightly different aggregate type, which essentially was a 6mm processed Greywacke stone and a Klipheuwel sand classified as 'Batch 1'. Although the grading of the mixes were similar (see Figure 9.4), with the alternate materials having a larger percentage of fine aggregate, the mixture using the alternate materials failed the slump flow test.

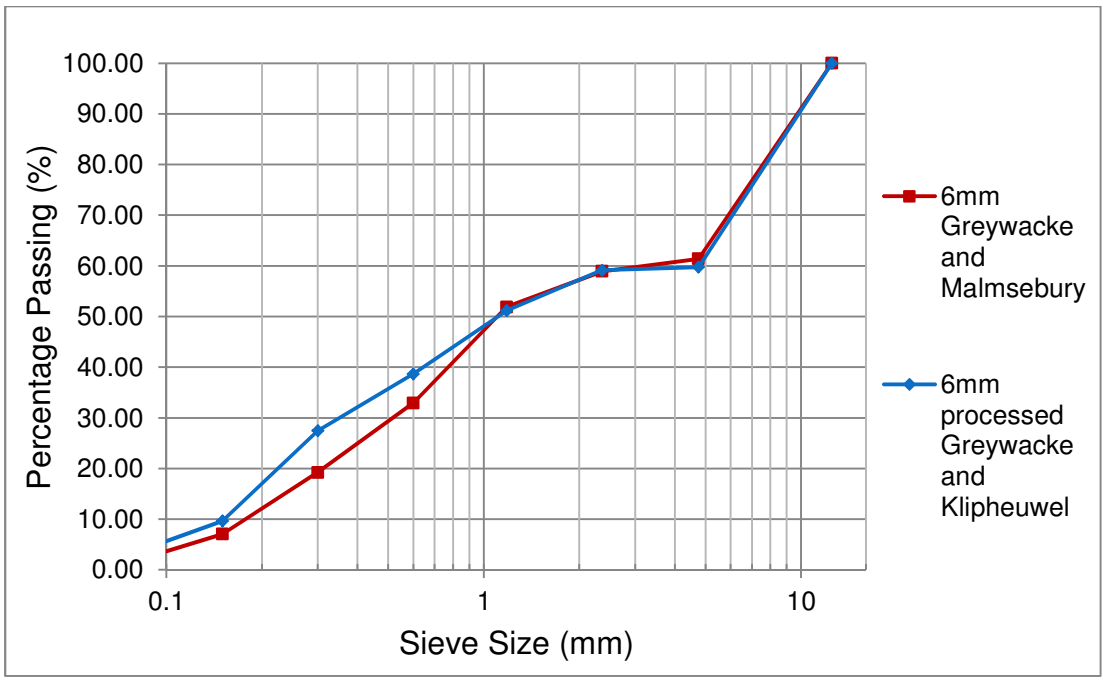

Figure 9.4 *Comparison of grading curve for Mix 2 using different materials*

Failure occurred as a result of the shape of the course aggregate particles, as the processed Greywacke stone had a more rounded shape as opposed to the initially used crushed Greywacke aggregate. This more rounded aggregate had a lower average particle surface area which thus reduced the paste requirement. When using the same mix design excess paste resulted (this was observed during trial mixing) which reduced the aggregate packing density and allowed fibres to entangle and thus restrict flow.

It must be noted that a similar mix design using the 6mm processed Greywacke stone was used for construction of the large scale flexural slab (see Section 8.3). The material was mixed at the concrete plant in the Ready Mix truck and a slump flow of 400mm was achieved. This was deemed suitable for construction purposes at the time.

Mix 3 was then generated using Klipheuwel sand Batch 1 and a 6mm Hornfels stone. In order to compensate for the larger volume of fines in the Klipheuwel sand the course aggregate percentage was increased from that used in Mix 2, whilst adjustments were also made to

water and SP volumes. A slump flow of 565mm was achieved. As a matter of reference Mix 3 was tested using a 13mm Greywacke stone as opposed to the 6mm Hornfels stone (see Figure 9.5). Again, due to the reduced packing efficiency of the larger aggregate particles failure resulted in the slump flow test.

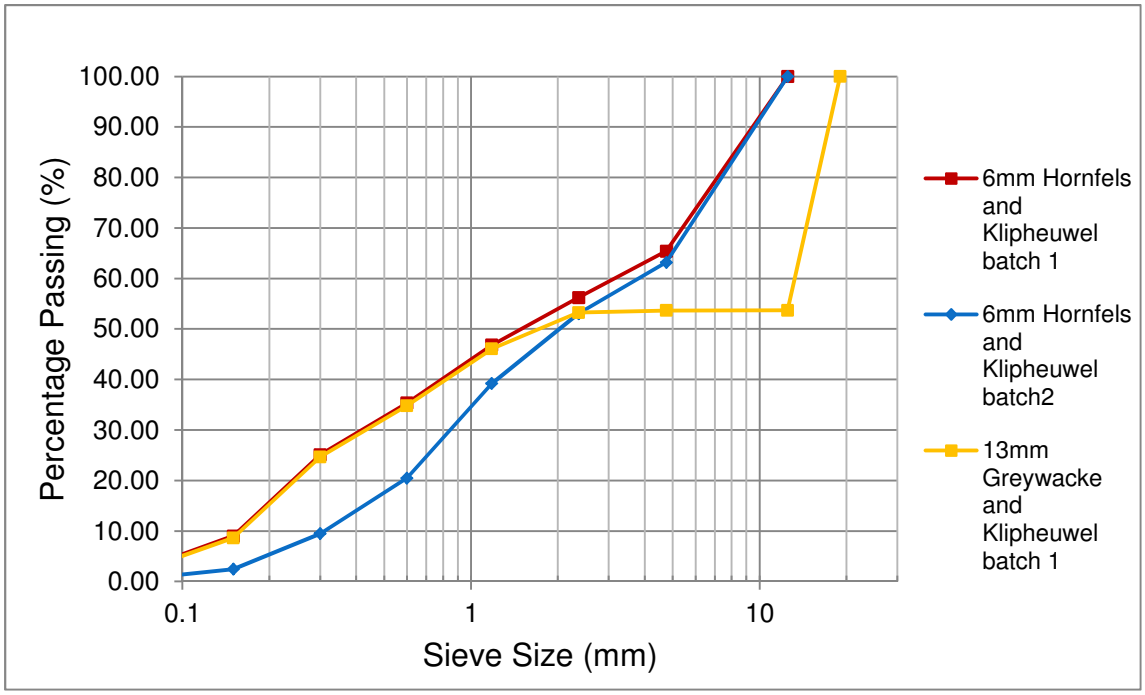

Figure 9.5 *Comparison of grading curve for Mix design 3 using differing materials*

As Klipheuwel sand Batch 2 had a reduced percentage of fines (as described in Section 9.1.2) in comparison to batch 1, Mix 3 was no longer valid and Mix 4 was incorporated. The design basis was similar to that of Mix 2, as the shape of the fine aggregate grading curve was similar to that of the Malmesbury sand. However, a higher percentage of fly ash was used to compensate for the reduced amount of fines. A slump flow of 500mm was attained for Mix 4.

It can be seen that although the fly ash volumes for Mixes 3 and 4 were the same, the flow of Mix 4 was more restricted. The stone and sand percentages differ between the mixes but it seems apparent that the major factor in this instance is the grading of the fine aggregates. Mix 4 has a reduced amount of intermediate fine particles in the range from 0.6mm to 0.15mm in

sieve size. Thus, in order to achieve adequate flow properties the grading of the aggregates in the mix design need to have a more linear distribution rather than an 's-shaped' distribution when plotting the percentage of material retained against the relevant sieve size on the logarithmic scale. A lack in fines cannot be compensated through adjustments of material quantities outside the intermediate range.

Through-out slump flow testing a non-homogenous flow shape, i.e. non-circular, for a majority of trial mixes occurred. Often, fibre bundling in the centre of the test sample resulted in failure of the trial mix. Due to the intrinsic nature of the slump flow test these bundles were inevitable (see Figure 9.6) but agitating the mixture very slightly with the fingers so as to disturb this bundle would assist the fresh state flow (note that this agitation was only for a short period so as to not assist the flow). Test samples that were deemed to have passed the test began to flow more easily after this step and distributed the fibres throughout. For specimens that had passed the slump flow test a more circular flow shape was achieved with a minimized flow restriction.

Figure 9.6 *Restricted flow due to fibre entanglement*

Concluding Summary

The fresh state performance is dependent on both the fibre type and aggregates used. The higher the aspect ratio of the steel fibre type the more restricted the expected flow and the use

of a finer course aggregate is recommended. The flow behaviour of a SCSFRC is highly dependent on the aggregate grading as well as the shape of particles. As a basic guideline the aggregate grading curve should be approximately linear as this assists in achieving an adequate matrix packing density, in which fibres are physically separated, and the potential for fibre 'balling' is reduced. The particle shape will need to be noted as this will influence the flow, overall aggregate surface area and thus packing efficiency again. The paste volume should be high enough so as to sufficiently coat all particles but excess paste must be avoided as this will increase the interspace volume and thus the potential for fibres to bundle.

This analysis briefly investigates the influence of the fibre and aggregate parameters on the fresh state flow properties. It was found that adjustments in the mix design need to be made with relevance to the parameter changed, and that through proportioning techniques it is possible to obtain a self-compacting SFRC mix. Four mixes were developed of which a minimum slump flow of 500mm was obtained for all mixtures passing the test. As the nature of the slump flow test initiates entanglement of the fibres, a degree of experience is required in visually assessing the flow during testing.

To obtain a SFRC self-compacting mix the mix design needs to have a high viscosity whilst maintaining the required flow properties, ensuring that fibres remain suspended in the mix and do not have a tendency to entangle. This analysis considered the influence of fibre type and, to a certain degree, aggregate grading and particle shape. The effects of differing cement types and mixing procedures has not been investigated and further research regarding these influencing parameters is necessary in order to obtain a suitable design procedure for SCSFRC.

9.2 Three-point Beam Testing

Three-point beam testing was conducted in order to determine the hardened state material properties of specific SFRC mix designs as well as to evaluate the influence of changes in mix constituents to these properties (see Figures 9.7, 9.8 and 9.9). Three mix designs, Mixes 1, 2 and 5 (see Sections 8.1 and 8.3.2 respectively), were selected as materials varied according to the fibre aspect ratio and concrete strength between the mixes. Material properties determined for Mixes 2 and 5 were used in theoretical models in predicting the punching shear and flexural slab failure loads respectively.

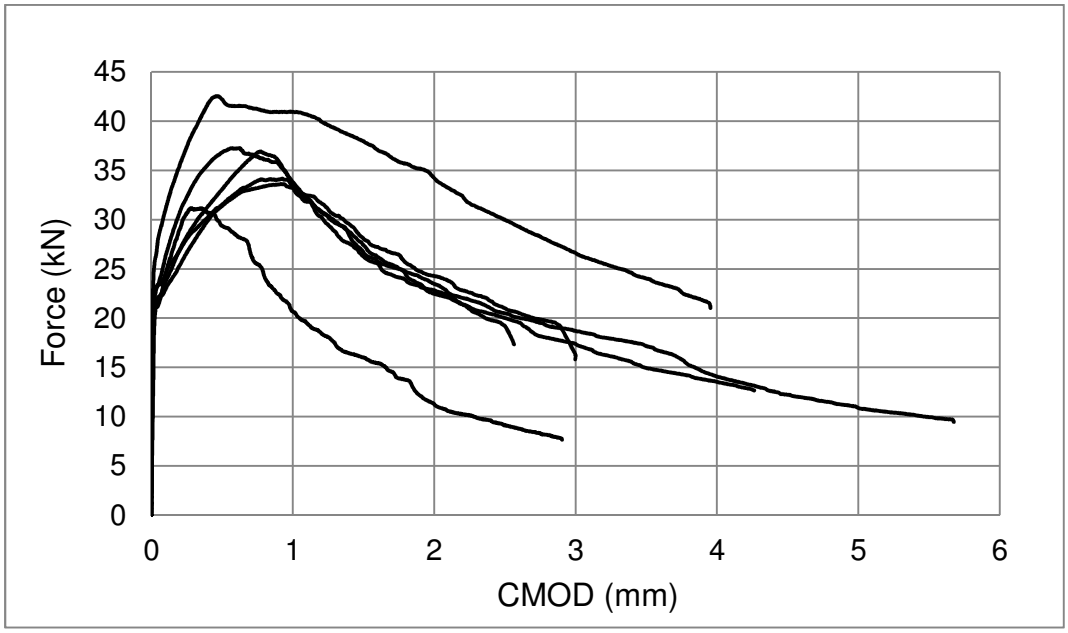

Figure 9.7 *Summary of Mix 1 three-point bending results*

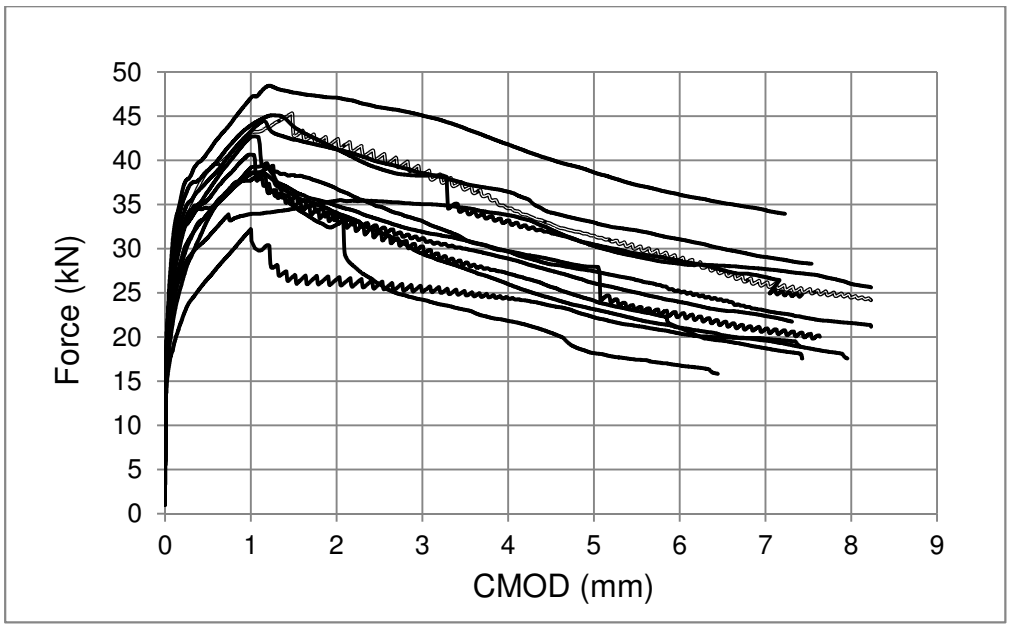

Figure 9.8 *Summary of Mix 2 three-point bending results*

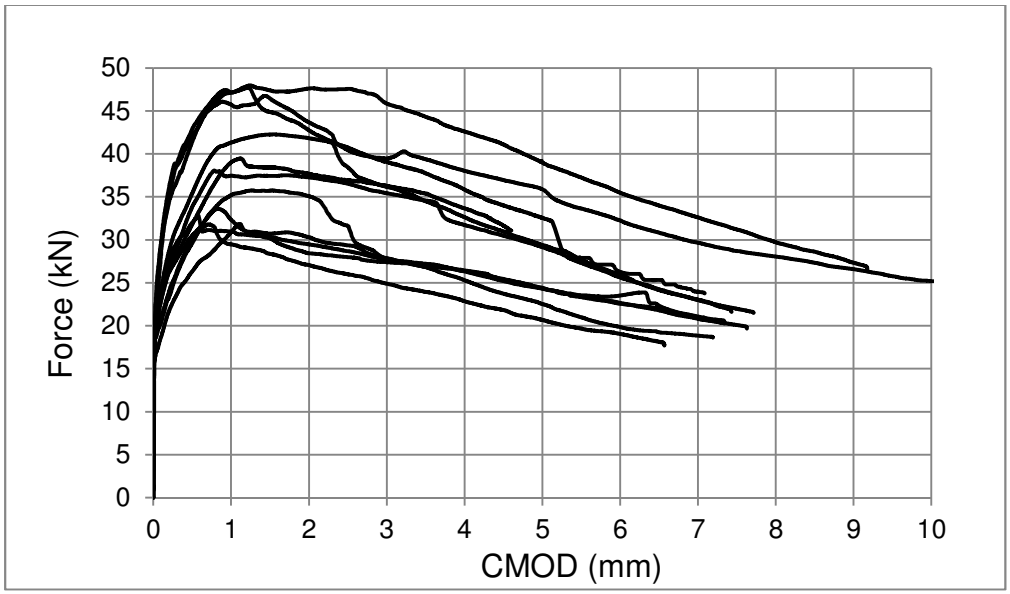

Figure 9.9 *Summary of Mix 5 three-point bending results*

Table 9.4 Mixes 1,2 and 5 characteristic material values

Mix Design	w/c ratio	Fibre	f_{cuk}		LOP_k		f_{R1k}		f_{R3k}	
		AR / L	N/mm^2	CoV (%)	N/mm^2	CoV (%)	N/mm^2	CoV (%)	N/mm^2	CoV (%)
1	0.6	55/30	55.32	2.15	5.4	11.3	7.45	13.7	4.1	19.3
2	0.53	80/60	39	4.78	6.2	9.45	9.43	10.3	7.82	17
5	0.52	80/60	47.2	5.82	4.96	11.4	7.86	16.4	7.5	19.2

The material values shown above in Table 9.4 are determined in accordance with the procedures as stated in RILEM TC 162-TDF (RILEM Technical Committee, 2003). From the results it can be seen that when determining the tensile material properties for SFRC mixes a larger variation in results can be expected than when performing standard compressive tests. However, the results indicate that a change to the fibre aspect ratio has an influence on the residual tensile material properties, especially in the latter loading stages when the crack width tends towards the ULS load state f_{R3} (2.5mm). It can also be noted that the degree of variation in results during the latter stages of tensile testing increases, which can be attributed to the intrinsic nature of SFRC regarding the fibre distribution and the crack bridging potential of the different fibre types.

With regards to the influence of the concrete compressive strength, which varies as a result of aggregate size, water/cement ratio's and cement type (see Sections 8.1 and 8.3.2), there is a suggestion from the results that an increase in strength will result in a lower tensile cracking strength. However, this is more likely as a result of a reduced fibre crack bridging potential due to either the length of fibres within the mix or the mixing and casting procedures implemented. The concrete strength though, may influence the residual tensile strength values at increased crack widths, where a higher compressive strength increases the fibre-matrix bond strength and thus influences the tensile residual strength reduction associated with early crack-width propagation.

Results and Discussion

According to the RILEM Technical Committee (2002) the limit of proportionality (LOP) is defined by the highest force value applied to the test beam up till the CMOD interval of 0.05mm. The residual stresses obtained thus give an indication of the number of fibres potentially bridging the initially formed crack, where a higher characteristic value can be expected for a larger number of fibres bridging the crack. It is clear that when comparing the LOP results between Mixes 1 and 2 that there is an increased fibre crack bridging potential associated with the longer fibre type. This has led to a greater variation between individual test specimen results for Mix 1. However, when comparing the results obtained for Mixes 1 and 5, Mix 5 has a slightly lower LOP value than Mix 1.

It is the opinion of the author that the lower LOP value for Mix 5 is as a result of the differences in the mixing and casting processes. Mix 1 was mixed using a pan mixer where an even distribution of fibres was more likely to be achieved under the controlled conditions. Mix 5 was mixed in the concrete supplier Ready Mix truck where the mixing process did not impose as much shear force to distribute the fibres. In addition, a much greater volume of SFRC was mixed in the truck, $4m^3$ as opposed to the pan mixer volume of $0.105m^3$, over a travel period of approximatley 1hr to the construction site. These two factors may have increased the potential of fibres to possibly bundle, or at least congregate in areas of the fresh SFRC mix, and thus yield SFRC beam specimens with a lower fibre content. This factor would also explain why the results obtained for Mix 5 have a greater degree of variation between test specimens (see Figure 9.10) when compared to the results obtained for Mix 2.

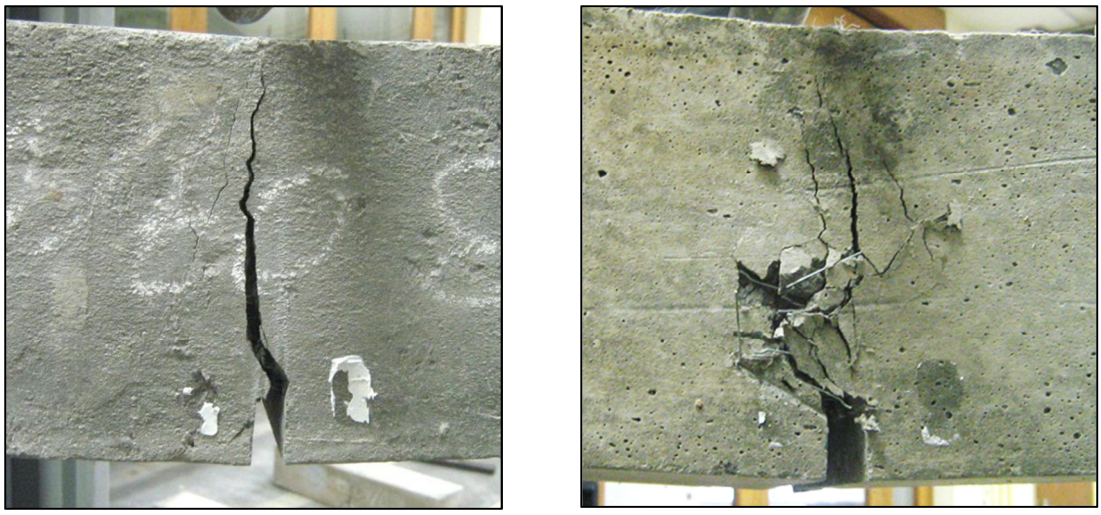

Figure 9.10 *Example of variation in behaviour between beam specimens for Mix 5*

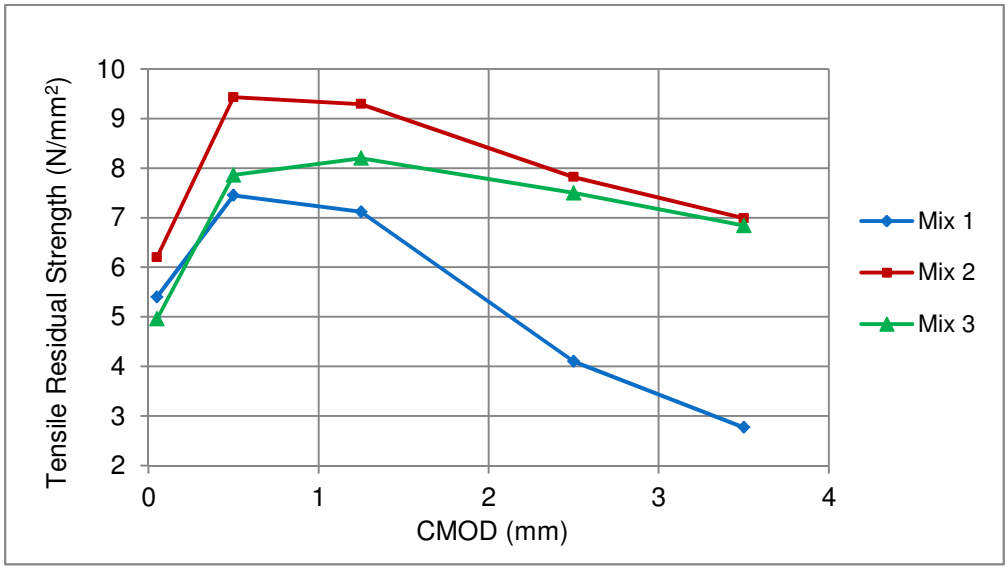

Figure 9.11 *Comparison of tensile residual strength with associated CMOD size*

Under increasing loads it is clear that all three SFRC mix types show a residual strength capacity (see Figure 9.11). For a CMOD of 0.5mm, the material property used in SLS design (RILEM Technical Committee, 2003), the load resistance offered by the tensile residual strength is greater than the initial cracking load. At a CMOD value of 0.5mm Mix 2 shows the greatest residual capacity which can again be attributed to the higher crack bridging

potential. For CMOD values greater than 0.5mm the influence of the various factors becomes more apparent. The tensile residual strength offered by Mix 1 reduces with increasing CMOD as the shorter fibres bridging the formed cracks begin to pull-out and lose their resistance to the imposed loads. This is further illustrated by the results obtained for Mixes 2 and 5, where the residual strength at greater crack widths is still significant. This characteristic thus illustrates that a greater ductility is achieved under ULS load conditions when using a longer fibre type.

In addition to this, results indicate that an improved ductility is also obtained for an increasing concrete compressive strength. As discussed in Section 2.1, an increased concrete strength results in a greater matrix-fibre bond which increases the resistance against fibre pull-out. This is evident in the results for Mix 5, where the values obtained at f_{R1} (0.5mm) are similar to those obtained at f_{R3} (2.5mm), with a small reduction in capacity as the CMOD increases to f_{R4} (3.5mm). The reduction in tensile residual strength of Mix 2, in which a lower compressive strength was obtained, from values obtained for f_{R1} to f_{R3} further illustrates this. The residual capacity offered at crack widths from f_{R3} to f_{R4} can be attributed to the frictional forces between the fibre and surrounding concrete matrix during the fibre pull-out mode. It was noted that during testing that none of the specimens failed as a result of rupture of the steel fibres themselves.

Concluding Summary

From the above results it is clear that the addition of steel fibres by 1% in volume to concrete provides a significant post-cracking tensile residual strength. Depending on the fibre type, with regards to the aspect ratio, the structural behaviour of the SFRC composite can differ. For shorter length fibres, it is clear that under increasing crack widths the residual resistance is limited and the composite can be characterised by a rather rapid decline in capacity once the crack width has exceeded SLS load conditions (i.e. 0.5mm). In addition to this, the variability of the composite performance can be considered greater than that experienced when using longer fibres due to the lower crack bridging potential. This restricts the

applications of the shorter fibres, where for structural applications generally a strain hardening or deflection hardening (see Section 2.2) post-crack behaviour is desired.

When using longer fibres a strain softening material can undergo deflection hardening, as a higher degree of ductility is achieved. This is evident from test results as fibres provide residual strengths that remain significant at crack widths even greater than that used in ULS design (i.e. greater than 2.5mm). The degree of ductility is further improved when using a higher strength concrete, in which the fibre-matrix bond strength is greater. The beneficial effects of this ductility were revealed during beam testing, particularly for Mix 2 beams, where deflection hardening was shown to occur (see Figure 9.12).

As discussed previously the variation in material performance between test specimens is an intrinsic property of SFRC but the degree of variation can give further insight into the material composition as well as the mixing and casting procedures. From the results obtained it is clear that the procedures used in industrial practice, and the volumes of material considered, will lead to a greater variability in performance. If the SFRC properties determined through characteristic testing such as three-point bending are to be used in construction design it is crucial to fully understand the laboratory procedures implemented and how these may vary when constructing on a larger scale.

Figure 9.12 *Multiple cracking patterns where deflection hardening is shown to occur*

9.3 Slab Testing: Flexural Analysis

A large scale SFRC only test slab was induced to flexural loading through simultaneous point load application. The test was conducted so as to evaluate the material potential of a SFRC only system for use in suspended flat slab construction. The expected load resistance was pre-determined through yield line theory in combination with various design models proposed for the determination of SFRC moment resistance (see Chapter 5). A summary of the test data (Figures 9.13, 9.14,9.15 and 9.16) and failure loads in comparison to those predicted by the various models (Table 9.5) can be seen below.

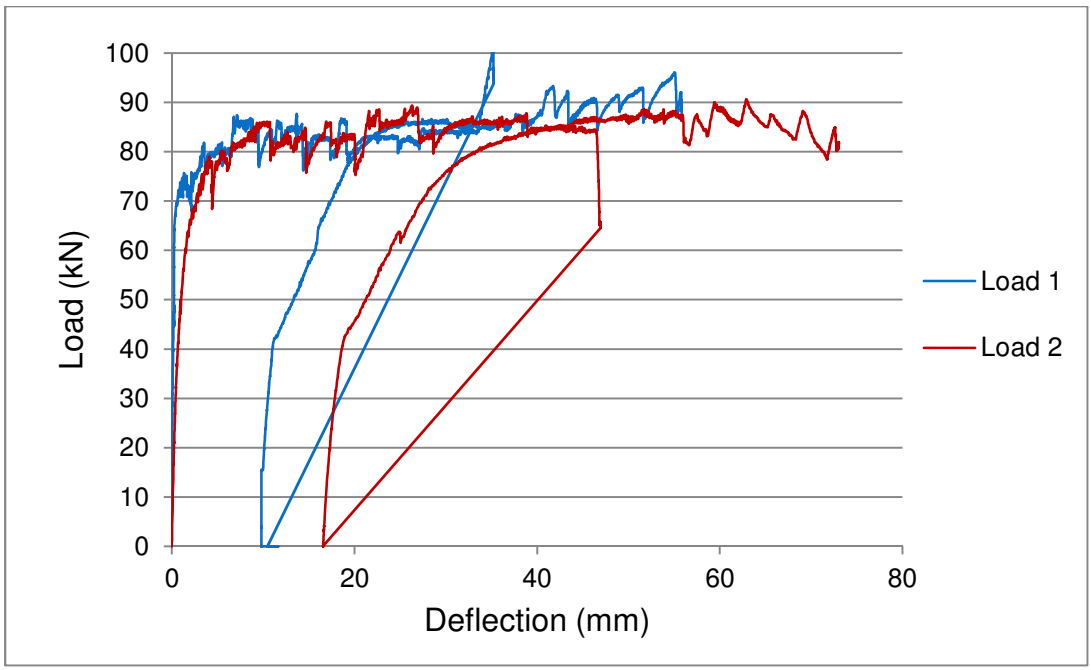

Figure 9.13 *Applied point load vs. deflection at load location*

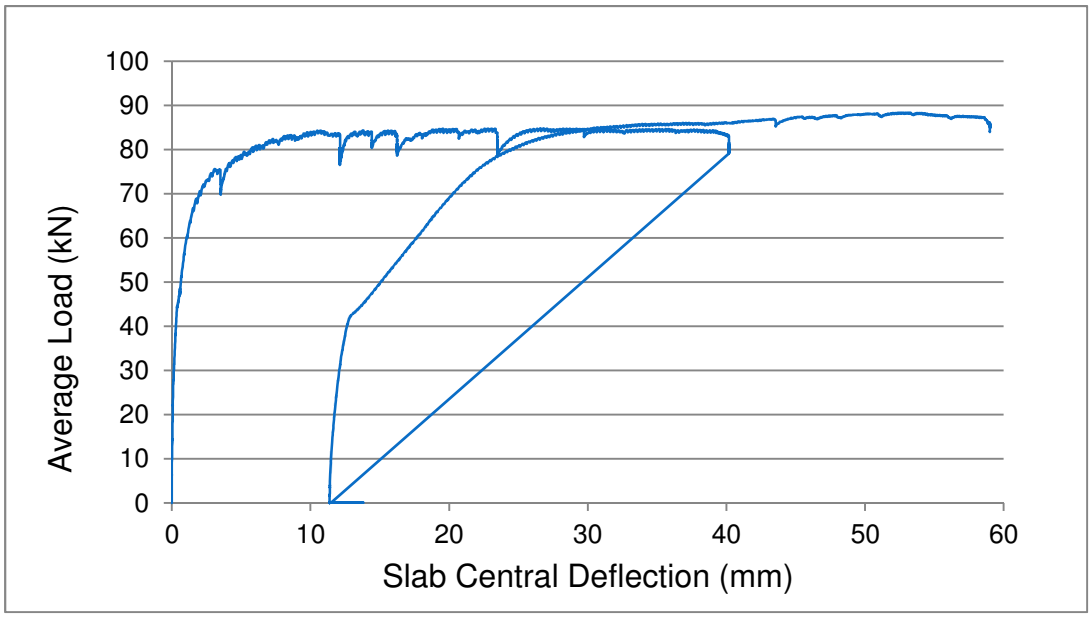

Figure 9.14 *Average of two point loads vs. deflection at slab centre*

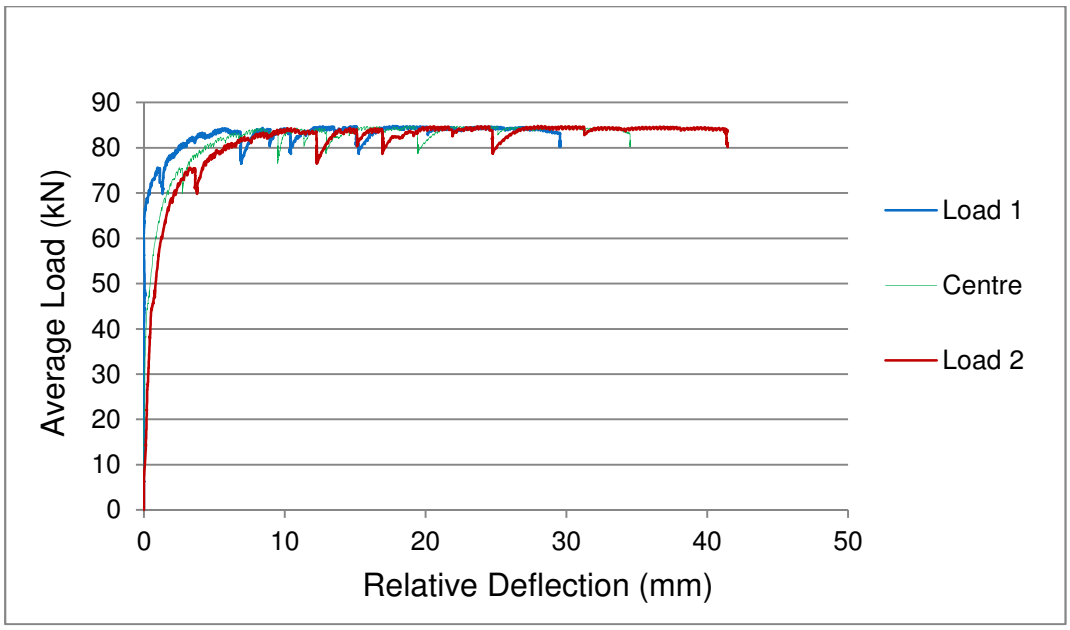

Figure 9.15 *Average load vs. relative deflection*

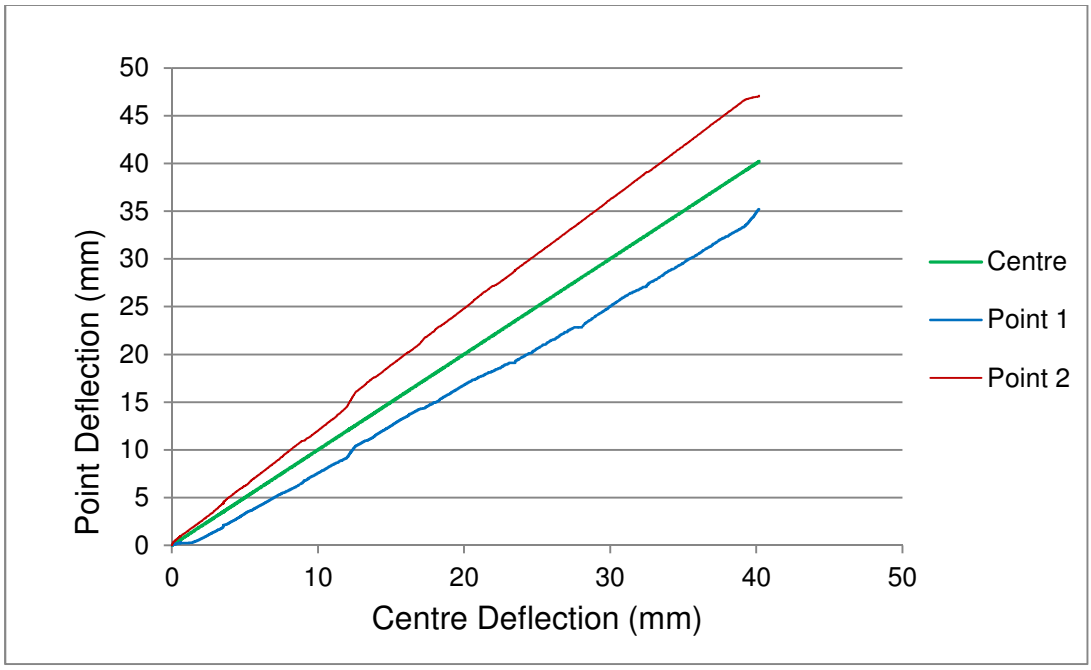

Figure 9.16 *Relative deflection vs. deflection at slab centre*

Table 9.5 Flexural test slab predicted load resistance vs. experimental load average

Design Model		Force Resistance		Error
		Moment (kNm)	Load (kN)	P_{exp} / $P_{predicted}$
SLS Load State	Test Load Average	14.93	74.65	1
	Rilem Stress-strain method	19.65	98.64	1.32
	fib Linear Model	23.49	117.92	1.58
	fib Rigid Plastic Model	-	-	-
	Closed-form solution	15.55	78.06	1.05
ULS Load State	Test Load Average	17.67	88.35	1
	Rilem Stress-strain method	17.10	85.84	0.97
	fib Linear Model	19.84	99.60	1.13
	fib Rigid Plastic Model	18.42	92.47	1.05
	Closed-form solution	16.23	81.47	0.92

The predicted force resistance values shown in Table 9.5 are determined (see Appendix B) according to characteristic material values obtained from three-point bending tests (see Section 9.2). The test beams were cast from the same material used to cast the flexural slab. The input parameters for the models are in accordance with the respective specifications (see Chapter 5) and are used in combination with a concrete material factor, $\gamma_m = 1.5$.

In Figures 9.13 and 9.14 it can be seen that after initial cracking of the flexural slab surface, at the point where the load resistance is no longer linear with respect to deflection, there is a small degree of deflection hardening for the strain softening material. The resistance increases from the initial cracking load of approximately 60kN to an ultimate resistance average of 88.35kN at each load point. In addition, the ULS failure mode for the flexural slab was extremely ductile in nature, in which the load resistance was maintained over a deflection range of 50mm at the centre of the slab (see Figure 9.14). Figure 9.15 shows that the load resistance at each load point was maintained without localised material failure but did, however, have varying deflection responses in resisting the applied load. This is further illustrated in Figure 9.16 in which the deflection at each load point is plotted against the deflection at the slab centre, where it can be seen that the deflection at Load Point 2 was much higher than that at Load Point 1.

As expected, rigid panels formed within the slab in resisting the applied loads. During the initial phases of loading the cracking pattern resembled that as predicted through yield line theory, where in the latter stages multiple crack patterns formed. Ultimate failure occurred in the cracks that formed initially, which acted as plastic hinges, once crack widths exceeded those prescribed in the various design models. It must be noted that failure of the system did not occur as a result of a loss in load resistance capacity. The applied load was released and then reapplied as shown in Figures 9.13 and 9.14, allowing one to evaluate the recovery state and resistance mechanism upon load reapplication.

Flexural Slab Crack Formations

Loads 1 and 2 were applied to the test slab in stages of which the crack pattern and crack widths were recorded at each load step. The first load increment was a simultaneous point load application of 50kN each (i.e. 100kN total load). No cracking on the slab tension surface was observed at this point, which was expected as the predetermined cracking load was 64kN at each load point. Non-linear load/deflection behaviour occurred at approximately 60kN average load in which no visible cracking could be observed. The loads were increased to 75kN each at which the onset of visible cracking occurred (see Figure 9.17).

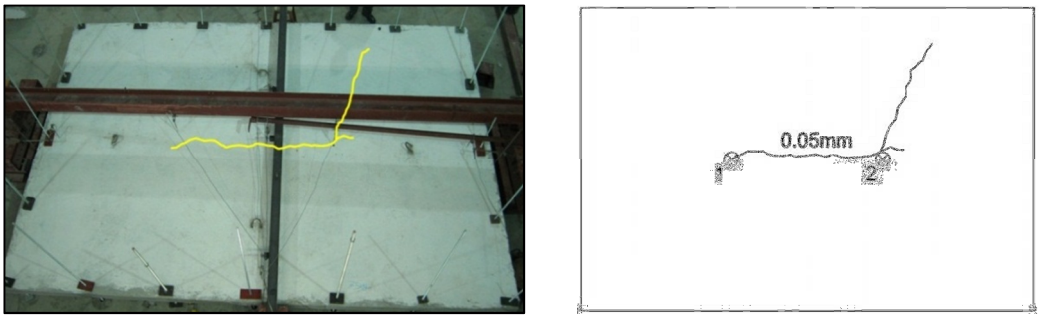

Figure 9.17 *Crack pattern and maximum crack width at load increment 1: 75kN*

The loads were then increased to approximately 85kN at each point load, upon which an increased degree of cracking had occurred. The crack pattern resembled that predicted

through yield line analysis, with the maximum crack width recorded for this stage occurring between the two point loads (see Figure 9.18). It was noted that the maximum crack width had exceeded the recommended serviceability limit state value of 0.5mm.

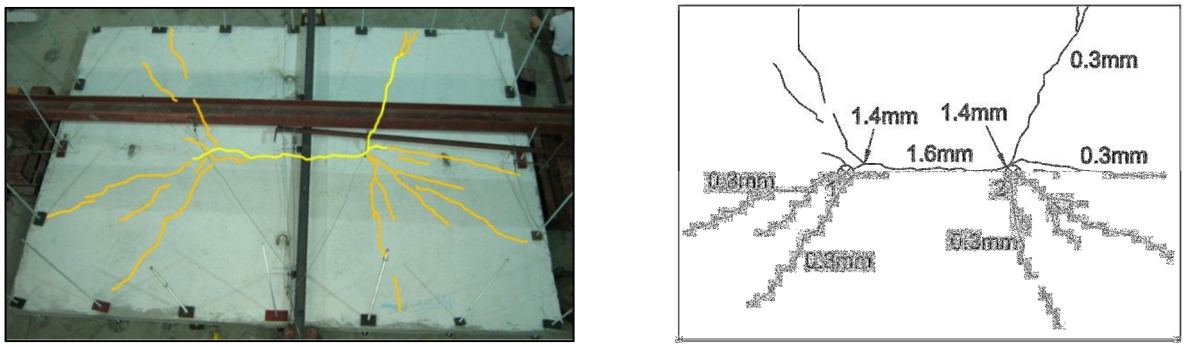

Figure 9.18 *Crack pattern and maximum crack width at load increment 2: 85kN*

Further load application from this stage resulted in little change to the resistance provided from the slab, indicating that the ultimate limit state loads had been reached. The loads were continued to be applied, increasing the slab deflection, until a crack width of 3.5mm had been reached (see Figure 9.19). At this stage the load resistance was constant at approximately 85kN indicating an extremely ductile failure mechanism for the SFRC only slab system.

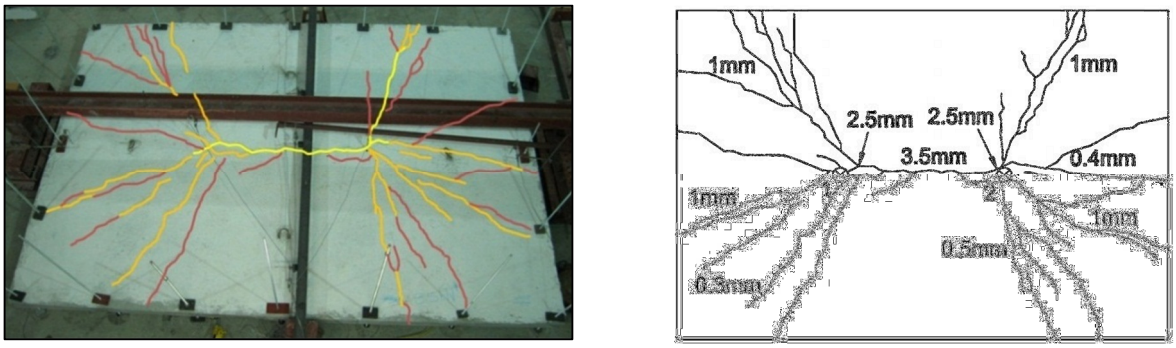

Figure 9.19 *Crack pattern and maximum crack widths at load increment 3: 85kN*

To obtain information regarding the failure mechanism after the ULS crack width design capacity had been reached additional loading was applied (see Figure 9.20). The load was

initially released to allow for adjustments to be made to the recording equipment and then reapplied. The average load resistance remained constant at 85kN, where even a slight increase in the resistance was observed at times. Load application was terminated once the loading jacks had reached the maximum displacement range.

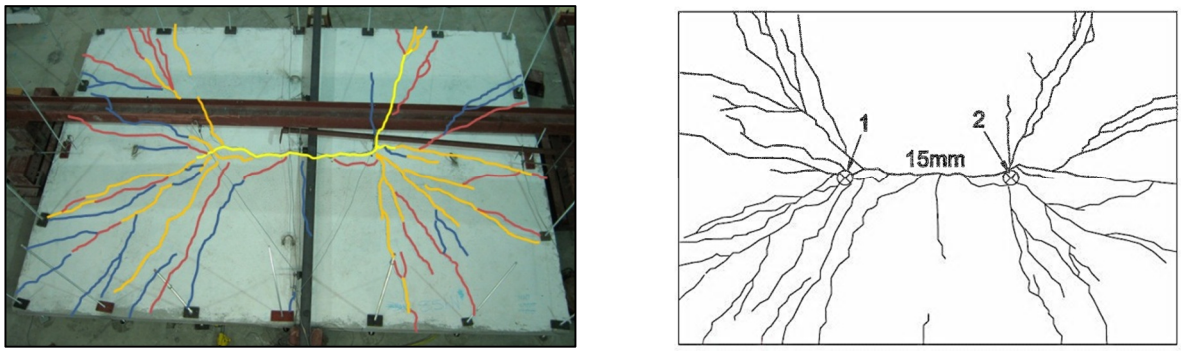

Figure 9.20 *Crack pattern and maximum crack width at load increment 4: 85kN*

Discussion: Slab Behaviour

During the initial load stages the slab behaviour was as to be expected with surface cracking and the associated non-linear behaviour occurring at approximately 60kN at each load point. Under an increasing load the initial crack pattern resembled that as predicted through yield line theory, where ultimate failure due to crack width limitations occurred at the location were initial cracking had taken place. It was clear that the dominant crack path had insufficient fibres bridging the crack in the centre of the panel, creating a hinge for the adjacent rigid panels to rotate about with reduced stiffness (see Figure 9.22).

This poor distribution of fibres within the centre of the panel may have been caused by inadequate casting techniques, in which the self-compacting material was placed at the centre of the slab mould and flowed outwards towards the edges. As a result, fibre concentrations were away from the panel centre (see Figure 9.21 for varied distributions). The poor fibre distribution in the central region induced a localised deflection softening response, which led

to ultimate failure of the system with little potential for redistribution of stresses. The ultimate load carrying capacity obtained was thus less than initially predicted using the design models.

Figure 9.21 *Cores taken from flexural slab showing varying fibre distributions*

Figure 9.22 *Hinge formation resulting from localised deflection softening*

Once the ULS load of 85kN had been reached the slab behaviour was extremely ductile when compared to conventional concrete. At increased deflection levels additional crack patterns developed, indicating a degree of localised deflection hardening. Although the load resistance had not increased past the ultimate failure load stress redistribution resulted, which enabled the system to maintain its load capacity. In regions where this multiple cracking had occurred it was clear that there was a greater local concentration of fibres in the initially formed hinge crack (see Figure 9.23), increasing the crack stiffness which enabled stress redistribution to the supports.

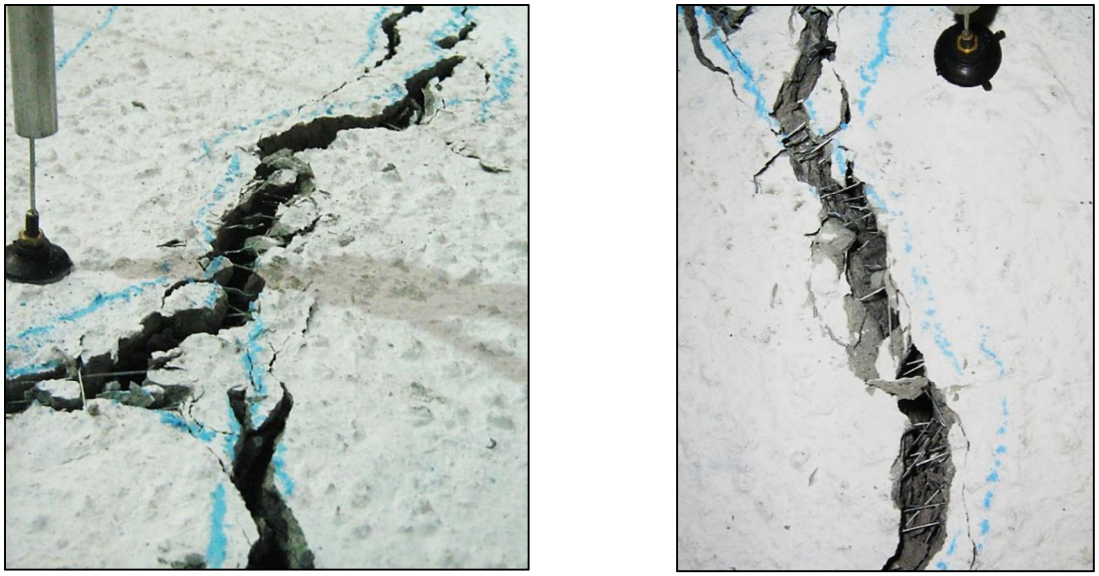

Figure 9.23 *Increased localised residual tensile strength due to fibre concentrations*

Within these deflection hardening regions the deflection response differed slightly between load application Points 1 and 2, with a larger deflection occurring at Load Point 2 (see Figure 9.24 and Figures 9.15 and 9.16). This increased deflection was also associated with a higher degree of cracking at Load Point 2 during the initial loading stages. As the load capacity was similar at both points it can be assumed that the response at Load Point 2 again resulted from an uneven fibre distribution, in which the stiffness of initially formed cracks was less than those formed at Point Load 1. Through additional cracking, as a result of the increased deflection, the activation of inert fibres took place which contributed to the load resistance

mechanism within the region of Point Load 2. This stress redistribution behaviour can also be related to the localised mechanism at Load Point 1, where the degree of cracking increased in the latter loading stages as fibre pull-out took place in the initially formed cracks. The load carrying capacity was thus maintained through the formation of additional cracks.

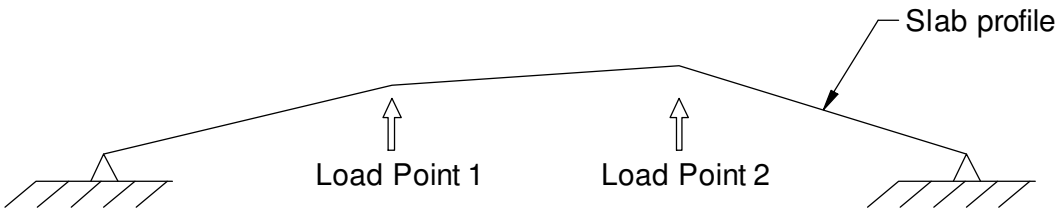

Figure 9.24 *Schematic of slab deflection profile in forming resistance mechanism*

The multiple cracking patterns observed can be attributed to the slab system support conditions. Although a premature hinge had formed in the centre of the slab due to deflection softening the potential for redistribution of stresses was further reduced as a result of the almost 'one way' span direction at the centre of the slab. Thus, the singular crack formation was considerably more dominant in this region than towards the ends (see Figure 9.25). The support edges at the ends were equal distances from the applied load and thus gave a greater potential for redistribution of stresses in this area.

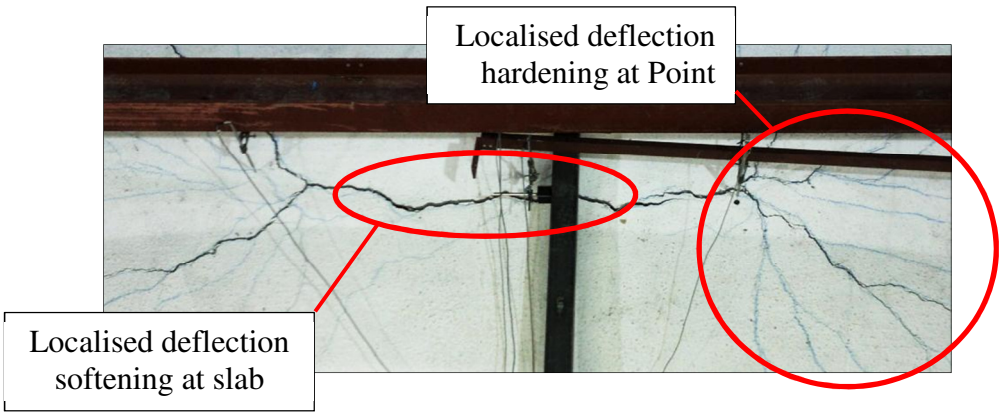

Figure 9.25 *Representation of localised response behaviours in test slab*

Discussion: Model Predictions

From the test results it is clear that the proposed models inadequately predicted the load resistance of the SFRC only test slab. In order to simplify the complex nature and behaviour of SFRC in the post crack stage assumptions need to be made with regards to residual stresses, crack widths and formations as well as the neutral axis location under increased loading. The results indicate, especially those for SLS load conditions, that modifications to the assumptions made are necessary for larger scale SFRC elements where the material variability is increased due to a greater potential for uneven fibre distributions.

When induced to initial load conditions the greatest concern is the lack of load resistance provided at the specified SLS crack width of 0.5mm. As the material properties determined are based on small scale test results the material variability due to fibre dispersion is far less than that experienced in full scale test slabs, thus overestimating the tensile residual stress values for cracks formed where there is a distinct lack of bridging fibres. In this test case the number of fibres at a dominant yield line location was insufficient, which allowed the formation of a plastic hinge with a reduced residual tensile resistance to that expected. An overestimation of the SLS load capacity thus resulted, particularly in both the RILEM and *fib* Model Code 2010 calculations where an assumption is made that the stress-crack width relation at 0.5mm determined through beam testing is valid at a larger test specimen scale. Both the RILEM and *fib* Model Code 2010 also make a simplification for the determination of the neutral axis location at this load state that may not be valid as it is based on observations made from small scale beam tests. This may further influence the moment response calculations.

The prediction made using the closed-form solution model had a closer relation to the results obtained as the determined SLS loads were based on limiting tensile strains as opposed to using residual stress values obtained at the SLS limiting crack width through beam testing. The strain limitation enables a more accurate prediction of the neutral axis location and thus the moment resistance provided by the residual stress. The model does not take into account a

change in tensile residual stress from SLS loading to ULS loading which may also assist in an improved prediction value due to its conservatism. However, the model did overestimate the resisting SLS capacity and again this is most likely as a result of the localised deflection softening, as the model is applicable to deflection hardening elements and considers a tensile strain over several cracks as opposed to the singular crack that formed in the test specimen.

In addition to the overestimation of the test slab SLS load capacity concern must be raised regarding the insignificant load increase from SLS limitations to the ULS load capacity, where an increase of only 10kN at each load point was recorded. However, it is clear that the use of steel fibres significantly improved the ductility of the slab system and that the various model predictions are more closely related to the test results obtained at failure. Through yield line theory the ULS load resistance determined was based on a singular crack formation and a stress-crack width relation.

As the calculations incorporated a material factor γ_m it is clear that the load prediction models would have significantly over estimated the ULS load capacity should the characteristic material properties determined through three-point bending have been used on their own. The reserve capacity obtained through the formation of additional cracks could not have been predetermined as this cracking pattern is considered random. The ductile response was thus expected, but its capacity as a result of stress redistribution is unpredictable in nature due to the inherent material variance that occurs in SFRC.

Of these models, the RILEM stress-strain and closed-form solution methods showed the best correlation to the test results. This was mainly due to a higher level of conservatism for the two models in comparison to those proposed in the *fib* Model Code 2010. Material property values used in the RILEM model were based on a much larger crack width at f_{R4} = 3.5mm and the closed form solution method used a reduction factor of 0.9 based on experience. This does not discredit the assumption that the *fib* Model Code 2010 model's make in that the ultimate limit state is achieved at 2.5mm, as in this case the ULS load was already achieved

at a crack width of 1.6mm, but that the residual stress determined at a 2.5mm crack width does not consider the influence of weak zones that may exist within the structure.

A common assumption made for all the proposed model's in the ULS state, excluding the RILEM stress-strain method, is that the neutral axis location within the bending section is extremely shallow and the compression zone is concentrated in the top fibre of the flexural member. These models thus assume that the majority of the section at ULS load conditions is in tension. This has led to load predictions for the differing models being quite closely related, where the differences in these predictions are mainly as a result of the characteristic material properties chosen. The relation of the predicted values to the test load ultimate capacity and slab behaviour under increasing load validates this assumption.

Concluding Summary

An intrinsic characteristic associated with SFRC is the variance in material behaviour under applied tensile loading. This attribute is directly related to the random dispersion and orientation of the fibres within the concrete matrix. Variation in material behaviour is present even in small test samples, such as beams used in three-point testing, but the degree of variation increases with the element size. This was apparent in the large scale flexural test slab. Uneven fibre distributions existed within the test slab due to fibre 'balling' and also, possibly, inadequate casting techniques. The result is regions in which there is an insufficient fibre distribution which may lead to local deflection softening and, ultimately, failure of the system.

Under increasing loads the initial crack formation will approximately relate to that expected through yield line theory predictions but once cracking occurs the element response is dependent on the fibre distribution. Unfortunately, in this test case, there was a distinct lack of fibres within the initially formed crack which resulted in a tensile residual stress insufficient to induce significant deflection hardening for the element and thus decreasing the

overall increase in post crack load capacity for the system. The poor fibre distribution gives insight as to the degree of quality control that is required during the mixing and casting process.

The design models applied to the flexural slab analysis inadequately predicted the SLS and ULS failure loads. The level of inaccuracy can be attributed to the material input parameters. The design assumptions made do not take account of weak zones within the element and an over estimation of the tensile residual stress, particularly for SLS load predictions, is made. This factor also influences the determination of the neutral axis position and thus the moment capacity in the SLS load state. It is clear that the SLS design using a SFRC only system is currently not suitable due to the potential for premature crack propagation as a result of poor fibre distribution. At a ULS loading state the model predictions are more closely related to the final load capacity. This may be attributed to the later stage in which the material properties are determined, where fibre pull-out behaviour has most likely been initiated, and the assumption that the majority of the section undergoes a tensile response in resisting the applied load. In both the SLS and ULS design models it is evident that a factor needs to be incorporated so as to account for the increased degree of material variability between small scale and large scale test samples.

It is the opinion of the author that this test example was a worst case scenario in which the fibre distribution was extremely poor in the region most likely to influence the overall specimen behaviour. Even with the poor load capacity encountered an ultimate moment resistance equivalent to that provided by 10mm diameter, high yield steel bars placed at 300mm c/c with an effective depth of 125mm was obtained. It can be assumed that the capacity of the system is predominantly influenced by the number of fibres bridging the initially formed cracks. In this case additional crack patterns to those initially formed only contributed significantly to the ductility response of the system.

The most positive aspect with regards to the flexural slab behaviour was the high level of ductility encountered under increasing deflection levels. This response behaviour is

significantly dependent on the support conditions of the system, as observed by the degree of cracking away from the centre of the test slab panel. The ULS load capacity was maintained at deflections levels as much as 60mm which indicates a high level of safety for such an implemented system.

This high ductility attribute of SFRC makes the material applicability most suitable to structures in which earthquake loading design is required. Structures designed to resist such loads require a high level of ductility of members in the ULS state. In addition to the ductility response, the design of such structures requires that plastic hinge formation occurs in predetermined regions as opposed to random locations within the structure as a whole. Thus, the use of SFRC in combination with conventional reinforcement becomes highly applicable. In such a case conventional reinforcing may be detailed so as to resist SLS load conditions, which also eliminates the influence of premature crack formation due to weak zones, and the resistance provided by the combination of the conventional reinforcement and steel fibres can account for the ULS load conditions. However, the use of steel fibres in combination with conventionally reinforced concrete under flexural load conditions exceeds the scope of this work.

9.4 Slab Testing: Punching Shear Analysis

Punching shear tests were conducted on three test specimens so as to evaluate the contribution of steel fibres to the load resistance. All three samples were constructed from the same concrete materials in combination with a 10mm steel so as to ensure a punching shear failure mode for the test specimen. The expected resistance load was predetermined using the shear models as described in Chapter 5. The load deflection curves (Figure 9.26) for all three tests and a summary of the load capacities (Table 9.6) is shown.

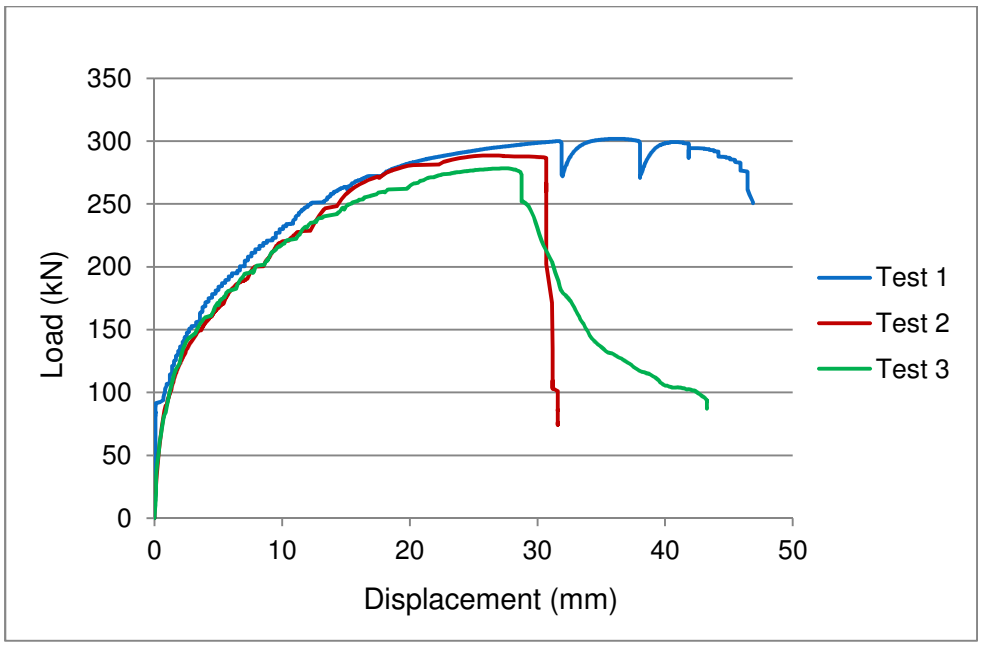

Figure 9.26 *Punching shear test sample load deflection response curves*

Table 9.6 Punching shear experimental results

Failure Characteristics	Test Sample		
	1	2	3
Failure mode	flx	PS	PS
ULS load (kN)	301.9	288.7	278.4
Model Prediction	P_{exp} / $P_{predicted}$		
SANS 0100-1	-	0.73	0.76
fib Model 2010	-	0.94	0.98
PS Mechanism model	-	0.92	0.95

The experimental results and comparison to the predicted failure loads can be seen in Table 9.6. The predicted SANS 0100-1 (2000) ULS failure load of 211kN was determined according to Clause 4.4.5 regarding the shear resistance of conventionally reinforced solid slabs without shear reinforcement (SANS 0100-1, 2000). The *fib* Model Code 2010 and punching shear mechanism model (see Section 5.3) ULS loads of 271.5kN and 265.7kN respectively were determined based on characteristic material properties obtained through three-point bending tests (see Sections 9.2.1 and 8.4.2). For both the applied models

considering the influence of steel fibres the characteristic residual tensile strength f_{Ri} was converted to a residual tensile stress by a factor of 0.4 so as to account for the differences between flexural testing and uni-axial tension tests (see Section 5.3.1). In all three models a material factor of γ_m = 1.0 was chosen as the samples were constructed in a controlled environment. None of the models directly considered the influence of reinforcing bars through dowel action.

Of the three tests conducted only two failed in punching shear. However, the results from these two specimens do indicate that the addition of steel fibres does improve the shear capacity of a flat slab system when compared to the ULS failure load determined according to SANS 0100-1. As the conventional failure mechanism caused by punching shear is considered brittle in nature these test specimens showed a degree of ductility, where the failure load is resisted over a small deflection range before punching shear failure occurs. The loads at which failure occurred are also of relative similarity of which the models considering the influence of the steel fibres adequately predicted. Once punching shear failure has occurred the capacity of the section is significantly reduced which is as expected with this type of failure mode.

Discussion

The behaviour of all three test specimens was similar during the initial stages of loading but when nearing the ultimate failure load differed slightly in their crack patterns, of which test Specimen 1 failed in flexure and Specimens 2 and 3 failed in punching shear (see Figures 9.27 and 9.28). The onset of non-linear load displacement behaviour began at approximately 75kN with visible cracking occurring at an approximate point load of 140kN. The initial crack formations were as a result of a flexural element response before circular cracking took place in the latter stages when Specimens 2 and 3 began to fail in punching shear.

It is the opinion of the author that the first specimen failed in a flexural mode due to a construction error in which the conventional reinforcing had settled near the centre of the test specimen at an approximate depth of 75mm, thus reducing the flexural resistance and possibly increasing the punching shear resistance (based on the theoretical failure mechanism, see Section 5.3.1). However, it is interesting to note the ductile manner in which flexural failure occurred for this specimen and the large degree of stress redistribution that occurred through multiple cracking. The failure load of 301.9kN was also higher than the 227.5kN load capacity determined according to the resistance provided by the conventional reinforcing. Thus, the failure load gives an indication that the steel fibres significantly contributed to the load resistance as the reinforcing had settled to the centre of the sample, reducing its contribution to the flexural resistance theoretically determined.

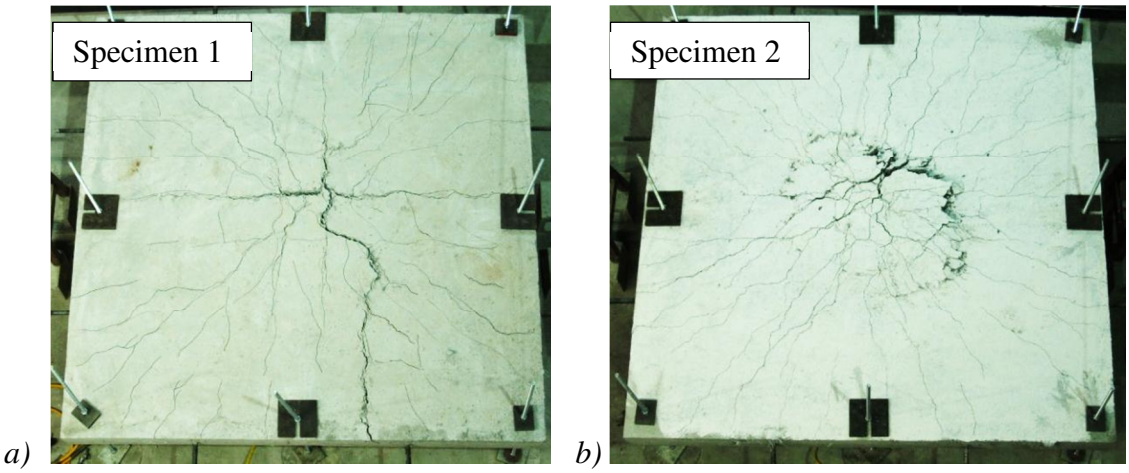

Figure 9.27 *Cracking pattern at failure for Specimens a) 1 and b) 2*

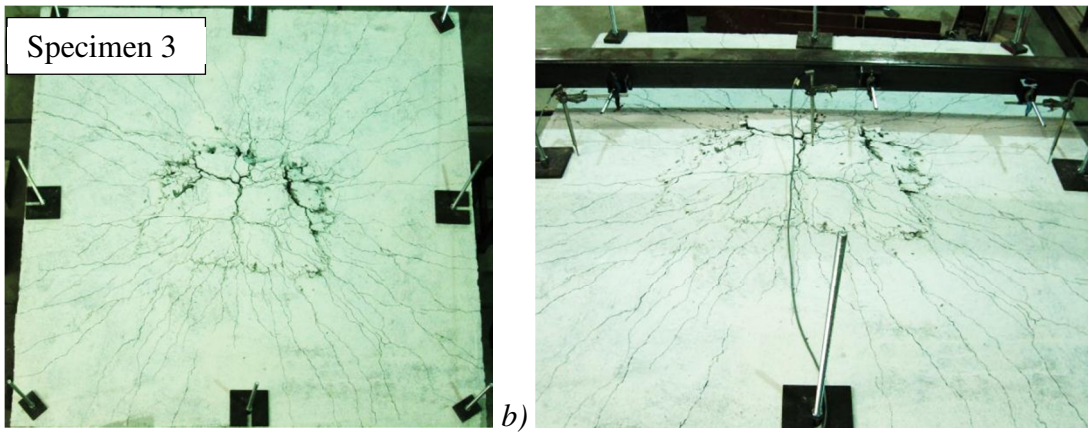

Figure 9.28 *a) Cracking pattern of Specimen 3 at failure, b) Specimen 3 in test position*

As described above Specimens 2 and 3 initially formed flexural crack patterns similar to that of Specimen 1. However, at approximately 200kN signs of circular crack patterns near the centre of the test panels began. Increased loading from this state led to flexural stress redistribution through multiple cracking but a significant amount of increased cracking occurred near the centre of the panels. Once nearing the failure load specimens showed significant deflection at their centre, soon after which a sudden failure occurred due to punching shear. Before the applied load was released the maximum flexural crack width for both specimens was measured at approximately 2mm in size, indicating a degree of flexural capacity remaining before the punching shear failure occurred. The ultimate failure mode was sudden as indicated in Figure 9.26 by a sudden drop in the load capacity. The punching shear failure crack pattern was oval in shape with a minimum/maximum diameter of 600/900mm and 550/850mm for Specimens 2 and 3 respectively (see Figure 9.29). Based on this information an average crack angle of 29° and 27° was determined for Specimens 2 and 3 respectively which is in correspondence to the assumed approximate design crack angle of 30° as observed by Choi et al (2007).

The design models used to determine the punching shear capacity show good correspondence with the experimental results obtained. Both models use an axial residual tensile strength as a defining parameter; however each differs in their computation of the final result.

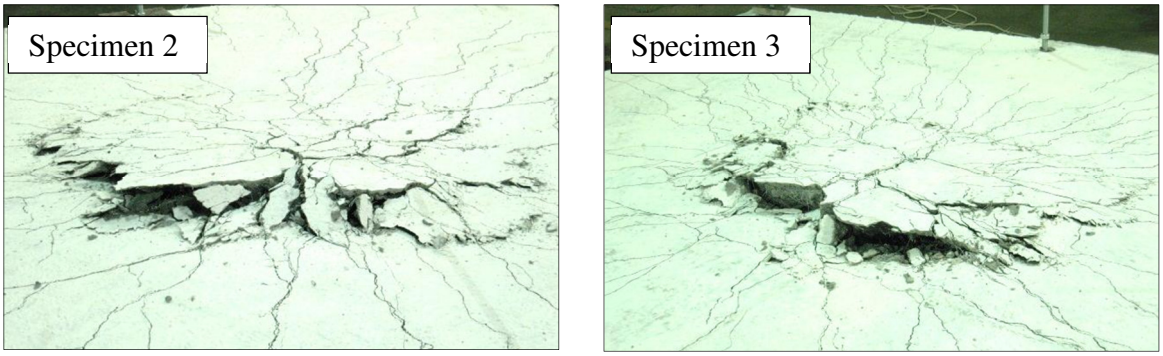

Figure 9.29 *Close up of punching shear failure for Specimens 2 and 3*

The punching shear mechanism model is more complicated and requires a better understanding in order to accurately predict the failure load. However, the description of the failure mechanism and its computation allow one to gain further insight into the model characterisation and thus reduces the level of uncertainty in the design shear strength associated with a lack of understanding. The increased capacity through dowel action of the reinforcing bars is neglected in the model and may account for the slight underestimation of the failure load. The punching shear design based on the *fib* Model Code 2010 is an adaptation of the shear design for SFRC structures in combination with conventional longitudinal reinforcing. Thus, in determining the results an assumption was made for the defining of the failure perimeter based on the experimental crack angle observations made by Choi et al. (2007). The ultimate failure load prediction is determined by a single function with simplified input parameters, making the calculation relatively easy. However, the origin of the function is undefined and there is little to no transparency with regards to how the influence of the parameters was determined. It is unclear as to whether the influence of dowel action is considered but as the predicted failure results match closely to the experimental results it can be assumed that this factor has been considered. In addition, the outside failure perimeter multiplied by the section effective depth does not accurately describe the area resisting punching shear through fibre pullout, but this may also be accounted for in one of the equation factors. The model has a similar design approach to that of conventional concrete punching shear design as per SANS 0100-1 (2000).

Concluding Summary

It is clear that the addition of steel fibres to conventionally reinforced concrete does improve the element resistance to punching shear. In the test cases in which punching shear failure did take place a theoretical shear resistance load increase of approximately 60-70kN was found as a result of the contribution from steel fibres. The test specimen behaviour up till failure was ductile in nature in which multiple cracking occurred as a result of stress redistribution. At the onset of failure the punching shear mode was relatively sudden as is associated with this type of mechanism. The punching shear failure loads for the specimens were relatively similar and this is most likely as a result of the controlled mixing and construction techniques implemented as well as the overall size of the test specimens, in which material variability is reduced when compared to that expected in industrial practice.

The design models considering the influence of steel fibres to the ultimate resistance showed good correlation with the results obtained. The models each have a different approach, in which the punching shear mechanism model accounted for the failure process and the *fib* Model Code 2010 gave a simplified function to determine the failure load, of which the assumptions made in both are verified through the test results. However, as both the models incorporate an axial residual tensile stress the assumptions made in this work regarding the conversion from results determined through flexure to an equivalent axial tensile stress need to be verified through an experimental analysis.

Chapter 10

Conclusions and Recommendations

This thesis is targeted at evaluating the feasibility of using SFRC only reinforced elements in the construction of in-situ cast flat slabs. For this it was necessary to develop an understanding of the material behaviour, on both a micro and macro scale, together with its current applications in industry. As its use as the sole form of reinforcement in structural systems is relatively new in Europe, and non-existent in South Africa, it was decided to take a more practical outlook with regards to the material characterisation, applicable design models, material behaviour in both the fresh and hardened state, and the structural performance of large scale systems under SLS and ULS load conditions. Through this work it was intended to highlight both the benefits and drawbacks of such systems regarding the design, construction and their implementation in an industrial context.

This investigation revealed the following:

- The design procedure used in SFRC generally differs from that of conventional concrete due to a non-linear post-crack behaviour. In order to simplify the complexity of the mechanism, design models make use of stress-strain or stress-crack width material relationships. It is important to fully understand the assumptions made in

these models as they may not always be suitable according to the intended application.

- Regarding steel fibres themselves, a defining attribute to their performance is the fibre aspect ratio. The higher the aspect ratio the better the performance of the individual fibres but this in turn is associated with a declining workability in the concrete fresh state. This has led to the development of self-compacting SFRC mix designs in which a homogeneous fibre distribution is more readily achieved.
- A volume fraction of 1% steel fibres will yield a tensile residual strength. Longer fibres have a greater chance of bridging cracks formed and can maintain a residual resistance at higher strain levels. As the degree of ductility is increased, the potential for a deflection hardening type behaviour is more likely. For these reasons, longer fibres are generally more desirable for structural applications.
- The flexural slab test loads resisted were lower than expected. It is believed that localised deflection softening took place in the plastic hinges, which can be attributed to a poor fibre distribution. This gives insight into the high degree of quality control that is necessary in large scale industrial construction.
- In the ULS load state the flexural slab showed high levels of ductility. This suggests that such an implemented reinforcement system is most suitable in combination with conventional reinforcing in structures designed to withstand earthquake loading.
- Punching shear tests revealed that, when used in combination with conventional reinforcement, the steel fibres contribute to the element shear capacity.

From the conclusions drawn in this investigation the following can be recommended as possible fields of future research:

- The most concerning factor regarding SFRC is its intrinsic variability in performance. It is imperative to define measures which mitigate this characteristic through the development of adequate and robust mix designs. In addition to this, the influence of different mixing of casting procedures on the fibre distribution should be further investigated.

- As the ductility of SFRC systems is high, another interesting field would be the modelling of SFRC in combination with conventional reinforcing in the SLS and ULS load states. This would particularly relate to areas of earthquake engineering in which predetermined plastic hinge locations within these structures is desirable in the ULS load state.
- As the material response varies according to the load conditions it is necessary to determine material properties with regards to the expected load state. However, this may not always be possible and the need for conversion factors between the different determination test procedures is required. Furthermore, the material properties determined may not always be representable of larger scale construction and again, suitable factors accounting for the increased, or decreased, degree of variability need to be statistically evaluated.
- Further work needs to be conducted with regards to SFRC only structural systems in which the true potential of SFRC can be realised. This may incorporate other forms of research such as using combinations of fibres in attaining a more consistent material behaviour and higher volume percentages whilst maintaining fresh state workability.

Reference List

Angerer, W. & Chappel, M., 2008. Design of Steel Fibre Reinforced Segmental Lining for the Gold Coast Desalination Tunnel. In *13th Australian Tunneling Conference*. Melbourn, VIC, 4-7 May, 2008.

ArcelarMittal, 2010. *Steel Fibre Reinforced Concrete (SFRC) for Industrial Floors Especially Without joints and Slabs on Piles*. [Online] (2.0) Available at: http://www.arcelormittal.com/distributionsolutions/repository/fanny/practical_guide_SFRC-UK.pdf [Accessed Spetember 2010].

Bayramov, F., Tasdemir, C. & Tasdemir, M.A., 2004. Optimisation of Steel Fibre Reinforced Concretes by means of Statistical Response Surface Method. *Cement and Concrete Composites*, (26), pp.665-75.

Bentur, A. & Mindess, S., 2007. *Fibre Reinforced Cementitious Composites*. 2nd ed. London: Taylor and Francis.

Bernard, S., 2003. Release of New ASTM Round Panel Test. *Shotcrete*, (Spring), pp.20-23.

Bhattacharya, A., Ray, I. & Davalos, J., 2008. Effects of Aggregate Grading and Admixture/Filler on Self-Consolidating Concrete. *The Open Construction and Building Technology Journal*, (2), pp.89-95.

Brandt, A., 2008. Fibre Reinforced Cement-Based (FRC) Composites after over 40 Years of Development in Building and Civil Engineering. *Composite Structures*, (86), pp.3-9.

Chanvillard, G., Banthia, N. & Aitcin, P.-C., 1990. Normalized Load-Deflection Curves for Fibre Reinforced Concrete under Flexure. *Cement and Concrete Composites*, (12), pp.41-45.

Chiaia, B., Fantilli, A.P. & Vallini, P., 2009. Combining Fibre-Reinforced Concrete with Traditional Reinforcement in Tunnel Linings. *Engineering Structures*, (31), pp.1600-06.

Choi, K.-K., Reda Taha, M.M., Park, H.-G. & Maji, A.K., 2007. Punching Shear Strength of Interior Concrete Slab-Column Connections Reinforced with Steel Fibres. *Cement and Concrete Composites*, (29), pp.409-20.

Colombo, M., di Prisco, M. & Felicetti, R., 2010. Mechanical Properties of Steel Fribre Reinforced Concrete Exposed at High Temperatures. *Materials and Structures*, (43), pp.475-91.

Construction Competenece and Consulting, 2011. *3-Co: Special Concretes- Steel Fibre Reinforced Concrete*. [Online] Available at: http://www.3-co.com/Pro/Engineers/Special.Concrete/sfrc.htm#Steel_Fiber_Reinforced_Concrete_(SFRC) [Accessed 27 May 2011].

De Hanai, J.B. & Holanda, K.M.A., 2008. Similarities between Punching and Shear Strength of Steel Fibre Reinforced Concrete (SFRC) Slabs and Beams. *IBRACON Structures and Materials Journal*, 1(1), pp.1-16.

Destree, X., 2009. Steel-Fibre-Only Reinforced Concrete in Free Suspended Elevated Slabs. *Concrete Engineering International*, (Spring 2009), pp.47-49.

Destree, X. & Mandl, J., 2008. Steel Fibre Only Reinforced Concrete in Free Suspended Elevated Slabs: Case Studies, Design Assisted by Testing Route, Comparison to the Latest SFRC Standard Documents. In W.a. Stoelhorst, ed. *Tailor Made Concrete Structures*. London: Taylor and Francis Group. pp.437-43.

di Prisco, M., Plizzari, G. & Vandewalle, L., 2009. Fibre Reinforced Concrete: New Design Perspectives. *Materials and Structures*, (42), pp.1261-81.

Dupont, D., 2003. *Modelling and experimental validation of the constitutive law (σ-ε) and cracking behaviour of steel fibre reinforced concrete (PHd)*. Heverlee, Belgium: Catholic University of Leuven.

Ellouze, A., Ouezdou, M.B. & Karray, M.A., 2010. Experimental Study of Steel Fiber Concrete Slabs Part I: Behaviour Under Uniformily Distributed Loads. *International Journal of Concrete Structures and Materials*, 4(2), pp.113-18.

Fantilli, A.P., Mihashi, H. & Vallini, P., 2009. Multiple Cracking and Strain Hardening in Fibre-Reinforced Concrete under Uniaxial Tension. *Cement and Concrete Research*, (39), pp.1217-29.

Ferrara, L. & Meda, A., 2006. Relationships between fibre distribution, workability and the machanical properties of SFRC applied to precast roof elements. *Materials and Structures*, 39, pp.411-20.

fib Special Activity Group 5, 2010. *fib Model Code 2010 First Complete Draft Volume 1*. 1st ed. Lausanne, Switzerland: the International Federation for Structural Concrete.

fib Special Activity Group 5, 2010. ISSN 1562-3610 *fib Model Code 2010 First Complete Draft Volume 2*. Lausanne, Switzerland: the International Federation for Structural Concrete.

Giaccio, G., Tobes, J.M. & Zerbino, R., 2008. Use of Small Beams to Obtain Design Parameters of Fibre REinforced Concrete. *Cement and Concrete Composites*, (30), pp.297-306.

Gohnert, M., 2006. Postulates on Shear in Reinforced Concrete. *Journal of the South African Institution of Civil Engineering*, 48(4), pp.9-13.

Graeff, A.G., Pilakoutas, K., Lynsdale, C. & Neocleous, K., 2009. Corrosion Durability of Recycled Steel Fibre Reinforced Concrete. *Intersections*, 6(4), pp.77-89.

Grunewald, S. & Walraven, J., 2001. Parameter-study on the influence of steel fibres and coarse aggregate content on the fresh properties of self-compacting concrete. *Cement and Concrete Research 31*, pp.1793-98.

Harajli, M.H., Maalouf, D. & Khatib, H., 1995. Effects of Fibres on the Punching Shear Strength of Slab-Column Connectios. *Cement and Concrete Composites*, (17), pp.161-70.

Hot Dip Galvanizers Association, n.d. *Corrosion Protetion of Reinforcement in Concrete Structures*. [Online] Hot Dip Galvanizers Association Available at: http://www.hdgasa.org.za/TechnicalPapers/Reinforcement%20of%20Concrete%20Structures.pdf [Accessed May 2011].

Khaloo, A. & Afshari, M., 2005. Flexural Behaviour of Small Steel Fibre Reinforced Concrete Slabs. *Cement and Concrete Composites*, 27, pp.141-49.

Kinnunen, S., 2001. Punching of Structural Concrete Slabs: Technical Teport. *Federation internationale du beton, Lausanne*, (Bulletin 12), pp.42-43.

Koehler, E. & Fowler, D., 2007. *Aggregates in Self Consolidating Concrete*. Final Report. Austin: University of Texas International Center for Aggregates Research.

Lau, A. & Anson, m., 2006. Effect of high temperatures on high performance steel fibre reinforced concrete. *Cement and Concrete research*, 36(9), pp.1698-1707.

Li, V.C. & Lepech, M.D., 2006. Long Term Durability Performance of Engineered Cementitious Composites. *Restoration of Building and Monuments*, 12(2), pp.119-32.

Lofgren, I., 2005. *Fibre Reinforced Concrete for Industrial Construction- a fracture mechanics approach to material testing and structural analysis*. Goteborg, Sweden: Chalmers University of Technology- Department of Civil and Environmental Engineering.

Mackechnie, J.R. & Alexander, M., 2001. *Repair Principles for Corrosion-Damaged Reinforced Concrete Structures*. Report Summary. Cape Town: University of Cape Town University of Cape Town; University of Witwatersrand.

Mills, G.M., 1970. *The yield-line theory : a programmed text for reinforced concrete slabs*. London: Concrete Publications.

Mueller, T. & Holschemacher, 2009. Self-Compacting Steel Fibre Reinforced Concrete- A Study About the Influence of Fibre Content and Concrete Compositions. In Shi, C., Yu, Z.,

Khayat, K.H. & Yan, P., eds. *Design, Performance and Use of Self-Consolidating Concrete SCC'2009*. Beijing, China, 2009. RILEM Publications S.A.R.L.

Olesen, J.F., 2001. Fictitious Crack Propagation in Fiber Reinforced Concrete. *Journal of Engineering Mechanics,* 127(3).

Oslejs, J., 2008. New Frontiers for Steel Fibre-Reinforced Concrete. *Concrete International*, (May, 2008), pp.45-50.

RILEM Technical Committee 188-CSC, 2006. *Casting of Self Compacting Concrete*. Final Report 35. Bagneux - France: RILEM Publications S.A.R.L RILEM Committee.

RILEM Technical Committee, 2002. RILEM TC 162-TDF: Test and Design Methods for Steel Fibre Reinforced Concrete- Bending Test. *Materials and Structures*, 35, pp.579-82.

RILEM Technical Committee, 2003 Part 1. Round-Robin Analysis of the RILEM TC 162-TDF Uni-Axial Tensile Test: Part 1. *Materials and Structures*, 36, pp.265-74.

RILEM Technical Committee, 2003 Part 2. Round-Robin Analysis of the RILEM TC 162-TDF Uni-Axial Tensile Test: Part 2. *Materials and Structures*, 36, pp.275-80.

RILEM Technical Committee, 2003. RILEM TC 162-TDF: Test and Design Methods for Steel Fibre Reinforced Concrete- Stress Strain Method. *Materials and Structures*, 36, pp.560-67.

Roesler, J., Lang, D. & Altoubat, S., 2004. Fracture of Plain and Fibre-Reinforced Concrete Slabs under Monotonic Loading. *Journal of Materials in Civil Engineering*, 16(5), pp.452-60.

Rostasy, F.S. & Hartwich, K., 1985. Compressive Strength and Deformation of Steel Fibre Reinforced Concrete Under High Rate of Strain. *The International Journal of Cement Composites and Lightweight Concrete*, 7(1), pp.21-28.

Rwelamila, P.D. & Wiseman, G.T., 1995. Concrete Quality Management: a Research Study of the General Contractor in South Africa. *Construction and Building Materials*, 9(3), pp.173-83.

SABS 0100-1, 2000. *The Structural Use of Concrete Part 1: Design*. 22nd ed. Pretoria: South African Bureau of Standards.

SANS 0100-2, 1992. *Structural use of concrete, Part 2: Materials and execution of work*. 2nd ed. South Africa: South African Bureau of Standards.

Self Compacting European Project Group, 2005. *The European Guidelines for Self Compacting Concrete- Specification, Production and Use*. Guidelines and specifications. European Project Group.

Sidumedi, K.S., 2010. *Investigation into the Relationship Between the Corporate Culture of South African Construction Frims and Performance*. PhD Thesis. Johannesburg: University of the Witwatersrand University of the Witwatersrand.

Soranakom, C. & Mobasher, B., 2007. Closed-form Moment-Curvature. *ACI Materials Journal*, 104-M39(July-August), pp.351-59.

Soranakom, C., Mobasher, B. & Destree, X., 2009. Numerical Simulation of FRC Round Panel Tests and Full-Scale Elevated Slabs. *ACI Journal*, SP-248, pp.31-40.

Soranakom, C. & Mobashir, B., 2007. Closed-form Solutions for Flexural Response of Fibre-Reinforced Concrete Beams. *Journal of Engineering Machanics*, 133(8), pp.933-41.

Soranakom, C. & Mobashir, B., 2009. Flexural Design of Fibre Reinforced Concrete. *ACI Materials Journal*, 106(5), pp.461-69.

Soranakom, C., Yekani-Fard, M. & Mobasher, B., 2008. Development of Design Guidelines for Strain Softening Fibre Reinforced Concrete. In Gettu, R., ed. *7th International Symposium of Fibre Reinforced Concrete: Design and Applications BEFIB 2008*., 2008.

Sukontasukkul, P., Pomchiengpin, W. & Songpiriyakij, S., 2010. Post-Crack (or Post-Peak) Flexural Response and Toughness of Fibre Reinforced Concrete after Exposure to High Temperature. *Construction and Building Materials*, (24), pp.1967-2974.

Tang, L. & Schouenborg, B., 2009. A Critical Review of Proportioning Techniques for Self-Compacting Concrete. In Shi, C., Yu, Z., Khayat, K.H. & Yan, P., eds. *Design, Performance and Use of Self-Consolidating Concrete SCC'2009*. Beijing, China, 2009. RILEM Publications S.A.R.L.

Theodorakopoulos, D.D. & Swamy, R.N., 2002. Ultimate Punching Shear Strength Analysis of Slab-Column Connections. *Cement and Concrete Composites*, (24), pp.509-21.

Tsai, C.-T., Li, L.-S., Chang, C.-C. & Hwang, C.-L., 2009. Durability Design and Applications of Steel Fibre Reinforced Concrete in Taiwan. *The Arabian Journal for Science and Engineering*, 34(1B), pp.57-79.

Walraven, J., 2009. High Performance Fibre Reinforced Concrete: Progress in Knowledge and Design Codes. *Materials and Structures*, (42), pp.1247-60.

Walraven, J.C. & Grunewald, S., 2001. Parameter Study on the Influence of Steel Fibres and Coarse Aggregate Content on the Fresh Properties of Self-Compacting Concrete. *Cement and Concrete Research*, (31), pp.1793-98.

Xu, B.W. & Shi, H.S., 2009. Correlations Among Mechanical Properties of Steel Fibre Reinforced Concrete. *Construction and Building Materials*, (23), pp.3468-74.

Zhu, B. et al., 2009. Optimized Design of Aggregate Particle Size Distribution for Self-Compacting Concrete. In Shi, C., Yu, Z., Khayat, K.H. & Yan, P., eds. *Design, Performance and Use of Self-Consolidating Concrete SCC'2009*. Beijing, China, 2009. RILEM Publications S.A.R.L.

Appendix A

Three-point Beam and Compressive Testing Data

Mix 1 Beams (700x150x150; 6 total)

Sample No	**LOP** (0.05mm)		**CMOD$_1$** (0.5mm)		**CMOD$_2$** (1,25mm)		**CMOD$_3$** (2.5mm)		**CMOD$_4$** (3.5mm)	
	P(kN)	f_L (N/mm^2)	P (kN)	f_{R1} (N/mm^2)	P (kN)	f_{R2} (N/mm^2)	P (kN)	f_{R3} (N/mm^2)	P (kN)	f_{R4} (N/mm^2)
1	28.55	8.22	42.27	12.17	39.6	11.40	30	8.64	24.04	6.92
2	21.93	6.32	31.35	9.03	31.15	8.97	21	6.048	14	4.03
3	22.167	6.38	33.13	9.54	30.42	8.76	19.27	5.54976	-	-
4	23.6	6.80	36.85	10.61	30.24	8.71	20.01	5.76288	14.93	4.30
5	23.41	6.74	31.58	9.10	29.54	8.51	20.5	5.904	17.16	4.94
6	21.13	6.09	29.64	8.54	29.22	8.42	19	5.472	14.64	4.22
Statistics										
Average	23.46	6.76	34.14	9.83	31.70	9.13	21.63	6.23	16.95	4.88
+	28.55	8.22	42.27	12.17	39.6	11.40	30	8.64	24.04	6.92
-	21.13	6.09	29.64	8.54	29.22	8.42	19	5.472	14	4.03
Std Deviation	2.66	0.77	4.67	1.34	3.93	1.13	4.17	1.20	4.14	1.19
CoV	11.34%	11.34%	13.68%	13.68%	12.41%	12.41%	19.27%	19.27%	24.40%	24.40%
f_{kt}	18.76	5.40	25.87	7.45	24.74	7.12	14.25	4.10	9.63	2.77

Mix 1 Cubes (100x100; 3 total)

Cube strengths						
MPa	Average	+	-	Std Deviation	CoV	**f_k**
59	57.66	59.00	56.57	1.237	2.15%	55.32
56.57						
57.4						

Mix 2 Beams (700x150x150; 12 total)

Sample No	**LOP** (0.05mm)		**CMOD$_1$** (0.5mm)		**CMOD$_2$** (1,25mm)		**CMOD$_3$** (2.5mm)		**CMOD$_4$** (3.5mm)	
	P(kN)	f_L (N/mm^2)	P (kN)	f_{R1} (N/mm^2)	P (kN)	f_{R2} (N/mm^2)	P (kN)	f_{R3} (N/mm^2)	P (kN)	f_{R4} (N/mm^2)
A1	22.8	7.30	36.76	11.76	34.7	11.10	26.23	8.3936	23.45	7.50
A2	23.8	7.62	35.8	11.46	36.1	11.55	30.5	9.76	26.4	8.45
A3	26	8.32	39.7	12.70	43.20	13.82	39.3	12.576	34.60	11.07
A4	18.36	5.88	27.62	8.84	28.15	9.01	25.9	8.288	24.69	7.90
A5	20.56	6.58	31.26	10.00	34.17	10.93	35.06	11.2192	33.80	10.82
A6	23.89	7.64	36.47	11.67	38.66	12.37	34.76	11.1232	31.00	9.92
B1	21.04	6.73	34	10.88	37.84	12.11	33.28	10.6496	30.95	9.90
B2	23.32	7.46	35.5	11.36	36.50	11.68	31.8	10.176	28.36	9.08
B3	24.57	7.86	38.9	12.45	45.10	14.43	39.1	12.512	34.46	11.03
B4	23.41	7.49	34.56	11.06	36.47	11.67	32.08	10.2656	29.99	9.60
B5	25.75	8.24	40.94	13.10	48.36	15.48	46	14.72	43.61	13.96
B6	23.76	7.60	37.66	12.05	43.21	13.83	39.79	12.7328	37.34	11.95
Statistics										
Average	23.11	7.39	35.76	11.44	38.54	12.33	34.48	11.03	31.55	10.10
+	26	8.32	40.94	13.10	48.36	15.48	46	14.72	43.61	13.96
-	18.36	5.88	27.62	8.84	28.15	9.01	25.9	8.288	23.45	7.50
Std Deviation	2.19	0.70	3.67	1.18	5.56	1.78	5.86	1.88	5.68	1.82
CoV	9.46%	9.46%	10.27%	10.27%	14.42%	14.42%	17.00%	17.00%	17.99%	17.99%
f_{kt}	19.36	6.20	29.48	9.43	29.02	9.29	24.45	7.82	21.84	6.99

Mix 2 Cubes (100x100; 12 total)

Cube strengths						
MPa	Average	+	-	Std Deviation	CoV	**f_k**
39.87	42.44	44.85	39.09	2.029	4.78%	38.97
39.50						
40.96						
43.4						
43.90						
39.09						
42.6						
43.64						
43.98						
43.23						
44.85						
44.26						

Mix 5 Beams (700x150x150; 12 total)

Sample No	**LOP** (0.05mm)		**CMOD$_1$** (0.5mm)		**CMOD$_2$** (1,25mm)		**CMOD$_3$** (2.5mm)		**CMOD$_4$** (3.5mm)	
	P(kN)	f_L (N/mm^2)	P (kN)	f_{R1} (N/mm^2)	P (kN)	f_{R2} (N/mm^2)	P (kN)	f_{R3} (N/mm^2)	P (kN)	f_{R4} (N/mm^2)
A1	22.861	6.58	42.862	13.72	47.982	15.35	47.582	15.22624	44.3	14.18
A2	25.38	7.31	41.437	13.26	45.746	14.64	40.413	12.93216	39.37	12.60
A3	19.141	5.51	30.124	9.64	28.99	9.28	25.981	8.31392	23.94	7.66
A4	17.246	4.97	26.334	8.43	30.91	9.89	29.348	9.39136	27.22	8.71
A5	20.813	5.99	31.831	10.19	38.54	12.33	36.917	11.81344	35.39	11.32
A6	25.109	7.23	42.085	13.47	47.559	15.22	40.731	13.03392	37.75	12.08
B1	20.919	6.02	31.996	10.24	30.525	9.77	27.994	8.95808	27.06	8.66
B2	19.459	5.60	29.618	9.48	35.74	11.44	31.631	10.12192	26.88	8.60
B3	20.624	5.94	33.844	10.83	37.364	11.96	36.54	11.6928	34.57	11.06
B4	21.79	6.28	35.445	11.34	41.955	13.43	38.424	12.29568	34.5	11.04
B5	-	-	-	-	-	-	-	-	-	-
B6	22.013	6.34	30.477	9.75	30.937	9.90	28.676	9.17632	26.83	8.59
Statistics										
Average	21.40	6.16	34.19	10.94	37.84	12.11	34.93	11.18	32.53	10.41
+	25.38	7.31	42.862	13.72	47.982	15.35	47.582	15.22624	44.3	14.18
-	17.246	4.97	26.334	8.43	28.994	9.28	25.981	8.31392	23.94	7.66
Std Deviation	2.44	0.70	5.61	1.80	7.14	2.28	6.72	2.15	6.52	2.09
CoV	11.41%	11.41%	16.42%	16.42%	18.86%	18.86%	19.24%	19.24%	20.04%	20.04%
f_{kt}	17.20	4.96	24.53	7.86	25.57	8.20	23.37	7.50	21.31	6.84

Mix 5 Cubes (150x150; 6 total)

Cube strengths						
MPa	Average	+	-	Std Deviation	CoV	**f_k**
49.4	52.63	56.96	49.12	3.065	5.82%	47.20
53.07						
52.3						
54.9						
56.96						
49.12						

Appendix B

Appendix B refers to all calculations made for predicted failure loads of both flexural and punching shear specimens. The prediction models implemented can be reviewed in Chapter 5. The material property input parameters are based on results obtained from small scale beam testing (see Appendix A), in which the characteristic values were determined through statistical analysis.

Flexural Test Slab

The design yield line pattern as shown below with continuous simple supports along perimeter was modelled. We assume maximum deflections at positions where point loads W were applied. Symmetry for panels A and B has been assumed. The design moment resistance m is determined according to the applicable models in Chapter 5.

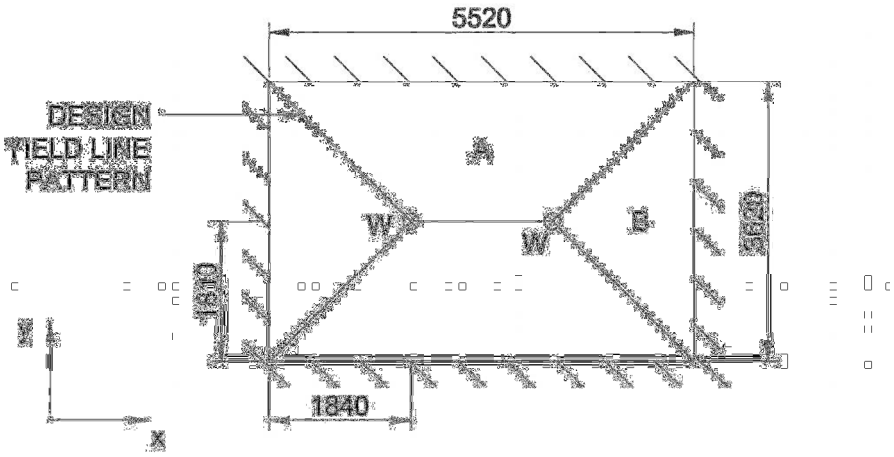

Panel	Rotation θx	Rotation θy	Moment Resistance	Length x	Length y	Mθ
A	1/1.81	NA	m	5.52	NA	3.05m
B	NA	1/1.84	m	NA	3.62	1.97m

Internal WD $= \Sigma M\theta = 2\ (3.05m + 1.97m) = 10.04m$

External WD $= F\ \delta = W.1 + W.1 = 2W$

Internal WD = External WD (i.e. $\Sigma M\theta = F\ \delta$)

$10.04m = 2W$

$W = 5.02m$

Load State	SLS		ULS	
	m (kNm)	W (kN)	m (kNm)	W (kN)
fib Linear Model	23.49	117.92	19.84	99.60
fib Rigid Plastic Model	-	-	18.42	92.47
RILEM σ-ε method	19.65	98.64	17.10	85.84
Closed-form solution	15.55	78.06	16.23	81.47

Punching Shear Test Slabs

The models that consider the influence of fibres incorporate an axial residual tensile stress. As the properties were determined through flexural testing the applicable tensile residual stress value was converted by an assumed factor of 0.4 (see Chapter 5) to approximate a representative axial residual stress. The test samples were constructed with 10mm high yield steel reinforcing at 200mm c/c with a cover of 25mm. An effective depth of 120mm was thus assumed.

SANS 0100-1 Punching Shear Design:

$v_{max} = \frac{V}{u_o d} \leq 0.75\sqrt{f_{cu}}$ *or* $4.75\ MPa$ clause 4.4.5.2

$where\ v_{max} = v_c = \frac{0.75}{\gamma_m}\left(\frac{f_{cu}}{25}\right)^{1/3}\left(\frac{100As}{b_v d}\right)^{1/3}\left(\frac{400}{d}\right)^{1/4}$ clause 4.3.4.1

$\gamma_m = 1$ assuming no material factor

$f_{cu} = 38.97\ MPa$ see Annex A

$$\frac{As}{b_v d} = \frac{474}{1000 \cdot 120} = 0.00395$$

$d = 120\ mm$

$$\therefore v_c = 0.75\left(\frac{38.97}{25}\right)^{1/3}(100 \cdot 0.00395)^{1/3}\left(\frac{400}{120}\right)^{1/4} = 0.862\ MPa$$

$\therefore 0.862 = \frac{V}{2040 \cdot 120}$ where u_0 is perimeter 1.5d away from column face, clause 4.4.5.2.3

$V = 211\ kN$

Punching Shear Mechanism Design:

In this model we need to determine the NA location according to the load state. In order to simplify the calculations it has been assumed that the neutral axis location is dominated by the conventional reinforcing in the failure state. Therefore:

$z = 0.95d$ *SANS 0100-1* clause 4.3.3.4

$$x = \frac{(d - z)}{0.45}$$

$$\therefore x = (120 - 0.95 \cdot 120)/0.45$$

$\therefore x = 13.33\ mm$ neutral axis depth

Compression zone resistance:

$$V_c = \lambda s \sqrt{f'_{ct}(f'_{ct} + \bar{\sigma})} \cdot Ac$$

where

$$\lambda s = \sqrt[4]{400/d} = \sqrt[4]{400/120} = 1.37$$

$$f_t = 0.3\left(f_{fck}\right)^{2/3} = 0.3 \cdot (38.97)^{2/3} = 3.45\ MPa$$

$$f'_{ct} = 0.9 f_t = 3.1\ MPa$$

$$\bar{\sigma} = \left(\alpha - \frac{\alpha^2}{3}\right) f_{cu} = \left(0.56 - \frac{0.56^2}{3}\right) \cdot 38.97 = 17.75\ MPa$$

$$Ac = (4 \cdot 150 + 4 \cot 30 \cdot 13.33) \cdot 13.33 = 9229\ mm^2$$

$$\therefore V_c = 1.37\sqrt{3.1 \cdot (3.1 + 17.75)} \cdot 9229 = 101.7\ kN$$

Tension zone resistance:

$$V_{fr} = \overline{f_{pc}} \cdot A_t \cdot \cos\theta$$

$$f_{ft} = 0.33\ f_{R3} = 0.33 \cdot 7.82 = 2.58\ MPa$$

$$f_{pc} = 0.4 \cdot f_{ft} = 1.032$$

$$\overline{f_{pc}} = 0.6 \cdot f_{pc} = 0.62$$

$$A_t = (4 \cdot 150 + 4 \cdot \cot 30 \cdot 120)\,(120 - 13.33)/\sin 30 = 305\ 372\ mm^2$$

$$\therefore V_{fr} = 0.62 \cdot 305\ 372 \cdot \cos 30 = 163.96\ kN$$

$$V = V_c + V_{fr}$$

$$= 101.7 + 163.96$$

$$= 265.66\ kN$$

FIB shear design model:

As the model is applicable to shear resistance in FRC beams an assumption of a crack angle of 30º was made based on observations by (Choi et al., 2007). The failure perimeter b_w was thus determined based on this assumption.

$$V_{Rd,F} = \left\{\frac{0.18}{\gamma_c} \cdot k \left[100\rho_1 \left(1 + 7.5\frac{f_{Ftuk}}{f_{ctk}}\right) \cdot f_{ck}\right]^{1/3}\right\} b_w \cdot d$$

$\gamma_c = 1$ assuming no material factor

$k = 1 + \sqrt{200/d} = 1 + \sqrt{200/150} = 2.32$

$but\ k \leq 2 \quad \therefore k = 2$

$$\rho_1 = \frac{474}{1000 \cdot 120} = 0.00395$$

$f_{ftuk} = 0.4 \cdot 8.9225 \div 3 = 1.19\ MPa$ conversion from flexural strength to axial stress

$f_{ctk} = 0.6 \cdot 6.2 = 3.72\ MPa$ conversion to axial stress as per RILEM TC-162 TDF (2003)

$f_{ck} = 30\ MPa$ cylinder strength

$b_w = 4 \cdot 150 + 8 \cot 30 \cdot 120 = 2263\ mm^2$ failure perimeter

$$\therefore V_{Rd,F} = \left\{\frac{0.18}{1} \cdot 2 \left[100 \cdot 0.00395 \cdot \left(1 + 7.5 \cdot \frac{1.19}{3.72}\right) \cdot 30\right]^{1/3}\right\} \cdot 2263 \cdot 120$$

$$= 271.5\ kN$$

Appendix C

Punching Shear Crack Formation Sequence

Sample 1

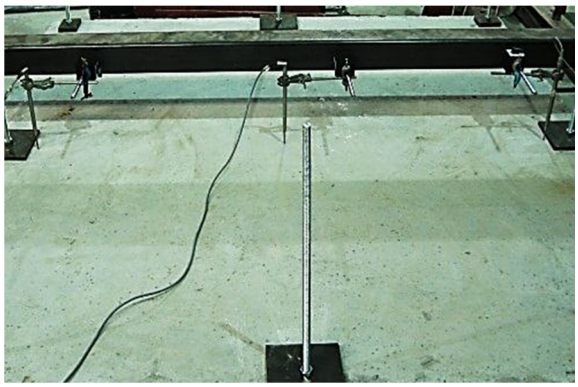

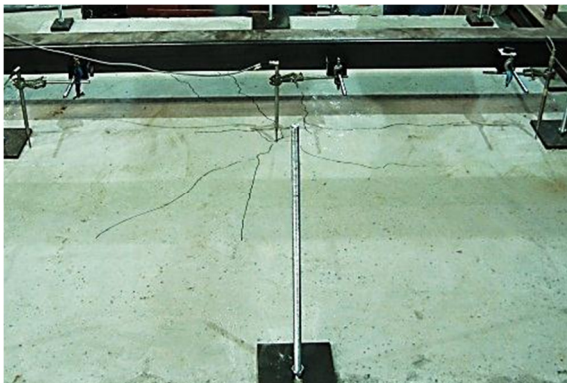

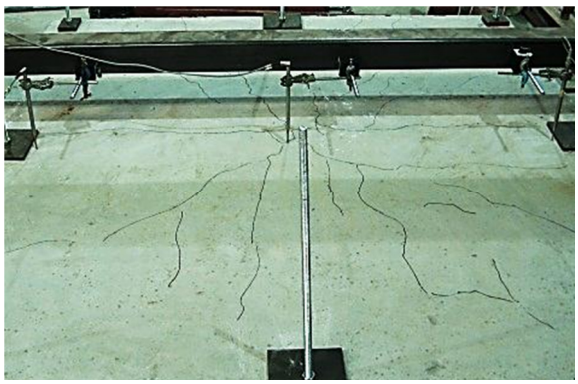

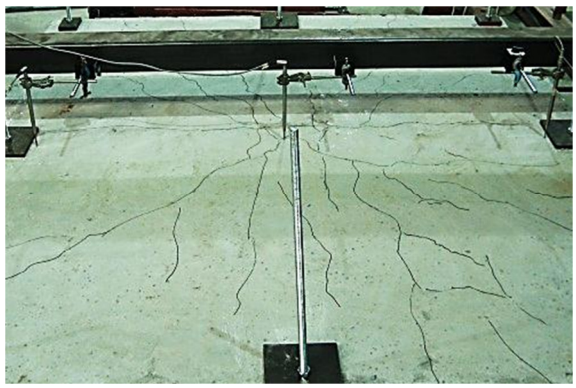

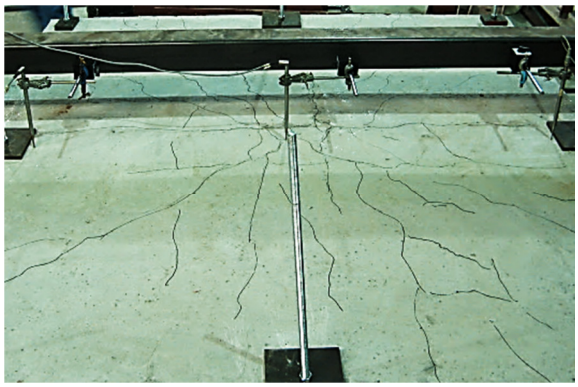

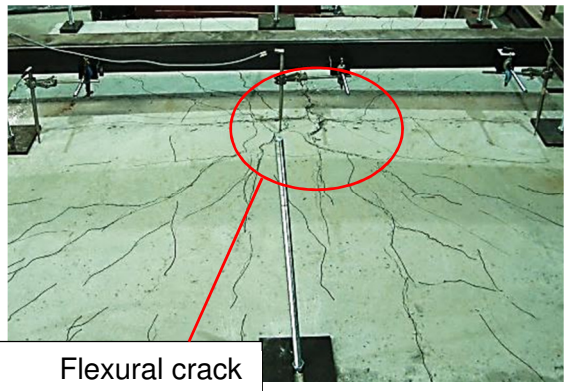

Sample 2

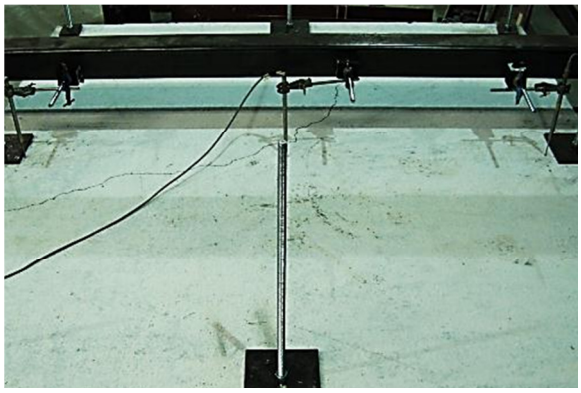
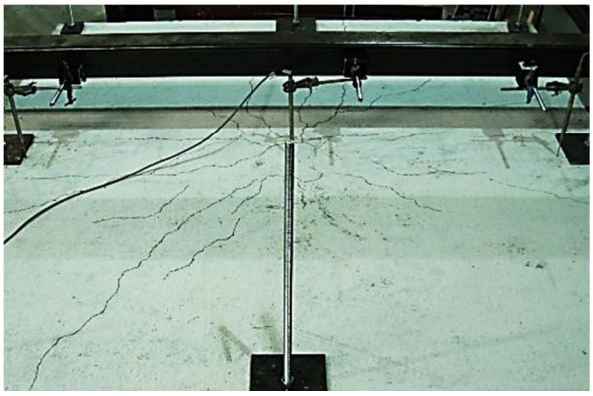
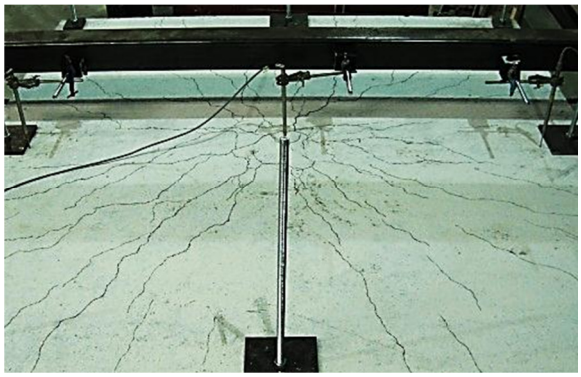
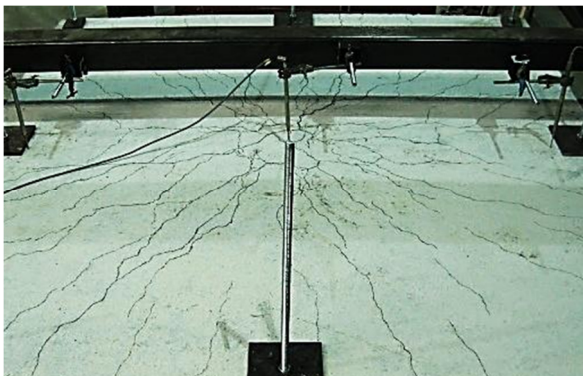
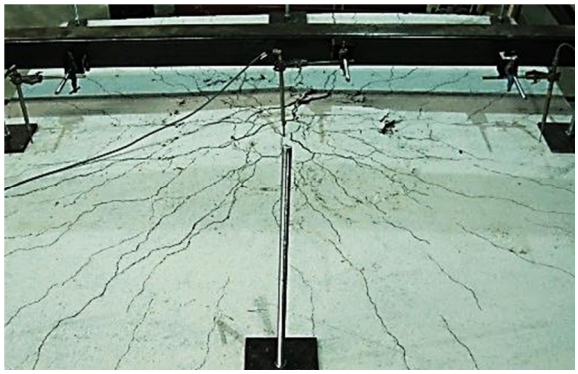
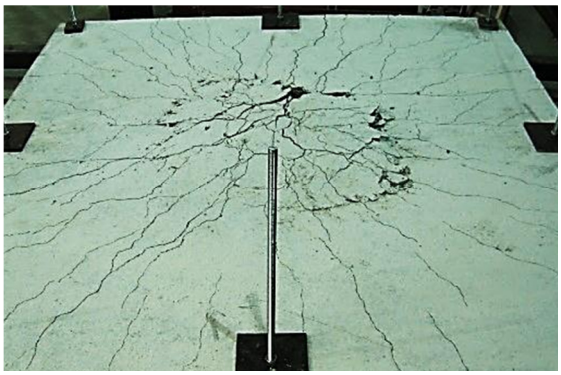

Sample 3